

FINAL  
CONTRACT REPORT  
VTRC 08-CR6

# FINITE ELEMENT ANALYSIS OF THE WOLF CREEK MULTISPAN CURVED GIRDER BRIDGE

JOHN C. LYDZINSKI  
Graduate Research Assistant

THOMAS T. BABER, Ph.D., P.E.  
Associate Professor

Department of Civil and Environmental Engineering  
University of Virginia



**Standard Title Page - Report on Federally Funded Project**

1. Report No. FHWA/VTRC 08-CR6	2. Government Accession No.	3. Recipient's Catalog No.	
4. Title and Subtitle Finite Element Analysis of the Wolf Creek Multispan Curved Girder Bridge		5. Report Date January 2008	
		6. Performing Organization Code	
7. Author(s): John C. Lydzinski and Thomas T. Baber		8. Performing Organization Report No. VTRC 08-CR6	
9. Performing Organization and Address  Virginia Transportation Research Council 530 Edgemont Road Charlottesville, VA 22903		10. Work Unit No. (TRAIS)	
		11. Contract or Grant No. 78966	
12. Sponsoring Agencies' Name and Address  Virginia Department of Transportation      Federal Highway Administration 1401 E. Broad Street                              400 North 8th Street, Room 750 Richmond, VA 23219                              Richmond, VA 23219-4825		13. Type of Report and Period Covered Final Contract Report	
		14. Sponsoring Agency Code	
15. Supplementary Notes			
16. Abstract  <p>The use of curved girder bridges in highway construction has grown steadily during the last 40 years. Today, roughly 25% of newly constructed bridges have a curved alignment. Curved girder bridges have numerous complicating geometric features that distinguish them from bridges on a straight alignment. Most notable of these features is that longitudinal bending and torsion do not decouple. Although considerable research has been conducted into curved girder bridges, and many of the fundamental aspects of girder and plate behavior have been explored, further research into the behavior and modeling of these bridges as a whole is warranted.</p> <p>This study developed two finite element models for the Wolf Creek Bridge, a four-plate girder bridge located in Bland County, Virginia. Both models were constructed using plate elements in ANSYS, which permits both beam and plate behavior of the girders to be reproduced. A series of convergence studies were conducted to validate the level of discretization employed in the final model. The first model employs a rigid pier assumption that is common to many design studies. A large finite element model of the bridge piers was constructed to estimate the actual pier stiffness and dynamic characteristics.</p> <p>The pier natural frequencies were found to be in the same range as the lower frequencies, indicating that coupling of pier and superstructure motion is important. A simplified "frame-type" pier model was constructed to approximate the pier stiffness and mass distribution with many fewer degrees of freedom than the original pier model, and this simplified model was introduced into the superstructure model. The resulting bridge model has significantly different natural frequencies and mode shapes than the original rigid pier model. Differences are particularly noticeable in the combined vertical bending/torsion modes, suggesting that accurate models of curved girder bridges should include pier flexibility. The model has been retained for use as a numerical test bed to compare with field vibration data and for subsequent studies on live load distribution in curved girder bridges.</p> <p>The study recommends consideration of the use of the finite element method as an analysis tool in the design of curved girder bridge structures and the incorporation of pier flexibility in the analysis.</p>			
17 Key Words Curved girder bridge, steel bridge, finite element analysis, natural frequencies and mode shapes		18. Distribution Statement No restrictions. This document is available to the public through NTIS, Springfield, VA 22161.	
19. Security Classif. (of this report) Unclassified	20. Security Classif. (of this page) Unclassified	21. No. of Pages 67	22. Price

**FINAL CONTRACT REPORT**  
**FINITE ELEMENT ANALYSIS OF THE WOLF CREEK MULTISPAN  
CURVED GIRDER BRIDGE**

**John C. Lydzinski**  
**Graduate Research Assistant**

**Thomas T. Baber, Ph.D., P.E.**  
**Associate Professor**

**Department of Civil and Environmental Engineering**  
**University of Virginia**

*Project Manager*

Jose P. Gomez, Ph.D., P.E., Virginia Transportation Research Council

Contract Research Sponsored by the  
Virginia Transportation Research Council

Virginia Transportation Research Council  
(A partnership of the Virginia Department of Transportation  
and the University of Virginia since 1948)

In Cooperation with the U.S. Department of Transportation  
Federal Highway Administration

Charlottesville, Virginia

January 2008  
VTRC 08-CR8

### **NOTICE**

The project that is the subject of this report was done under contract for the Virginia Department of Transportation, Virginia Transportation Research Council. The contents of this report reflect the views of the authors, who are responsible for the facts and the accuracy of the data presented herein. The contents do not necessarily reflect the official views or policies of the Virginia Department of Transportation, the Commonwealth Transportation Board, or the Federal Highway Administration. This report does not constitute a standard, specification, or regulation.

Each contract report is peer reviewed and accepted for publication by Research Council staff with expertise in related technical areas. Final editing and proofreading of the report are performed by the contractor.

Copyright 2008 by the Commonwealth of Virginia.  
All rights reserved.

## ABSTRACT

The use of curved girder bridges in highway construction has grown steadily during the last 40 years. Today, roughly 25% of newly constructed bridges have a curved alignment. Curved girder bridges have numerous complicating geometric features that distinguish them from bridges on a straight alignment. Most notable of these features is that longitudinal bending and torsion do not decouple. Although considerable research has been conducted into curved girder bridges, and many of the fundamental aspects of girder and plate behavior have been explored, further research into the behavior and modeling of these bridges as a whole is warranted.

This study developed two finite element models for the Wolf Creek Bridge, a four-plate girder bridge located in Bland County, Virginia. Both models were constructed using plate elements in ANSYS, which permits both beam and plate behavior of the girders to be reproduced. A series of convergence studies were conducted to validate the level of discretization employed in the final model. The first model employs a rigid pier assumption that is common to many design studies. A large finite element model of the bridge piers was constructed to estimate the actual pier stiffness and dynamic characteristics.

The pier natural frequencies were found to be in the same range as the lower frequencies, indicating that coupling of pier and superstructure motion is important. A simplified “frame-type” pier model was constructed to approximate the pier stiffness and mass distribution with many fewer degrees of freedom than the original pier model, and this simplified model was introduced into the superstructure model. The resulting bridge model has significantly different natural frequencies and mode shapes than the original rigid pier model. Differences are particularly noticeable in the combined vertical bending/torsion modes, suggesting that accurate models of curved girder bridges should include pier flexibility. The model has been retained for use as a numerical test bed to compare with field vibration data and for subsequent studies on live load distribution in curved girder bridges.

The study recommends consideration of the use of the finite element method as an analysis tool in the design of curved girder bridge structures and the incorporation of pier flexibility in the analysis.

## **FINAL CONTRACT REPORT**

### **FINITE ELEMENT ANALYSIS OF THE WOLF CREEK MULTISPAN CURVED GIRDER BRIDGE**

**John C. Lydzinski**  
**Graduate Research Assistant**

**Thomas T. Baber, Ph.D., P.E.**  
**Associate Professor**

**Department of Civil and Environmental Engineering**  
**University of Virginia**

## **INTRODUCTION**

One of the most significant innovations in bridge design over the last forty years has been the development of horizontally curved girder bridges. These bridges are particularly advantageous for the construction of roadways in areas that have serious geographical or man-made impediments. In addition, they allow for more economical construction relative to straight girder chords that are aligned in a curved fashion, since they often allow the use of fewer piers and longer spans. Their utilization is especially common on major highway overpasses and on highway on-ramps and off-ramps. Today, horizontally curved bridges account for nearly one quarter of newly constructed bridges (NCHRP, 1999). The most common steel curved girder bridge configuration uses I-girder construction. Such girders, in their straight form, are familiar to most engineers, and superstructures constructed of I girders have a well established form, consisting of several parallel (or radially concentric) girders connected by cross-frames or diaphragms at intermediate stations, and diaphragms at the piers.

Although common, the use of I-girders in curved bridge construction significantly complicates bridge analysis and design. Such complications exist at every level, from the behavior of the plates that make up the girder flanges and webs, to the individual girder behavior, to the behavior of the girder/slab systems that comprise the bridge superstructure. Additional complications, not widely reported in the literature, may also occur as a result of the interaction between the curved girder alignment and certain types of intermediate piers. A number of studies carried out in recent years indicate clearly that several aspects of curved girder bridge behavior are significantly different than straight girder bridge behavior. Specifically,

- Flange local buckling stresses on the inner and outer side of the web differ from each other, and from those in the straight girder case. Moreover, flange local buckling behavior differs considerably depending upon the degree of restraint provided by the web. In addition, the inner half of a curved girder tension flange may also buckle, a phenomenon that does not occur in straight girders. Although this phenomenon is relatively unimportant at small curvatures, its importance increases as the curvature of the girder increases.

- Curved web plates under bending membrane stresses, or under a combination of bending and shear do not experience classical buckling instability as do webs in straight girders. Instead, S-shaped bending of the web occurs at the onset of loading, increasing continually with the load, and introducing a decreased web efficiency. Therefore, the flange stresses, and the stresses at the web-flange juncture tend to increase, while stresses lower in the web tend to decrease, and the ultimate load capacity of the curved girder is reduced, albeit not by a large amount. This effect is most pronounced in very slender webs, and may or may not be important in thicker webs.
- Longitudinal stiffeners in curved girders may provide a significant stiffening benefit in both the compressive *and* the tensile portions of the web, since both the compression and tension zones participate in the S-shaped lateral web bending. By comparison, longitudinal stiffeners provide no significant benefit in the tension web region of straight girders.
- Bending and torsion of curved girders do not decouple. Consequently, in the presence of warping, flange stresses under uniform loads are not uniform, and the girders tend to rotate as well as translate under load.
- Individual girders undergo twisting under self weight thus introducing construction stresses, unless the cross-frames, or diaphragms are designed to accommodate the twisting deformation of the girders, or the girders are supported during construction to prevent twisting. Typically the girder webs will only be vertically aligned under one stress state, and the designer and fabricator must be clear about what this state is, to prevent construction problems.
- Cross frames, or diaphragms tend to transfer a larger percentage of the load toward the outer girders in a curved girder system. Consequently, cross-frames become primary load carrying members in curved girder bridges. Stresses in cross-frames may be significant, and outer girders may carry a larger percentage of the total load than the inner girders. Another way to think about this phenomenon is that when the girder system twists and bends as a unit, the torsion and bending on the outer edge are additive, while the torsion and bending on the inner edge tend to cancel somewhat.

All of these factors complicate both the analysis and design of curved girder bridges, and as a result, curved girder specifications have lagged those for other bridges in efficiency. Because a curved alignment creates additional complications at the plate element, girder, and system levels, developing modeling procedures for such structures that can adequately account for the complex behavior is of paramount importance.

Prior to the early 1960s, many engineers avoided designing and constructing horizontally curved bridges due to the complexity of their behavior. Extensive research conducted from the late 1960s until today have allowed many of the complications involved with these structures to be identified, and permitted significant advancements in structural design efficiencies. Additional understanding of the dynamic response characteristics of curved bridges is needed.

The construction of computational models for curved bridges that account for the complicating factors discussed above, and evaluate the influence of other possible effects as well is the focus of this study.

## **Background**

The background relevant to this research may be subdivided into several areas. Extensive research has been carried out on extending thin-walled beam theory to model individual curved girders, and has led to a number of theoretical and computational models. Such models typically share the limitations of thin-walled beam theory, in that they are able to model beam action, but not plate action. As such, they cannot predict local stability behavior of curved girders, although they can predict lateral stability limits, provided the proper terms are included. To compensate for this limitation, a number of analytical and experimental models have been constructed to evaluate the behavior of curved flange and web plates. Much of this work has been directed toward evaluating the stability limits of these elements, although strength and residual stress influences have also been considered. The analytical work has used closed form solutions, where available, and either finite difference or finite element methods where closed form analytical solutions are not available. Finally, several experimental studies of scale model, and full scale curved girder bridges have been carried out that are relevant to the proposed work. The major focus of this work has been to investigate the interaction between members in a curved girder system.

### **Curved Girder Research**

The most important distinction of curved girder behavior from that of a straight girder is the significant primary influence of so-called lateral flange moments, which are developed as a result of constraint against torsional warping. These moments have the greatest impact directly on the flanges, where significant normal stresses are created by three main factors in addition to the usual flexural bending: warping stresses due to non-uniform torsion, radial bending due to curvature, and load induced second order effects due to lateral deflection of the compression flange (NCHRP, 1999). The magnitude of these stresses is influenced by span length, flange width, and degree of curvature. The vertical flange moment is characterized by the load applied through the girder's shear center, the restoring forces in connecting members between girders, and the shift of load from interior girders to exterior girders (NCHRP, 1999). In addition, transverse displacements of the web may occur, and along-axis stresses in the web may have a nonlinear distribution (Davidson et al., 2004; Hall, 1996). This web behavior also tends to increase the normal stresses in the compression flange.

Torsional rotation of the cross-section commences upon the initial application of lateral and vertical moments to the girder cross section. Distortion of the cross section out of plane as a result of the accompanying warping displacements contradicts the Navier assumption that plane sections remain plane. Warping stresses develop when a torque is applied to a member that is constrained against warping displacements, or when the torsion acting on a member is non-uniform. The resulting system of flange stresses is termed the bimoment.

The bimoment is a function of the girder's depth, and is proportional to the second derivative of the angle of twist (Davidson et al., 2004). As the bimoment develops, the resulting flange shear resultants are directed toward the center of curvature in the tension flanges and away from the center of curvature on the compression flanges. The resulting system of stresses leads to a pair of self-equilibrating torsional moments, (hence the name bi-moment), in order for the system to resist torsion. The magnitude of the resulting bimoment varies significantly depending on the location in the system, with peak values often found near the diaphragms, where warping constraint is particularly significant.

Such warping effects are also present in straight girders, but only develop during lateral-torsional buckling. By contrast, the torsion found in curved girders is a primary response mechanism and therefore tends to have a much greater effect on the structure's overall behavior and strength than it does in straight girders.

In a girder system, additional complications arise because of the interaction between members. As the individual members displace, the magnitude and distribution of the resulting stresses vary as a function of the stiffness and spacing of the lateral bracing, or diaphragms, and the radius of curvature of the girders (NCHRP, 1999). Web plates are subjected to higher bending stresses than in a straight girder, but the peak bending stress is primarily found in the tension flange. The total stress magnitude, which ultimately governs the strength of the system, is higher in beams with a larger curvature, as a result of second order forces, generated from lateral displacements and twisting of the sections (Liew et al., 1995).

Shear stresses in the girders develop as a result of three distinct mechanisms: shear flow associated with vertical bending, the pure twisting of the beam during which all sections are free to warp, known as St. Venant torsion, and transverse bending with non-uniform axial deformation, known as warping torsion (Oden, 1967). AASHTO curved girder provisions ignore the interaction that exists between torsional shear stress and bending stress, as long as elastic bend buckling limits are implemented for the web. Recent research results have supported this assumption (Hall, 1996).

Curved girders typically fail by flexure or lateral-torsional instability, or due to an interaction of the two modes (Liew et al., 1995). Limiting the cross section's lateral movement is the key to preventing lateral instability failure. The most effective system level prevention against lateral instability is achieved by the use of lateral bracing or diaphragms. The diaphragm members connect girders to one another, transferring large lateral loads, and thus decreasing the secondary out-of-plane stresses associated with the flange plates.

Lateral bracing is particularly important in the initial stages of bridge construction when the concrete deck is not in place, and therefore does not restrain significant lateral and torsional movements of the top flange. Even when the deck is in place, there are still some concerns because horizontal and vertical displacement, and rotations of the horizontally curved beam will always occur to some degree regardless of the applied moment or brace spacing (Nakai and Yoo, 1988).

The first study on the analysis of curved structural members has been attributed to St. Venant in his memoir of 1843 (Tilley, 2004). However, in depth analysis of curved beams did not commence until nearly a century later. Gottfeld (1932) was the first to present a complete analysis of thin-walled curved girders. Umanskii (1948) presented a theoretical analysis of doubly symmetric curved I-members (Nakai and Yoo, 1988). Their respective contributions were subsequently followed by the work of Vlasov (1961), who is generally credited with providing the most extensive early theoretical foundation for analyzing curved beams (Rajasekaran and Padmanabhan, 1989). Vlasov began with the governing equations already developed for straight girders and substituted appropriate curvature terms to compensate for the change in geometry (Rajasekaran and Padmanabhan, 1989). Subsequently, Dabrowski (1968) provided an in depth analysis of curved girders that culminated with a series of design charts for single and multispan girders. Yoo (1979) developed slightly different equations than Vlasov's by substituting curvature terms into the potential energy equations for a straight beam. Rajasekaran and Ramm (1985) concluded, based upon results of numerous buckling studies, that curved girder actions agreed more closely with Vlasov's equations than with Yoo's (Rajasekaran and Padmanabhan, 1989).

Since that time, a number of additional curved analytical and computational models have been generated for individual curved girders. The vast majority of those models incorporate some form of the Navier assumptions for bending behavior, and the Wagner assumptions for constrained warping. Thus they are capable of predicting beam level behavior, but are unable to predict web plate bending, or local deformation in the vicinity of diaphragms. The vast majority of research beyond the fundamentals of curved members, in particular multi-girder systems, and investigations into local plate behavior, did not commence until the advent of more advanced mathematical techniques, specifically the development of finite element analysis in 1957 (Shore and Landsberry, 1975).

### **Modeling Web and Flange Plate Behavior**

A major focus of early work carried out as part of the Consortium of University Research Teams (CURT) was the stability behavior of web and flange plates. A number of papers by Culver and his co-workers (Culver and Frampton, 1970; Culver, Dym and Brogan, 1972; Culver, Dym and Uddin, 1973; Culver and Nasir, 1971) explored both elastic and inelastic behavior of curved flange and web elements, and formed the basis for many of the early code provisions. A significant limitation of their work is that it was only able to examine individual flange or web panels at one time, and was unable to incorporate them into overall structural system models. Moreover, they were unable to construct fully accurate models of web plate behavior at that time. More recent work by Lee and Yoo (1996) used finite element models to predict the strength of curved I-girder webs in pure shear. Davidson, Ballance, and Yoo (1999a, 1999b, 2000a) combined analytical and nonlinear finite element models to more fully address the behavior of curved I-girder webs under bending, and under a combination of bending and shear. They also examined the benefit of incorporating longitudinal stiffeners into curved girder designs (Davidson, Ballance and Yoo, 2000b).

## **Finite Element Models**

When finite element analysis was developed in the late 1950s, it gave researchers an effective tool for subdividing girders into multiple sections, in order to more closely analyze the associated stresses and strains. At least a portion of that work has been directed toward developing thin walled curved beam elements. Two approaches have been used in developing finite equations for curved girders. The first, and the most popular, is displacement based models based on a minimum potential energy formulation. The second encompasses some form of multi-field variational principle (Gendy and Saleeb, 1992). As an alternative to this approach, which retains all of the underlying assumptions of thin-walled curved beam theory in some form, it is possible to model curved girders using thin-shell finite elements. The latter approach has the advantage of producing a much more comprehensive model of curved girder behavior, but at the expense of much larger numerical models.

Due to its potential for high accuracy and flexibility in modeling complex configurations, the finite element method has become the most popular curved girder bridge modeling technique in recent years. Finite element analysis has tended to replace more simplistic two-dimensional modeling methods, such as the Dabrowski and Vlasov method and the grillage or grid analysis method.

In the 1970s, the advent of large-scale computational software made it much easier to develop full-scale models to determine the associated stresses, strains, and displacements with curved girder bridges. Much of the subsequent research, shifted to understanding the more complex second order effects of the bridges.

Fukumoto and Nishida (1981) were able to obtain an analysis of the inelastic, ultimate strength of horizontally curved beams using a transfer matrix method. The transfer matrix method was especially useful at the time, because unlike previous methods used, the transfer matrix method included the second order effects associated with geometric and material nonlinearities, including residual stresses (Liew et al., 1995). Liew et al. (1995) conducted detailed elasto-plastic studies of instability using several different finite element models constructed using ABAQUS, and compared the results with those obtained from several experimental studies and with simple bounding methods using second order elastic and rigid-plastic models of curved girders. Lee and Yoo (1996) used finite elements to predict strength of curved webs in pure shear. Davidson, Ballance and Yoo (1999b) conducted detailed large deformation finite element analyses of curved girder webs under bending, and compared those results with an analytical formulation. Galambos et al. (2000) compared construction stresses obtained from a finite element model with field measured stresses.

## **Vibrational Effects**

Charles Culver, who was a major contributor to the CURT project, was the first to calculate the natural frequencies of a curved simple span (Culver, 1967). Chang and Volterra (1969) followed Culver's work and were able to determine the upper and lower bounds of curved

girder frequencies by using the Lehman-Maehly method. The Ritz method, however, is now commonly used in determining bridge frequencies (Huang et al., 1998).

Culver, with help from Tan and Shore, was able to determine that two free vibration frequencies are associated with each mode shape in horizontally curved beam systems as a result of coupling of the torsional and flexural vibrations (Snyder and Wilson, 1992). Ayre and Jacobsen recognized that natural frequencies tend to occur in clusters, depending on the number of spans in a multispan system. According to their findings, there are  $N$  frequencies in a cluster in an  $N$  span system (Snyder and Wilson, 1992).

Some of the more recent research has focused primarily on the vibrational effects on the girders of shear deformation. Shear deformation has a significant influence upon frequencies associated with higher modes and occasionally lower modes in deep beams, (Piovan et al., 2000).

Tan and Shore (1968) were the first to develop a curved girder's dynamic response to moving vehicle loads (Snyder and Wilson, 1992). The dynamic solution was found by combining a Laplace transformation with the dynamic stiffness method. In this method, the dynamic stiffness matrix and nodal loading vector were formulated based on the Frobenius method (Huang et al., 1998).

Yang et al. (2001) used modal superposition to investigate the forced vibration of a curved girder under both vertical and horizontal moving loads. They showed that, in determining the participating mode shapes, care must be given in accounting for the types of loading crossing the span. One of the most complex cases is that of multiple moving loads. In this case, the modal contributions were found by the superposition of the vibrations induced by each load, with attention paid to the period and time lag of each event (Yang et al., 2001).

### **Overall Curved Girder Bridge System Design and Response**

As discussed in the previous section, lateral and torsional movements, and subsequent deformations of the girders, is widely viewed as the most complicated aspect of curved bridge analyses. There are other aspects of curved bridges, however, that demand just as much attention. Of particular concern is the interaction between adjacent girders through the diaphragms or cross-frames, the connection between the concrete deck and the steel girders, the fabrication method of the steel girders, and the bridge construction process. The curved girder alignment produces much higher torsional stresses in a cross-section than in its straight counterpart, which subsequently can generate fairly significant lateral and vertical displacements in the flanges and in the web. However, because girders are connected to each other by diaphragms, the twisting tendency of the girders is restrained and load transfer between girders occurs. The girder torsion thus forces diaphragm members to act as primary load carrying members.

Girder failure in horizontally curved bridges typically occurs as the result of flexural and/or torsional buckling. The buckling failure can either occur on a global scale, such as lateral flange buckling, or due to localized effects, such as web bend buckling. The most critical failure of the two is on the local scale, between the support points (Nakai and Yoo, 1988). As one of the

exterior girders in the system fails or commences to yield, its stiffness drops significantly, which in turn reduces the amount of load it can receive from an inside girder by way of the diaphragms.

The diaphragms are designed to transfer the lateral forces between girders and reduce internal girder stresses, and tend to transfer load toward the outer girders. Once the outside girders yield, however, the moments in the inside girders increase rapidly, since they cannot transfer the excess loads. This results in additional stress to the inside girders, which can lead to their failure as well. Consequently, properly accounting for the interaction between adjacent curved girders in a bridge framing system is much more vital than in straight girders, where weight is usually more uniformly distributed and only limited load transfer between the girders takes place (NCHRP, 1999).

Properly determining the interaction between the concrete deck and the steel girders is also important. Composite action is necessary for the bridge, not only to reduce lateral and torsional movements associated with the girder system, but also to provide adequate compressive strength for the concrete deck and ensure that longitudinal negative bending moments do not occur in the concrete slab. Shear studs are typically placed to generate the composite action. This joining of girders and the concrete slab interface resists the majority of the prevalent torsional shear stresses that could lead to debonding of the composite section. In the case of floor beam connections to girders, as well as long span plate connections, additional high tension bolts are prescribed to resist both shearing and the torsional moments associated with the I-girders (Nakai and Yoo, 1988).

Often overlooked, a secondary and potentially costly problem can develop during the fabrication of the girders. Curved girders are most often fabricated by one of two methods, cold working or heat curving. Cold working is conducted by bending rolled steel girders or plates through a machine process, once the steel has already hardened. This method can be particularly harmful by creating sufficiently large strains that the steel metallurgy is seriously affected. In current practice the cold working method is not as widely used, primarily due to the large size of the girders that are required for bridge spans. Instead of cold working, heat curving is the typical preferred method of fabrication. Heat curving is performed by shaping the flange and web plates before the steel reaches a hardened state. Flange plates may also be created by cutting the curved sections from wider and more standard plate sections, thus limiting the fabrication effects to the edges of the plates. After the flange sections have cooled, or alternately are cut, they are then welded to the heat curved web to form the curved girder. The welds, however, create thermal stresses at the joints and can also lead to the development of additional residual stresses away from the weld. Usually the residual stresses can be minimized by initial reverse-welding procedures, but the stresses cannot be completely avoided (Nakai and Yoo, 1988). The increased residual stress decreases the overall yield strength, and results in slight inelastic action during initial loading (NCHRP, 1999). This problem is not peculiar to curved girder bridges, but the residual stress pattern may be different in curved girders than in their straight counterparts.

Because of its super elevation, and the curved path that vehicles take in traversing the bridge, curved bridges are excited in both vertical and radial and directions simultaneously; creating significant coupled vibrations due to the automobiles moving at fairly high speeds (Shore, 1975).

Grid analysis, or the grillage method, is an alternative two dimensional analysis method that was developed by Lavelle and Boick (1965) and with advancements in computer technology, replaced the Dabrowski and Vlasov method (Zureick and Naqib, 1999). This method utilizes two-dimensional grid members with three degrees of freedom, two rotational and one translational. This allows the model to be created quickly. The grid analysis method recognizes St. Venant torsion, but typically disregards warping torsion. The grillage method is often accompanied by the assumption laden V-Load Method, which was developed to approximate the effects of warping. It is possible, in principle, to include warping torsion in the grid members, but this has not usually been done. Significant errors may be associated with the grillage method due to the assumptions needed to convert a composite girder/slab system into a system of one dimensional elements. These assumptions compromise the overall accuracy, in addition to limiting the types of models that can be built (Topkaya and Williamson, 2003).

The space-frame method was developed by Brennan and Mandel (1973). Unlike grid analysis and the Dabrowski and Vlasov method, the space-frame method is three-dimensional. It was one of the first three dimensional modeling methods introduced, and works by modeling curved members using three-dimensional straight girder segments, with diaphragms acting like truss members that can only carry axial loads. The space-frame method also disregards the effects of warping. Like the grid models, warping can be included in space frame models with the addition of an extra degree of freedom at each node, but most available software does not do this. Unlike the grid method, the space-frame method does have the ability to model vertical as well as horizontal curvature.

In recent years, finite element modeling has become, by far, the most often used analysis method, at least in research studies. Unlike the previous three methods, finite elements can model three-dimensional structures and it includes the effect of warping torsion. In finite elements, the structure is broken down into a large number of elements with multiple degrees of freedom. Predictions of the structure's behavior are based on the nodal displacement and nodal stresses or element stresses associated with a given element. With the finite element method there is considerable flexibility in implementing boundary conditions, intricate geometries and varying loads that can be used to generate a complex model that easily determines the static and dynamic properties of a structure.

Several techniques can be applied in the finite element modeling process to improve the overall results. Increasing the overall element number will obviously increase accuracy, but it has been found that fewer, higher order elements, with more interpolation nodes can be much more efficient in time and accuracy than many lower order elements (Saje and Zupan, 2003). One of the drawbacks of having a very large number of elements is the high cost associated with the time required to build the model and run the analysis.

Although it is a valuable modeling tool, especially in research, finite element modeling is not without its limitations, particularly in a design setting. Properly describing the details of the girder and diaphragm configuration is time consuming, and does not always lead to an adequate model, especially of connection details. The same can be said of modeling composite action between girders and the deck slab. In addition, slab cracking in negative bending regions is a complex phenomenon that is not easy to model efficiently. Even for relatively simple bridges,

introducing somewhat different modeling approximations can lead to significantly different results, as reported by Tilley (2004), who considered models of the same structure using ABAQUS, ANSYS, and SAP2000 to model the single span test bridges at the Turner-Fairbanks Laboratory. One major finding of Tilley's work is that boundary condition approximations can significantly influence the accuracy of response predictions.

Subsequent work by Simons (2005), while not directed toward curved girder bridges did introduce an interesting option for coupling girders and slabs when plate elements are used to model the girders. Simons observed that rigid link models often lead to local distortion of the girder flanges, and replaced the rigid links with plate elements. The resulting response predictions appeared much more reasonable than those obtained using rigid links.

The process is further complicated if non-linear geometry, material nonlinearity, and residual stresses are to be included. In addition, including nonlinearity can lead to very long run times, and large output files that may be difficult to quickly interpret for design purposes. (NCHRP, 1999). An additional difficulty can occur if a curved composite bridge is modeled using plate elements. It may be desired to obtain the bending and twisting moments at a section. Not only is this information not given directly by the plate model, but also the stresses may be in a Cartesian coordinate system that does not line up with the beam axis at a point. Therefore, calculating bending and twisting moments, or even axial stress may require additional transformations of stress that are not implicit within the finite element code. While the needed transformations are possible, they significantly complicate the post-processing phase of the analysis.

A final complication is introduced by load modeling. In principle, it is possible to run vehicular load models across a structure in either a static, or a dynamic mode. However, load placement is not trivial on a structure whose potential load points may number in the tens of thousands, which has been generated by a mesh generation scheme.

## **PURPOSE AND SCOPE**

The purpose of this study was to create a finite element model to predict the dynamic bridge response characteristics of a recently constructed three-span, horizontally curved girder bridge over Wolf Creek in Bland County, Virginia. The model will then become a numerical test bed for use in conjunction with subsequent field studies of the bridge response.

The Wolf Creek Bridge, shown in Figure 1, is located on Route 644 in Bland County. The bridge is a replacement bridge recently designed using the MDX bridge design software and is scheduled for completion in 2006. The bridge is a three-span I-girder bridge, with spans of 56'-0", 76'-0", and 56'-0" built on a circular curve with a centerline radius of 260'-0", subtending a total angle of 41°24'. The piers are radially oriented, and the bridge consists of four plate girders fabricated of ASTM A709, Grade 50W steel. The diaphragms are C15x33.9s, attached to ½" x 6 ½" plates directly below the top flanges of the girders by bolted connections. Since the separation between the diaphragms and the bottom flanges are roughly 13", the diaphragms rely upon the bending stiffness of the channels, and the ability of the connection

plates to transfer loads to the channels to restrain the girder compression flanges in negative bending regions. The piers are of a T-type, also known as a hammerhead pier, with 5'-0" diameter columns 14' high between foundation and pier cap. The bridge is nearly level, with only a 0.09% gradient along the bridge. Cross-deck slope is 0.02 ft. per ft. along the entire bridge. The bridge was designed using allowable stress design options in MDX for HS20-44 loading. The undersides of the girders are approximately twenty feet above grade, and the bridge surface is located about twenty four feet above grade. For additional details of the bridge, see Lydzinski (2006).

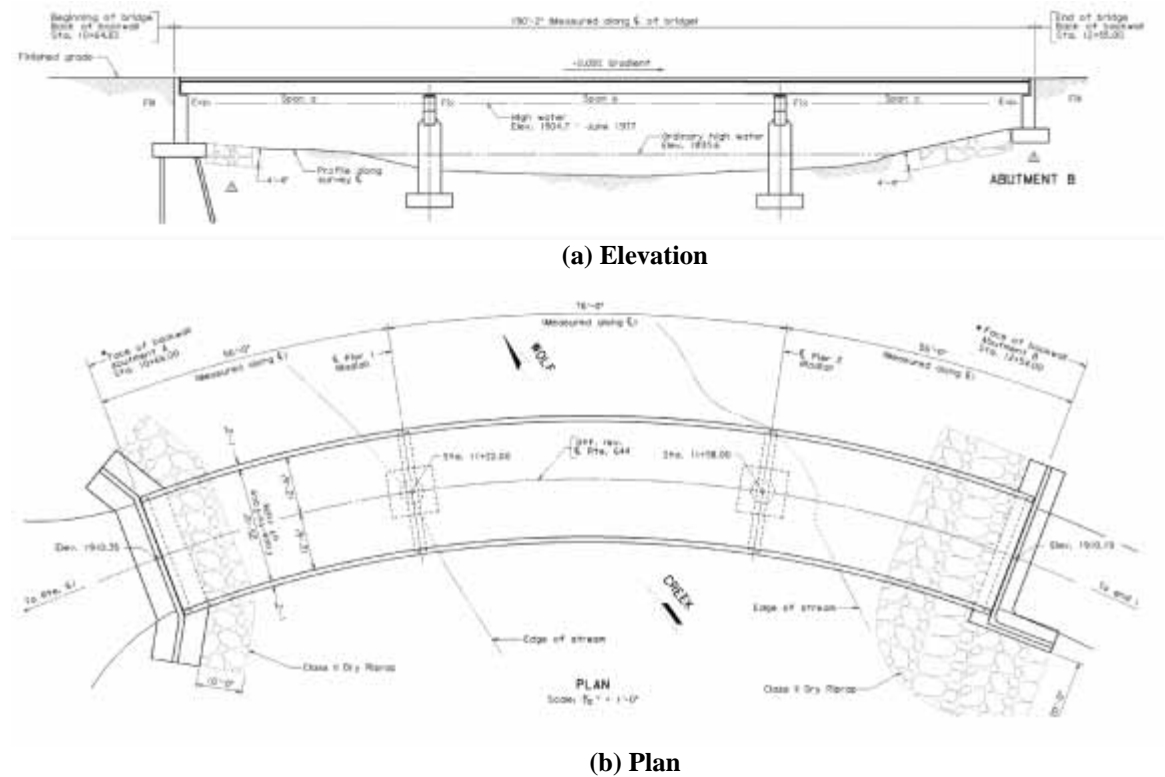


**Figure 1. The Wolf Creek Bridge**

Although the Wolf Creek Bridge is relatively small, it has several features that make it almost ideal as a field “test bed” for curved girder bridges. Unlike bridges tested previously in laboratory studies, the Wolf Creek Bridge has three spans, which makes it an excellent structure for evaluating interaction of spans in a curved alignment. Equally important, access to the bridge is almost unlimited, since it has only a very light volume of low speed traffic.

To fulfill the purpose of the study, several stages of modeling were undertaken. Although these are discussed in greater detail subsequently, it is useful to outline the nature of the numerical studies here. These include:

1. A series of convergence studies on composite girder beams, intended to validate the modeling procedure

2. A baseline “rigid pier” model of the superstructure, intended to replicate a model typical of many design models
3. A detailed pier model, intended to determine the flexibility of the intermediate piers with a fairly high degree of accuracy
4. A simplified pier model, intended to facilitate inclusion of pier flexibility into the superstructure model
5. A “flexible pier” model, including the detailed superstructure model and the simplified pier model.

During the study, it was decided to include slab stiffness for an uncracked slab in the negative bending regions, since experience with previous studies, together with field data, has tended to show that free vibration characteristics of a bridge are adequately modeled by the uncracked slab.

Several models were generated during the current study in order to satisfy the overall objective. Based upon previous experience in modeling bridge structures, it was decided to model both the slab and the plate girders using shell elements, since such elements are capable of predicting a more complete and accurate response than can be obtained using beam elements for the girders. Specifically, the web and flange plate distortions frequently observed in curved girders cannot be modeled using beam type models. Initially, a series of convergence test studies were conducted to determine the level of discretization needed to construct a satisfactory bridge model using the shell elements. Based upon the results of the convergence studies, a bridge superstructure model was then carefully constructed to ensure the maximum accuracy possible, while staying within the bounds of the model size allowed by the software license. Initially, the superstructure model was isolated from its surroundings, and placed upon idealized rigid supports. This model was used to provide a baseline for comparison with more complete models, and is typical of approximations frequently introduced during design of bridges.

Following analysis of the baseline structure, a separate detailed model was constructed of an individual pier. The pier was modeled down to, and including the footing. No attempt was made to model subgrade stiffness. The purpose of this model was to determine whether including pier flexibility is likely to significantly change the superstructure response. Based upon the results of this study, it was decided to introduce a flexible support model. Because of the already large number of elements present in the superstructure model, and the large number of elements required for the detailed pier model, a separate, simplified pier model was introduced with the intent of reproducing the essential flexibility and mass properties of the piers with many fewer degrees of freedom. The simplified model that was used in the present study was comprised of three-dimensional frame elements, and was constructed after several trials.

Following the completion of the curved bridge model, several analyses were performed. One of the main investigations considered whether centralized piers should be modeled in detail, or if the use of simple support boundary conditions is acceptable.

## METHODS

### Convergence Studies

Finite element (FE) structural models can produce either very good, or very poor results depending upon whether the level of discretization is adequate. At the same time that inadequate discretization may produce poor results, using too many elements may lead to a very inefficient model that may lead to overly long execution times, or worse, may not run at all, either because of poor numerical convergence or because the model size exceeds the available computer capacity. In the current case, it was understood that the ANSYS licensing agreement places an upper limit upon the model size that can be generated. Although that upper limit is relative large, it is still possible to exceed it when modeling an entire structure.

It was decided early during the study to model the entire superstructure, including the bridge deck, the railings, the girders, and the diaphragms, using plate elements. Although it is possible to model the girders and diaphragms using beam elements, considerable information about the bridge response is lost in such models, and difficulties have been encountered in achieving complete displacement compatibility between the girder and deck models in past studies. Numerous other researchers have used finite element modeling techniques for bridge structures with plate elements, e.g., Tilley (2004), Simons (2005), and references cited by those authors, but relatively little has been reported about convergence of those models. Therefore, it was decided that an important first step in the current study must be a convergence study, to determine the minimal level of acceptable discretization. As part of the studies it was planned to model the bridge superstructure both before and after the slab was placed, so it was considered important to model several distinct elements separately. A single span, 48 ft. long girder was modeled, using the SHELL63 Element from ANSYS. Because of the additional complications in imposed boundary conditions that would be introduced by curving the single span girder, a straight girder was used for the convergence studies. The bottom flange of the girder used for convergence tests was 19 inches wide and 1.25 inches deep, the top flange was 16 inches wide and 0.875 inches deep, and the web was 30 inches deep and 0.5 inches thick. The girder was supported by pinned supports at one end and by roller supports at the other. Bearing stiffeners were placed at either end, and the supports were applied across the flange width to minimize any problems associated with local end distortion. The convergence test girder was subjected to 20 kip downward loads at the center of the top flange that are applied along six-foot intervals beginning at the ends, as shown in Figure 2. Several convergence studies were conducted.

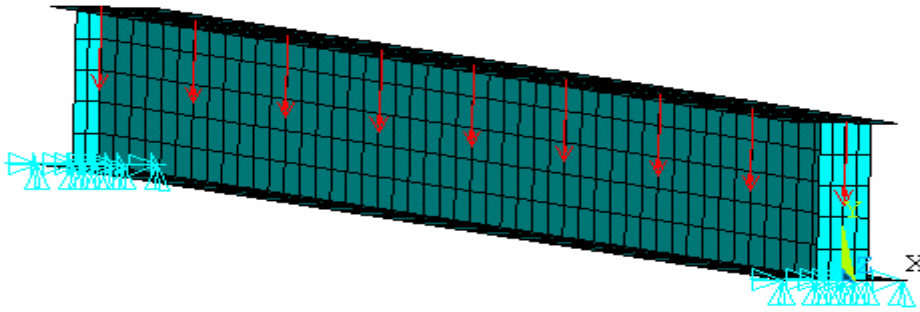


**Figure 2. Convergence Girder Test Model**

### **Girder Convergence Studies**

Three different convergence studies were conducted on the bare girder. In the first study, the number of elements through the height of the web was varied. In the second study, the number of elements across the flange width was increased, and the number of web elements was again varied. In the Third study, the number of flange and web elements used at the cross-section was held constant, and the subdivision along the length of the beam was varied. The organization of these studies is summarized in Table 1.

**Table 1. Girder Convergence Studies**

	<b>Number Of Flange Elements (Each Flange)</b>	<b>Number Of Web Elements</b>	<b>Number Of Elements Along The Length</b>
Study No. 1	4	2, 3, 4, 5	48
Study No. 2	6	2, 3, 4, 5	48
Study No. 3	4	4	8,16,24,48,96,144,576

### **Girder Plus Slab convergence Studies**

With the girder convergence tests completed, the concrete haunch and deck were added. The haunch was modeled using a technique developed by Simons (2005), who found that using vertical shell plates to connect the girder to the deck provides a reasonably accurate representation of the haunch's response, and eliminates local flange distortions that have sometimes been observed in rigid link models. The shell elements representing the haunch connect the nodes that define the top flange to corresponding nodes that compose the deck directly above. This creates elements that run vertically along the length of the girder, as seen in Figure 3. The plates used to define the haunch can be varied to create the same overall width as the actual section. This model may slightly underestimate the lateral stiffness of the haunch, but because the lateral deformation of the haunch is generally negligible, this error is considered acceptable. An alternative, not explored in this study, would be to model the haunch using solid elements. An eight-foot wide deck was added to the 48-foot girder and haunch to complete the convergence studies. Concrete for the haunch and deck was assumed to have an elastic modulus of 3605 ksi and a Poisson's Ratio of 0.2. Four convergence tests were performed, as outlined in Tables 2 and 3.

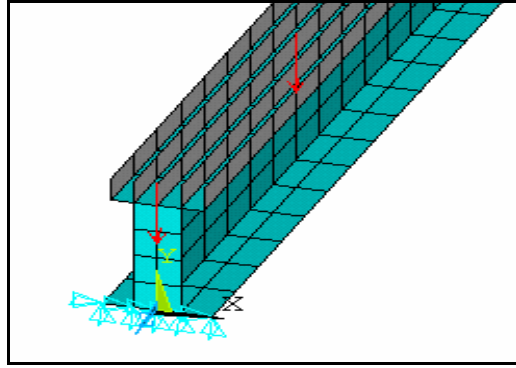


Figure 3. Girder with Haunch

Table 2. Convergence Studies for Girders with Haunch and Deck

Study No. 4	Number of web elements varied (4 flange elements)
Study No. 5	Number of web elements varied (8 flange plates)
Study No. 6	Number of elements along length varied
Study No. 7	Number of deck elements transverse to beam varied

Table 3. Convergence Tests for Girder with Haunch and Deck – Grid Variations

	Flange Elements	Web Elements	Deck Elements	Elements Along Length
Study No. 4	4	2, 3, 4, 5, 6	24	48
Study No. 5	8	2, 3, 4, 5, 6	24	48
Study No. 6	4	4	24	8,16,24,48,96,144,576
Study No. 7	4	4	6,8,12,24,44	48

### Diaphragm Convergence Studies

The final set of convergence studies was conducted for a channel section representative of the diaphragms used in the Wolf Creek Bridge. The representative diaphragm member studied is a C15 x 33.9, eight feet long. For the convergence studies, the girder was fixed at the ends, and loaded at mid-span with a ten kip load, as shown in Figure 4. Three studies were conducted, as summarized in Table 4.

In study 8, a single flange element was used, and the number of web elements through the height was varied. In study 9, the web element study was repeated with two elements across each flange. In study 10, 1 flange element and 4 web elements were used, and the number of elements along the diaphragm was varied.

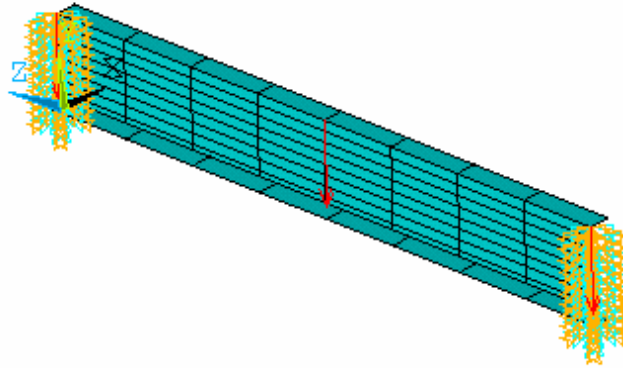


**Figure 4. Diaphragm Convergence Model**

**Table 4. Diaphragm Model Convergence Studies**

	<b>Flange Elements</b>	<b>Web Elements</b>	<b>Element Along Length</b>
Study No. 8	1	1, 2, 3, 4, 5, 9	8
Study No. 9	2	1, 2, 3, 4, 5, 9	8
Study No. 10	1	2	2, 4, 8, 16, 32

## **Pier Models**

The Wolf Creek Bridge is supported at two intermediate points along its length by two hammerhead piers. At the beginning of the study, one of the objectives was to ascertain whether it is important to consider pier flexibility to correctly determine the bridge superstructure dynamic response characteristics. At first, a detailed, three dimensional solid model was constructed. That model had a very large number of degrees of freedom, which made its explicit inclusion in the bridge model impractical. The detailed model was used as a basis of comparison for a simplified model of the bridge using beam elements, which was calibrated against the three dimensional model and subsequently used in the full bridge model.

### **Pier Model using Three-Dimensional Solid Elements**

Complete modeling of a reinforced concrete pier can be quite complex, so several simplifying assumptions were introduced. It was assumed that the amount of cracking of the pier is not sufficient to significantly reduce stiffness. It was further assumed that, in the absence of significant cracking, the gross cross section of concrete dominates the design, so detailed modeling of reinforcement is unnecessary. The pier concrete was given the same properties as A3 concrete, which was prescribed in the plans for the bridge substructure. The properties specified include a modulus of elasticity of 3,122 ksi, a Poisson's ratio of .17, and a density of  $2.172 \times 10^{-7}$  kips-sec<sup>2</sup> per square inch. Finally, it was assumed that the sub-grade below the base of the pier is sufficiently stiff that it may be considered to provide rigid support to the footing, since modeling the surrounding impact of the soil characteristics is beyond the scope of this project, and such additional refinement is not justifiable, given the approximations introduced in modeling the pier as an isotropic elastic body. It is clear that all of these assumptions are

approximations at best. Thus, the model presented here must be regarded as a baseline model, which should be subject to critical evaluation based upon observed field behavior.

The detailed pier model, shown in Figure 5, was constructed using SOLID95 elements within ANSYS. These are 20 noded quadrilateral elements that permit quadratic variation of displacements within an element. The model was generated using the solid modeling capability of ANSYS along with the meshing tool to automatically generate the mesh. The resulting model has 21,941 nodes and 14,361 elements. Each node has 3 degrees of freedom, so, accounting for the restrained nodes at the base, the model has over 60,000 degrees of freedom.

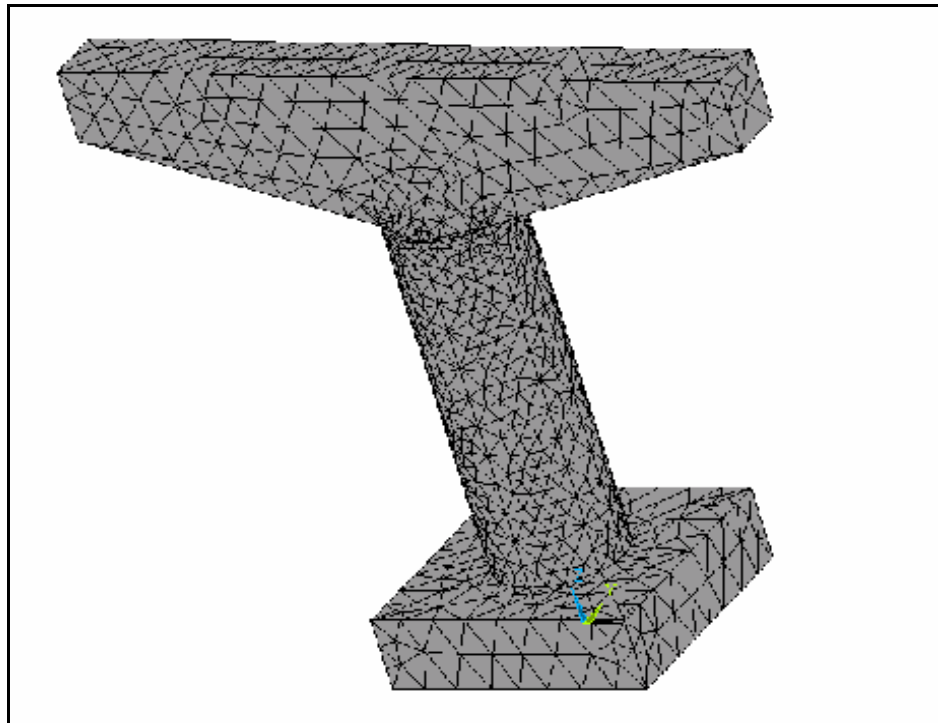


**Figure 5. Finite Mesh Model of Pier**

### **Simplified Pier Model Using Beam Elements**

Including the detailed pier model in the structure definition proved to be impractical, because of the limitation on the number of degrees of elements that could be included in the model. Therefore, an approximate model for the piers was constructed, using beam elements. The final model is shown schematically in Figure 6.

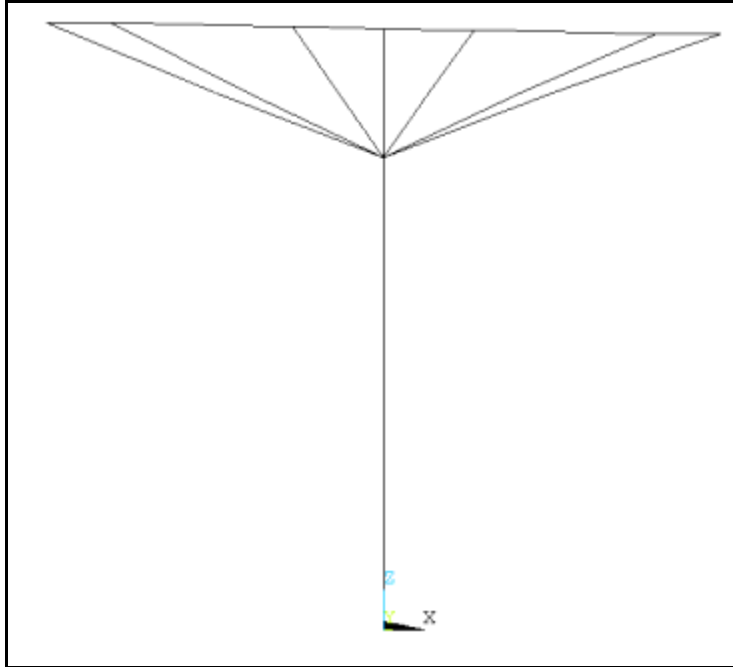


**Figure 6. Schematic of the Beam Pier Model**

The beam model was created with the same concrete and density properties as the actual pier. Several different beam element models were created, with the intent of mimicking the behavior of the full pier model as closely as possible. In the final frame model, the over 14,000 solid elements were reduced to only thirty-two beam elements. The elements used in the beam model were BEAM4 elements, which are three dimensional with tension, compression, torsion, and bending capabilities.

Due to the large reduction in element numbers, and the relatively massive size of the joint regions of the pier, between the circular columns and the tapered pier cap, the only way to accurately capture the nature of the finite mesh model was to alter the size of each beam element individually by varying its cross section. This was accomplished through a trial and error process, by varying the element arrangement and cross section until the displacement characteristics of the beam model closely matched that of the solid element mesh model under the same loading conditions.

In order to evaluate the performance of the BEAM4 pier models against the SOLID95 model, two groups of tests were used. The first series of tests was carried out by applying static point loads to both the SOLID95 model and the BEAM4 model, and the deflections under load were compared. Four point loadings were used:

1. Test 1: A 100 kip load applied was horizontally in the plane of the pier (the  $x$  direction) at the highest point, directed toward the column.
2. Test 2: Four 100 kip loads were applied vertically (the  $z$  direction) at the girder locations along the pier
3. Test 3: A 200 kip horizontal load was applied perpendicular to the plane of the pier (the  $y$  direction), at the location of girder three, at the top of the pier.

4. Test 4: A 50 kip load was applied in the  $x$ -direction at the same point as in test one. Meanwhile, horizontal loads were applied perpendicular to the plane of the pier ( $y$  direction) at four points across the pier cap. On one side of the column, two 75 kip loads were applied in the  $+y$  direction, and on the opposite side two 75 kip loads were also applied in the  $-y$  direction, creating a torque in the column.

Using these four test loadings as a guide, the BEAM4 pier models were adjusted by trial and error to reproduce the displacements of the SOLID95 model as closely as possible.

Once the stiffness of the BEAM4 models was established to be as close as possible to those of the SOLID95 model, a second, dynamic test was conducted. In this final test, the first three natural frequencies and mode shapes of the BEAM4 and SOLID95 models were computed, and compared.

With the large reduction in element size, Figure 6 shows that the final beam model barely resembles the actual pier. However, the most important objective is that the final beam model displays very similar stiffness and mass characteristics to the solid element mesh model when subjected to the same varying loading conditions, as is shown in the next section. If it is not feasible to reproduce the stiffness and mass equally well, it was decided to emphasize stiffness, since the mass of the superstructure, which is more accurately modeled, may be expected to dominate the mass of the pier.

### **The Bridge Models**

Using the convergence studies as a guideline, the superstructure of the bridge was modeled using SHELL63 elements. Two bridge models were then constructed. The first model, designated as the *rigid pier model* assumes simple pinned support conditions at the pier locations, and roller supports along the tangential direction at the abutments, consistent with the bearings used in the structure. The second model, which will be called the flexible pier model, incorporated the BEAM4 model of the piers discussed above.

### **Modeling the Girders**

Each girder flange was discretized into four elements, at least in part to accommodate the diaphragm connection plates and bearing stiffeners. In order for the diaphragms to be adequately modeled, the girder web cross section was modeled using five elements through the height. This accommodates the three diaphragm web plates that connect into the girder webs, and allows the girder webs to be properly represented as well. Beginning at the end of span (c), the nodes needed to define the end cross section coordinates for the four girders and the deck slab were created, generating a total of fifteen end nodes per girder cross section. In the ANSYS cylindrical coordinate system, the end nodes were then copied and swept at incremental angular distances by varying the subtended angle. The angular increments were selected so that the largest nodal arc length in the outer girder is one foot, the maximum length prescribed by the convergence tests. By sweeping the nodes through the entire length of each girder, the girder outlines were formed with a total of 217 lines of cross section nodes, or 3,255 total nodes per girder.

Once the nodal pattern was established, SHELL63 elements were generated by using the nodes as corner points for the plate element boundaries. The SHELL63 element does not allow curved boundaries, so the bridge model consists of numerous flat elements. Since the web element lengths are a maximum of one foot, the flat elements provide a reasonable representation of the curved flange plate boundaries, and the curved web geometries, as shown in Figure 7.

Girder element material properties for the steel were defined with a modulus of elasticity  $E = 29,000$  ksi, a Poisson's ratio  $\nu = 0.3$ , and a material density  $\rho = 7.35 \times 10^{-7}$  kips - s<sup>2</sup> / in<sup>4</sup>.

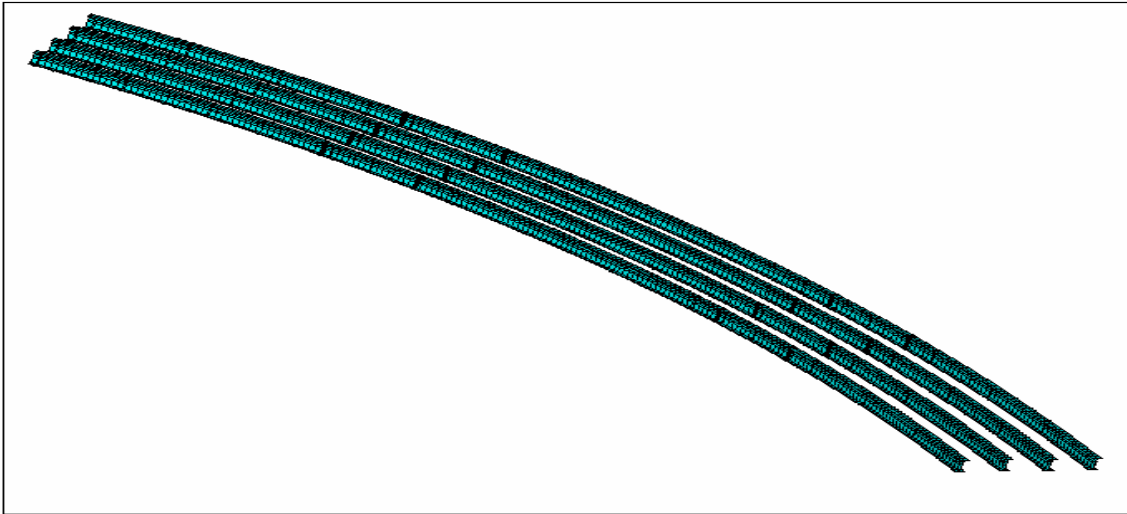


**Figure 7. Layout of Girders in ANSYS**

The bearing and web connection plates were likewise modeled with SHELL63 elements, using the identical material properties as the girders. The web to diaphragm connection plates in the Wolf Creek Bridge are 6.5 inches wide, while the bearing stiffener plates are eight inches wide. To simplify the girder mesh, it was decided to model both plates as 6.5 inches wide, and change the thickness of the bearing connection plates to provide equivalent stiffness characteristics. The element section properties were then varied, in order to accommodate the reduction in both volume and stiffness. A typical connection plate detail is shown in Figure 8, which also illustrates the meshing of the girder cross-section in greater detail.

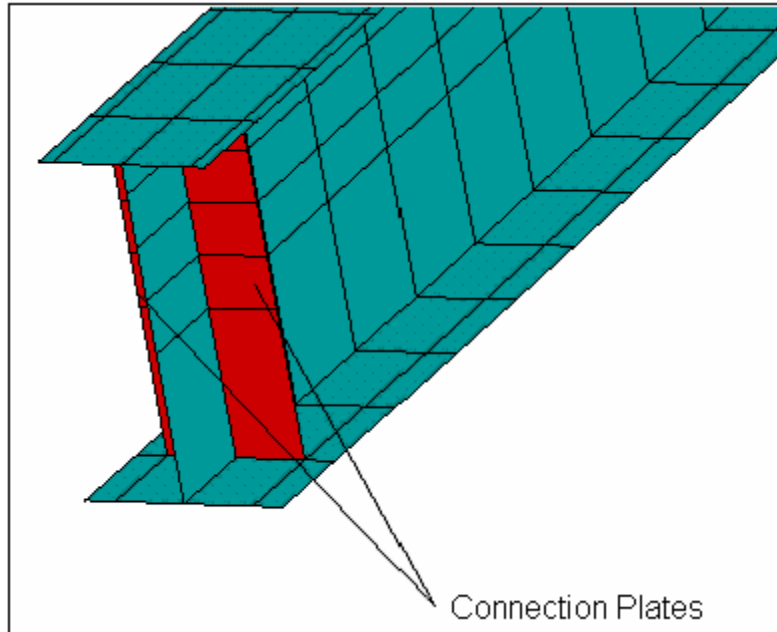


**Figure 8. Example of Connection Plate Elements on Girders**

### **Modeling the Diaphragms**

Based upon the convergence tests, it was decided that the diaphragm webs should be modeled with four plates in the vertical cross section. The diaphragm flanges were modeled using one element per flange, given the relatively small width of these members, and the relative insensitivity of the diaphragm models to a change in the number of flange elements. Lengthwise, the diaphragms were discretized into seven elements, each element being one foot long.

The diaphragm end nodes were positioned to coincide with the top nodes on the web of each respective girder. The newly created line of nodes was subsequently copied and offset vertically, with four total rows equally spaced, to form the outline of the first diaphragm web. The top and bottom diaphragm rows were subsequently offset horizontally to form the outline of both diaphragm flanges. Once the initial diaphragm was created, it was copied and swept to the specified locations of each row of diaphragms on the bridge.

In the design specifications, the diaphragms are joined to the girders through bolted connections on the connection plates. Since modeling bolted connections is beyond the scope of this project, an alternative method was used. In reality, the diaphragms are joined to the connection plates at a distance of approximately 0.5 inches from the edge of the girder web. In the ANSYS model, however, they were joined at the edge nodes of the connection plates, and therefore act as a continuous member between the girders and diaphragms. The accuracy of this approximation will be evaluated in subsequent measurements on the actual structure.

To make up for the lost stiffness where the diaphragms overlap the connection plates in the model, the thickness of the connection plate elements over the sections where the diaphragms connect was increased to include the thickness of both the diaphragm webs and the connection plates. This approximation assumes that the bolts provide an effectively rigid connection

between the diaphragms and the connection plates. In the FE model, the diaphragm flanges start at the outside edge of the connection plates. The effect of losing the flange length over the connection plates should be insignificant on the global scale, although it may be expected to introduce local errors in the diaphragm flange stresses. Since the primary purpose of the current model is not to model local diaphragm stresses, the approximations are considered to be adequate. Figure 9 shows a layout of a portion of the bridge with diaphragm members present.

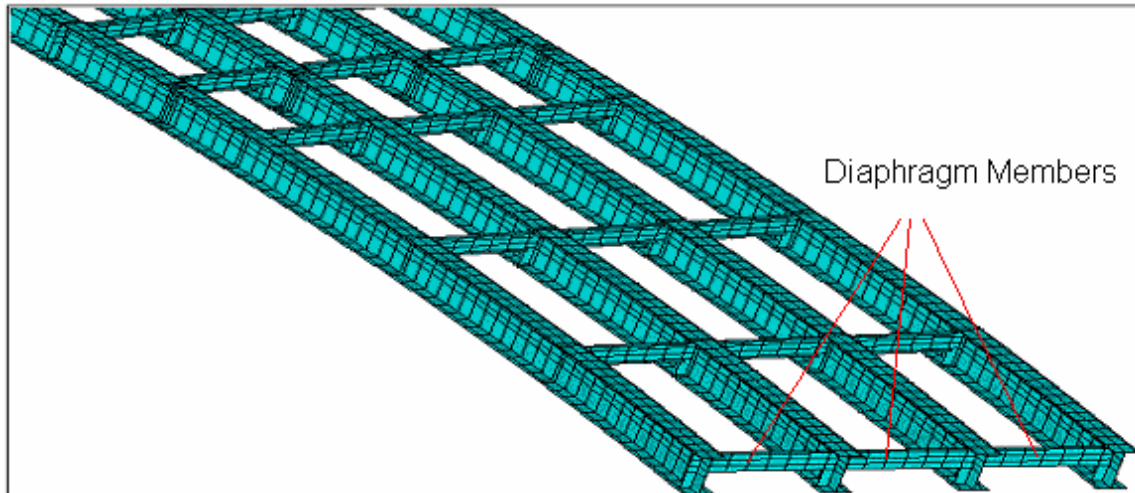


**Figure 9. Layout of Bridge Girders with Diaphragms**

### **Modeling the Haunches**

The haunches connecting the girders to the slab were modeled using the plate element approach developed by Simons (2005). In this model, SHELL63 elements are oriented vertically, parallel to the girder web, and extend from the nodes on the top flange of the girder to the nodes on the mid-plane of the slab. The thicknesses of the plate elements making up the haunch collectively replace the full width of the haunch. As noted above, this model tends to somewhat underestimate lateral shear stiffness of the haunches, but since lateral shear stiffness of the haunches is several orders of magnitude higher than the lateral stiffness of the elements to which the haunches are connected, this underestimate is not considered to be of great consequence. Moreover, the stiffness of each respective row of haunch elements can easily be altered by varying the shell thickness in order to obtain comparable overall section stiffness properties. As shown in Figure 10, the location and length of each haunch element, shown in green, was specified by the corresponding location and length of the element and nodal boundaries of each girder below.

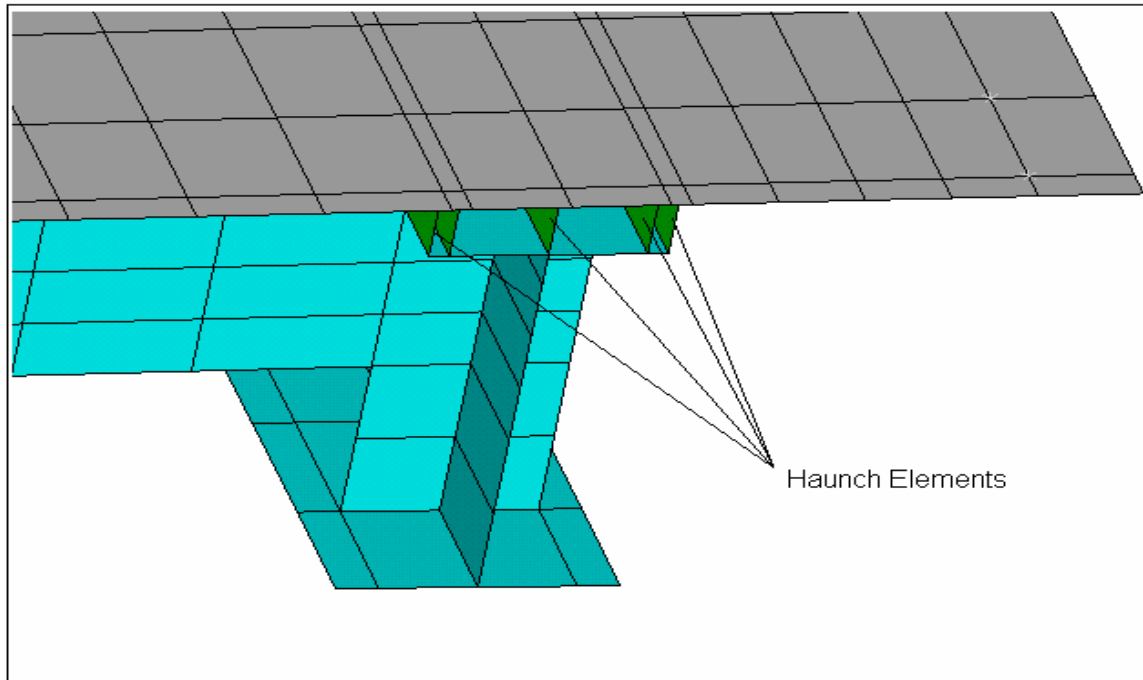


**Figure 10. Diagram of SHELL63 Haunch Elements**

A4 concrete was used to model the haunches, with  $E = 3,605$  ksi;  $\nu = 0.15$ , and  $\rho = 2.2245 \times 10^{-7}$  kips - s<sup>2</sup> / in<sup>4</sup>. The haunch sections on girders two and three were modeled identically, but on girders one and four, the design was slightly different due to the additional three inches of haunch width on the inside of girder four and on the outside of girder one. Table 5 specifies the thickness of each row of shell elements over each girder.

**Table 5. Thickness of Haunch Element Rows**

	<u>ROW 1</u>	<u>ROW 2</u>	<u>ROW 3</u>	<u>ROW 4</u>	<u>ROW 5</u>
<b><u>GIRDER FOUR</u></b>	3.688	4.005	6.625	4.005	0.688
<b><u>GIRDER THREE</u></b>	0.688	4.005	6.625	4.005	0.688
<b><u>GIRDER TWO</u></b>	0.688	4.005	6.625	4.005	0.688
<b><u>GIRDER ONE</u></b>	0.688	4.005	6.625	4.005	3.688
*** Rows from inside of bridge to outside, thickness in inches					

### **Modeling the Deck and Parapets**

The deck and parapets, or railings, were also modeled using A4 concrete. The top flange girder nodes were used as a basis for the layout of the deck nodes, since the deck nodes are positioned on the bridge deck directly above the girders. Using the results of the convergence tests, the distance between the outer edges of adjacent girders' top flanges was subdivided into seven elements transversely. The three deck elements adjacent to the girders are 8.5 inches wide, and the element midway between the girders is 17 inches wide, in order to minimize model size. The width of the deck on the outside of the inner and outermost girders was subdivided into five rows of elements, with a maximum width of seven inches.

The length of each girder element along the bridge axis prescribes the length of the deck elements above. The lone exception was at the ends of the bridge, where there is an additional 1.5 inches of deck on each end of the structure beyond the girder ends. Therefore, an extra row of deck elements is provided on each end of the bridge to accommodate the added length. An end section of the bridge model, showing the deck discretization, including the extra row of elements at the end of the bridge is shown in Figure 11.

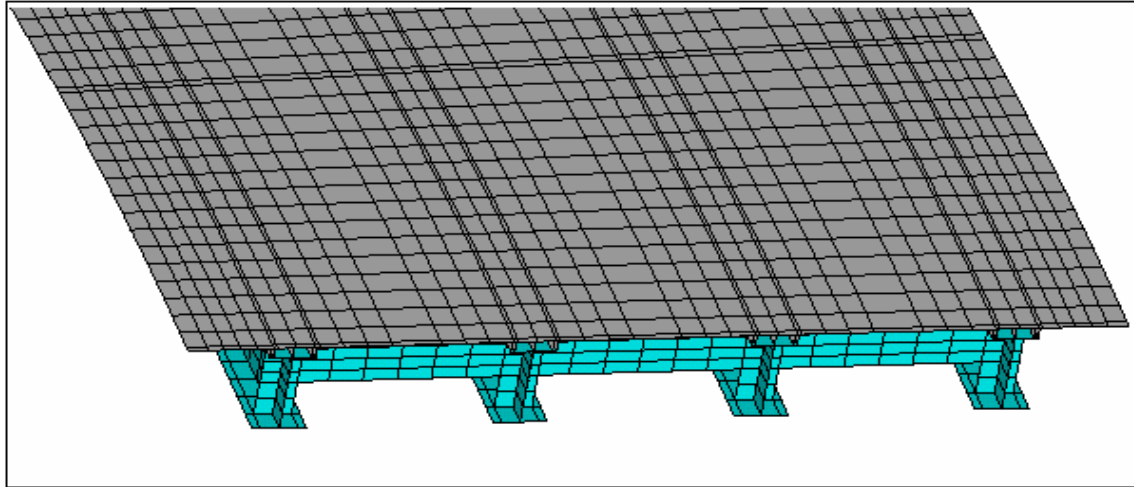


**Figure 11. End Section of Bridge with Deck Plate Elements**

The parapets were produced in similar fashion, using SHELL63 elements with the same material properties as the deck and haunch members. Two deck rows of nodes, including the second row of nodes from the outside on both sides of the bridge, are copied and offset vertically to create two new rows of nodes on each side. These form the outline of the parapets. The first row of nodes corresponds to the 13” height of the base of the parapets and the second row outlines the top of each parapet at a height of 27” above the bridge deck.

Design specifications call for each base of the parapets to be spaced at a maximum of seven feet from each other, end to end, with an unspecified maximum base width. Since these distances were to be specified by the general contractor, on a bridge that had not been erected at the time that this model was constructed, the exact dimensions could not be accurately modeled and therefore had to be approximated.

Using the element length prescribed by the girders and subsequently the deck nodes, the outside parapet close to girder one in the ANSYS model was created with a maximum base-to-base distance of approximately seven feet. Base parapet elements were modeled with a thickness of twelve inches, while the top elements have a thickness of thirteen inches. A similar inside railing was generated close to girder four, but its base-to-base length was slightly less due to the change in radius at these respective sections of the bridge, as shown in Figure 12. This difference may introduce small errors in the results. It is, however, expected that these necessary approximations will not extensively impact the overall accuracy of the model since the added stiffness and mass of the parapets is relatively small compared to that of the overall structure.

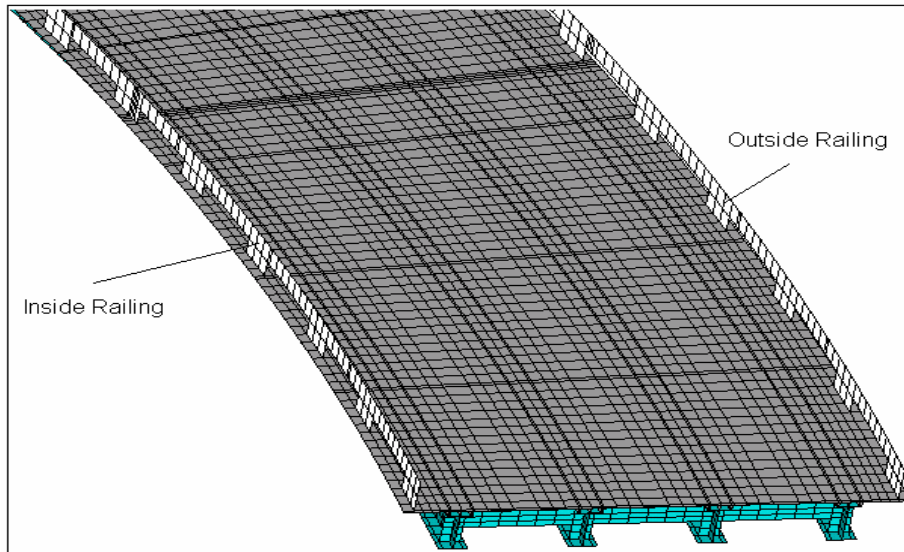


**Figure 12. Model of Deck with Parapets**

## **Modeling the Support Boundary Conditions**

The supports shown on the Wolf Creek Bridge plans indicate pinned supports at intermediate piers and rollers that permit tangential motion at the abutments. To eliminate large local distortion that can occur when single point supports are applied to plate element models, and to simultaneously provide support conditions that are more realistic from a physical standpoint, the supports on each girder were spread over three nodes in the radial direction, the node at the bottom of the flange, and one node to either side, corresponding to the edges of the idealized bearing plates. For modeling purposes, it was assumed that the abutments are sufficiently stiff, relative to the girder to be considered rigid, so the nodes located at the center of the abutment support were constrained against radial and vertical translation. Three consecutive nodes in the radial direction were supported, but only one nodal line in the tangential direction was constrained, since to constrain more than one nodal line against vertical translation would effectively fix the ends of the beam against rotation.

Two different models were used for the intermediate piers. In the first model, the assumption that the piers act as rigid support bases for the superstructure was introduced. This assumption is often made during the design phase, when the precise stiffness of the substructure is not known. For this *rigid pier model*, a line of three radial nodes centered on each of the girder flanges was simply constrained against translation in the radial, tangential, and vertical direction. Rotations are allowed, but the presence of three constrained nodes on a radial line effectively constrains rotation about the vertical and tangential directions. Thus, only radial rotation of these nodes remains feasible.

The second model incorporated the simplified BEAM4 pier model to approximate the pier flexibility described above. The two piers were generated in such a manner that the pier cap nodes' at the support points have the same  $x$ ,  $y$ , and  $z$  coordinates as the bottom flange elements on the girders above. The bottom of the pier model is fixed, which effectively introduces the

assumption of a rigid footing. The top nodes of the piers, which correspond with nodal locations on the girders, were joined together with the bottom flange nodes on the girders using the coinciding nodes feature in ANSYS. This method allows the piers and girders to act as a pinned boundary condition system, since the pier cap elements are now connected to the nodes on the girders. The bridge with adjoining piers is shown in Figure 13.

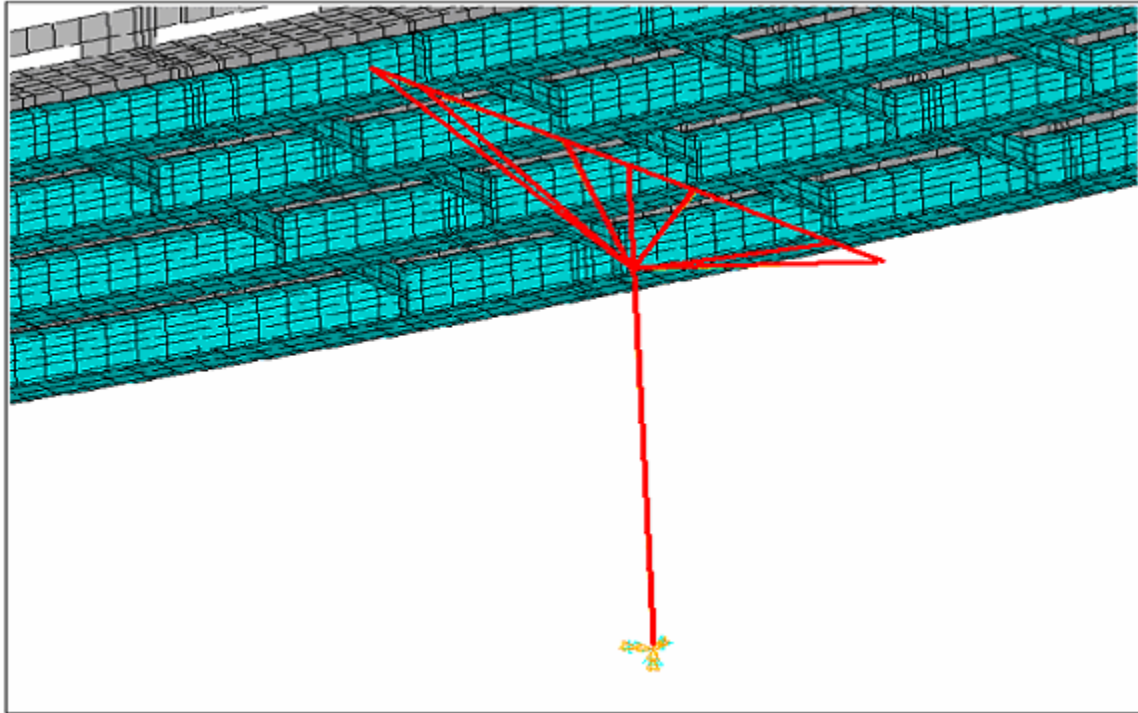


**Figure 13. Bridge With BEAM4 Pier Model**

To provide a basis for comparison, modal analyses were carried out for both the rigid pier and flexible pier models. Systematic shifts in natural frequencies and mode shape comparisons were carried out for both models. Additional modes occurring in one model but not the other were also examined. Additional forced vibration studies were also conducted as a precursor to planned field studies, but those will not be discussed further.

## **RESULTS**

### **Convergence Studies**

#### **Girder Convergence Studies**

The midspan deflection of the girder models obtained by varying the number of web elements in study 1 (4 elements per flange) and study 2 (6 elements per flange) are shown in Figure 14. It appears that a small change in the results occurs as the number of flange plates is increased from 4 to 6. However, the difference between all of the predicted displacements is only about 0.0065%, which is expected to be much smaller than errors introduced by other sources. The reason for the insensitivity of the model to the number of elements used are discussed shortly.

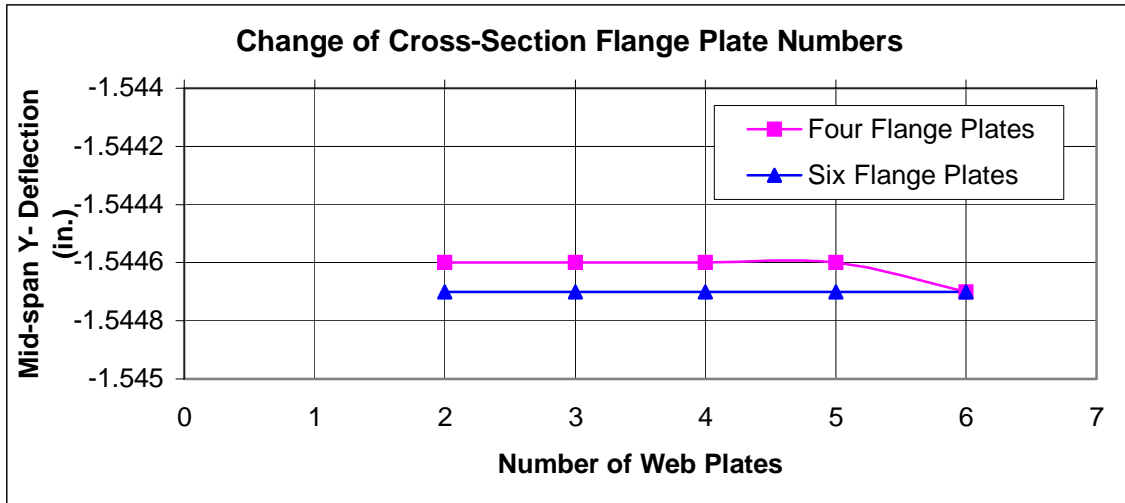


Figure 14. Changing the Number of Elements in Girder Cross Section

Figure 15 illustrates the results of girder convergence study 3, in which the number of elements along the length of the girder is varied. It is seen that the effect of varying the number of elements along the length of the girder is somewhat larger than that of varying the number of elements within the cross-section. Even so, most of the change in the results has occurred by the time the element lengths have been reduced to 12", and the difference between the midspan deflection predicted by 48 elements along the length and 576 elements along the length is less than 0.08%, still well within the error limits to be expected from the plate modeling approximation.

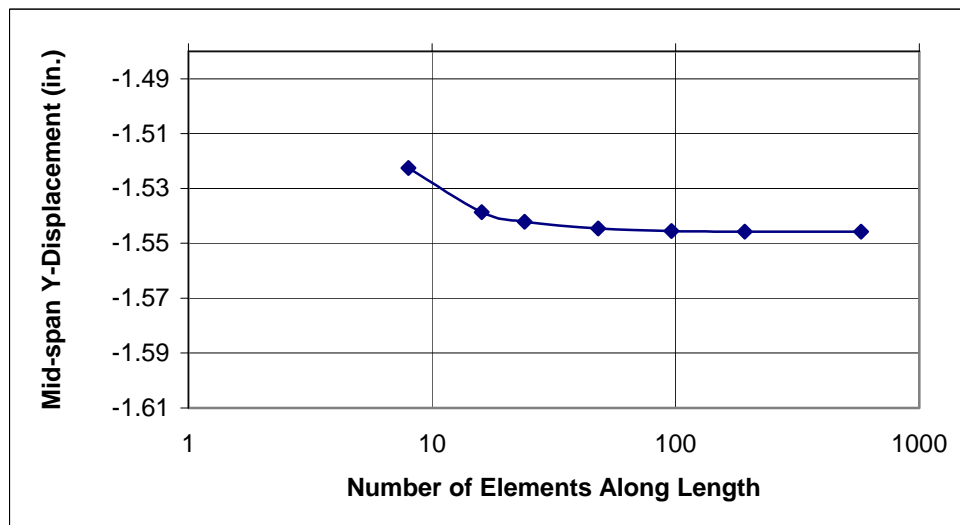


Figure 15. Changing Plate Length Along Girder

### Girder Plus Slab Convergence Studies

When the slab is added to the girder, the convergence properties of the girder/slab combination are somewhat different from that of the girders alone. The results of varying the number of web plates in Study 4 (4 flange plates) and Study 5 (8 flange plates) are shown in

Figure 16. The influence of doubling the number of flange plates is quite small, only leading to a shift of the two convergence curves by about 0.004%. Increasing the number of elements over the height of the web has a more significant although still small effect. Increasing the number of web elements from two to six leads to roughly a 0.04% increase in displacement. This change is still small, but is more significant than the change introduced by changing the number of flange elements.

Increasing the number of elements along the length of the girder/slab combination has a much more pronounced effect, as shown in Figure 17. Convergence is almost complete when 96 elements are taken along the length, but 48 elements still provides results that are within 0.18% of the final model with 576 elements along the length, and may also be considered an acceptable model.

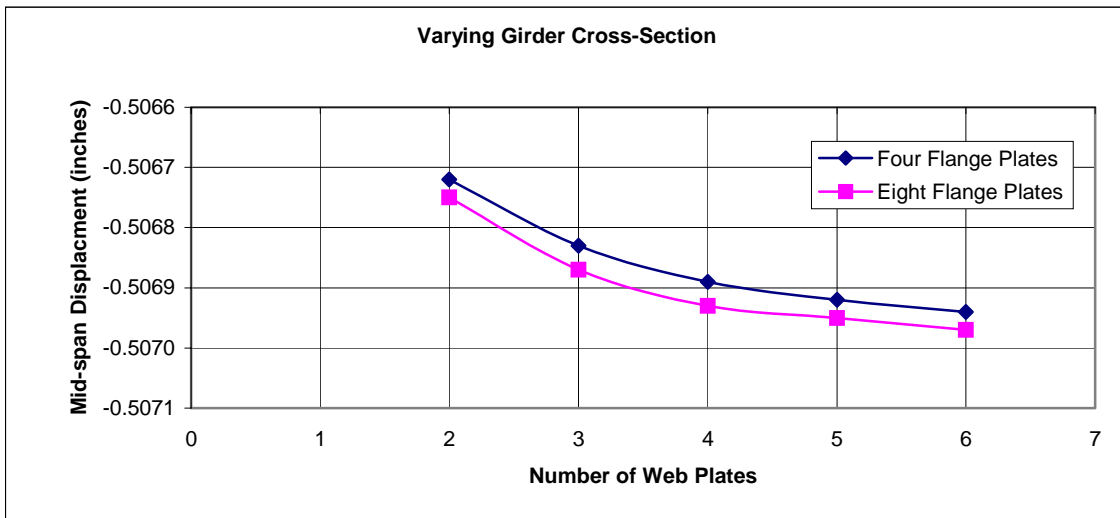


Figure 16. Changing Number of Plates in Girder Cross Section with Deck



Figure 17. Varying the Number of Elements Along Length

The final convergence study on the girder/slab combination examined the effect of increasing the number of slab elements across the width. The results of this study, which were conducted with 4 elements in each flange, 4 web elements, and 48 elements along the length, is shown in Figure 18. This result appears to be relatively insensitive to the number of elements, provided at least eight elements are used across the width of the slab.

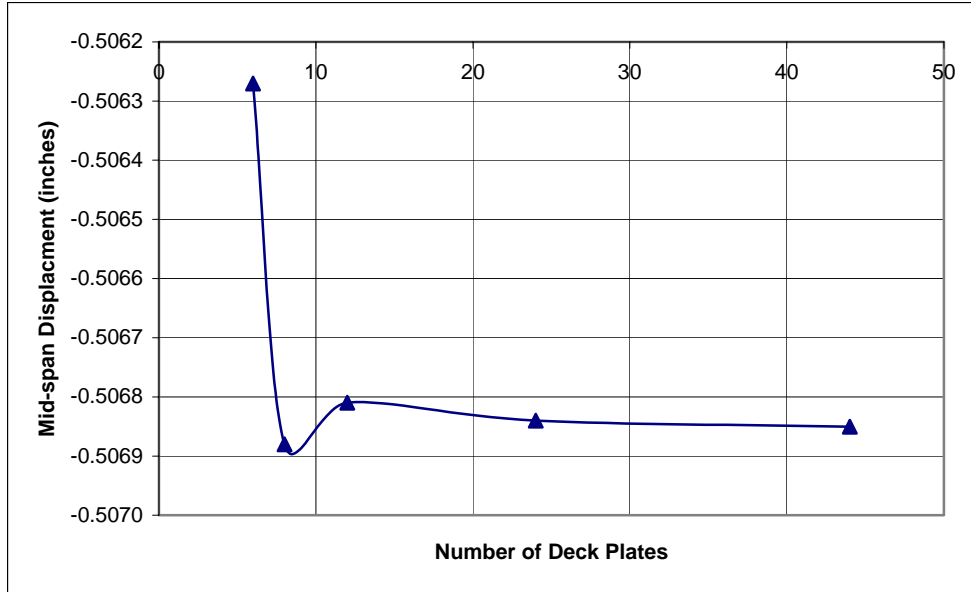


Figure 18. Varying Number of Deck Elements Across Width

### Diaphragm Member Convergence Studies

The diaphragm member studies provided interesting results that did not display the monotonic convergence properties observed in the girder and girder/slab models. Figure 19 shows the results of studies 8 and 9. Doubling the number of flange elements led to about a 0.36% increase in the displacements, which is not a very large change, but is significantly larger than the changes that had been observed in the previous models. Regardless of the number of flange elements, increasing the number of web elements had a more substantial effect. When the number of web elements was increased from one to two, a decrease in the measured mid-span deflection occurred. Subsequently, additional elements resulted in an increase in the deflections. Increasing the number of web elements from two to nine resulted in about a 2.5% increase in deflection, which is significant. This trend was almost identical regardless of the number of flange elements.

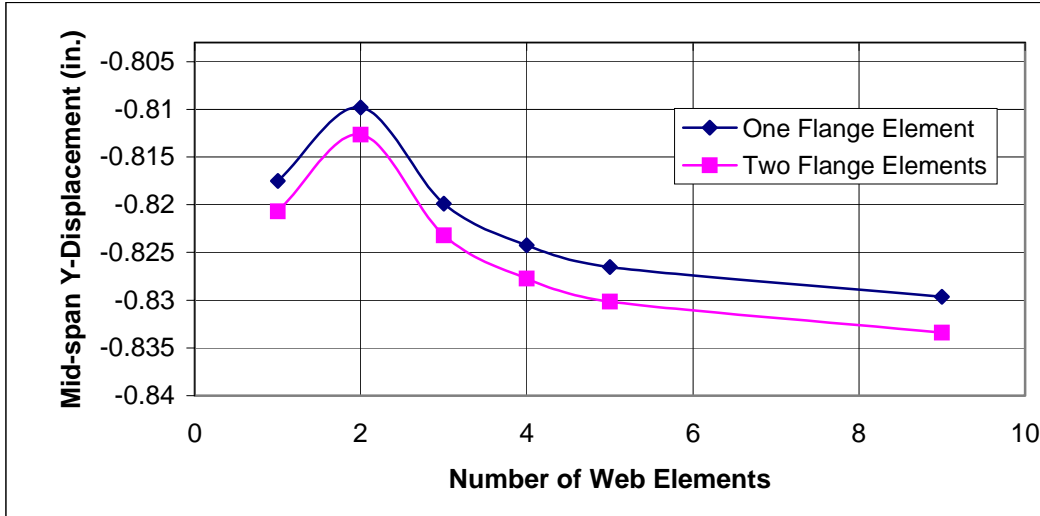


Figure 19. Changing Number of Elements in Diaphragm Cross-Section

The results of study 10 are shown in Figure 20. In this study the influence of increasing the number of elements along the span was considered in a model with 1 flange plate and 2 web plates. This study reveals the typical monotonic convergence. It is apparent that the minimal number of acceptable elements is at least eight (12" long elements), and if more precise data is to be obtained, the 44 element model appears to be about 4.8% more flexible. It should also be noted from Figure 20 that convergence is not quite complete, even with 44 elements along the beam.

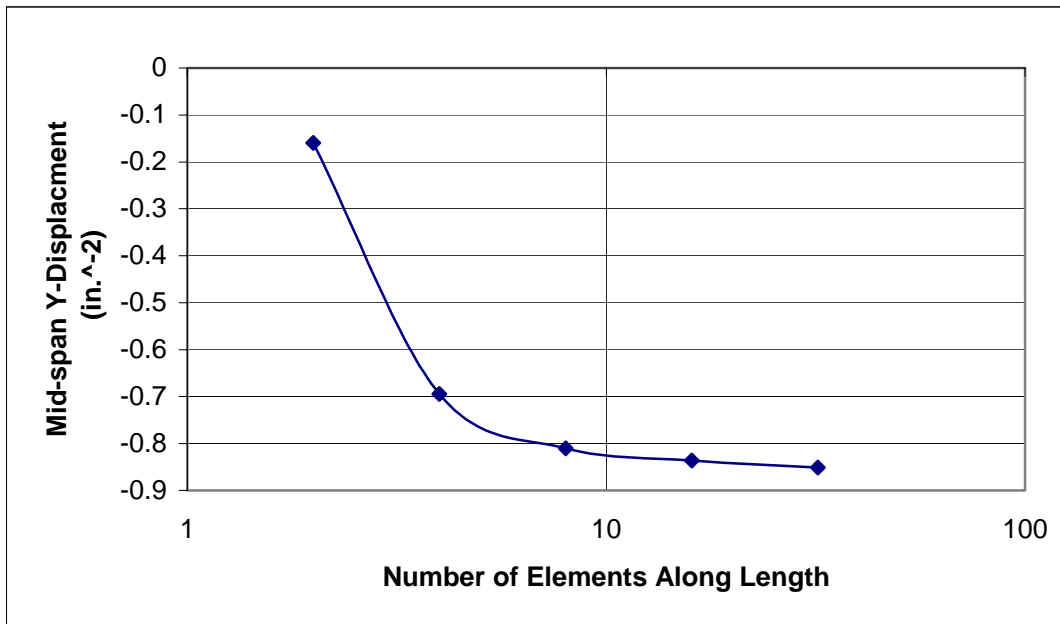


Figure 20. Changing Element Length Along the Diaphragm

## Pier Models

Since several different BEAM4 pier models were evaluated for inclusion in the final bridge model, only the results obtained from the final model are discussed here. Under the Test 1 loading, the displacements shown in Table 6 were obtained. The two most important displacement components under this loading are the  $x$  (transverse) and  $z$  (vertical) components. Error in the  $x$ -displacement, or lateral displacement, is limited to an average of 3.8 percent. The average error in the  $z$ -displacement, or vertical displacement, is slightly higher, at 11.5 percent. The  $y$  displacement components are negligible for this test.

When the Test 2 loading was applied, the displacements shown in Table 7 were obtained. This loading is also in the plane of the pier, so the  $y$  displacements are again negligible. The  $z$  displacement components are most important in this loading, which mimics the application of a uniform superstructure dead load on all four girder locations. Some  $x$  displacements also occur at the top pier level as a result of the bending rotation of the pier cap, but direct comparison of these quantities is probably not as important. Under this loading, the BEAM4 pier model is within 3.7% of the SOLID95 model, and again is slightly more flexible.

**Table 6. Test One, 100 kip Load in the X-Direction (results in inches)**

SOLID ELEMENT MODEL				BEAM MODEL			
<u>NOD</u> <u>E</u>	<u>DX</u>	<u>DY</u>	<u>DZ</u>	<u>NOD</u> <u>E</u>	<u>DX</u>	<u>DY</u>	<u>DZ</u>
29	<b>0.37959</b>	-5.05E-03	<b>0.3117</b>	28	<b>0.37316</b>	0	<b>0.3365</b>
42	<b>0.36088</b>	-1.49E-04	<b>0.2413</b>	30	<b>0.37259</b>	0	<b>0.27003</b>
63	<b>0.35146</b>	-1.27E-04	<b>7.63E-02</b>	33	<b>0.36754</b>	0	<b>8.73E-01</b>
66	<b>0.34684</b>	-1.04E-04	<b>-7.99E-02</b>	37	<b>0.36352</b>	0	<b>-9.42E-01</b>
69	<b>0.34428</b>	-8.34E-05	<b>-0.23883</b>	40	<b>0.3606</b>	0	<b>-0.27777</b>
40	<b>0.34429</b>	-7.62E-05	<b>-0.29573</b>	42	<b>0.36069</b>	0	<b>-0.34369</b>

**Table 7. Test Two, Four 100 kip Loads in the Z-Direction (results in inches)**

SOLID ELEMENT MODEL				<i>BEAM MODEL</i>			
<u>NODE</u>	<u>DX</u>	<u>DY</u>	<u>DZ</u>	<u>NODE</u>	<u>DX</u>	<u>DY</u>	<u>DZ</u>
29	-1.29E-02	2.53E-05	<b>-5.23E-02</b>	28	-1.08E-02	0	<b>-5.25E-02</b>
42	-1.31E-02	1.84E-04	<b>-4.78E-02</b>	30	-9.93E-03	0	<b>-4.49E-02</b>
63	-6.53E-03	-1.08E-04	<b>-2.30E-02</b>	33	-4.88E-03	0	<b>-2.39E-02</b>
66	5.21E-03	1.73E-04	<b>-2.26E-02</b>	37	8.55E-03	0	<b>-2.35E-02</b>
69	1.12E-02	4.91E-05	<b>-4.68E-02</b>	40	1.35E-02	0	<b>-4.57E-02</b>
40	1.12E-02	6.22E-05	<b>-5.21E-02</b>	42	1.40E-02	0	<b>-5.51E-02</b>

The displacements under the Test 3 loading are given in Table 8. This loading should cause a combination of displacement perpendicular to the plane of the pier, and twisting of the pier column. The  $y$  displacement component is dominant under this loading. Referring to Table 8, it is seen that the BEAM4 model produces slightly smaller displacements than the SOLID95

model under this loading, indicating that the out of plane stiffness of the BEAM4 model is slightly higher. However, the average error is roughly 0.34% in this case, which is insignificant, given the approximations inherent in both models.

The displacements of the two models under the Test four loading are given in Table 9. This loading produces non-negligible displacements in all three directions, with the largest displacements in the y direction. The x and y displacements in the beam model compared very favorably with the finite model, with errors of 3.5 and 6.0 percent respectively. The z displacement error is somewhat larger, with an average error of 11.74 percent between the BEAM4 and SOLID95 models. The BEAM4 model appears to be slightly stiffer in x and y directions, and somewhat more flexible in the z direction.

**Table 8. Test Three, Positive 200 kip Y-Direction (results in inches)**

**SOLID95 MODEL**

<u>NODE</u>	<u>DX</u>	<u>DY</u>	<u>DZ</u>
29	-1.78E-03	<b>9.80E-01</b>	-5.61E-03
42	-1.77E-03	<b>9.37E-01</b>	-4.68E-03
63	-1.05E-03	<b>8.21E-01</b>	-2.12E-03
66	-3.51E-04	<b>6.61E-01</b>	-2.00E-03
69	7.24E-05	<b>5.41E-01</b>	-3.54E-03
40	8.13E-05	<b>5.00E-01</b>	-4.20E-03

**BEAM4 MODEL**

<u>NODE</u>	<u>DX</u>	<u>DY</u>	<u>DZ</u>
28	5.97E-04	<b>9.64E-01</b>	-7.55E-03
30	7.59E-04	<b>9.22E-01</b>	-6.58E-03
33	1.87E-03	<b>8.12E-01</b>	-3.49E-03
37	3.81E-03	<b>6.54E-01</b>	-4.96E-03
40	4.73E-03	<b>5.32E-01</b>	-1.09E-02
42	4.83E-03	<b>4.92E-01</b>	-1.31E-02

**Table 9. Test Four, X and Y Direction Combined Loading (results in inches)**

**SOLID95 MODEL**

<u>NODE</u>	<u>DX</u>	<u>DY</u>	<u>DZ</u>
29	<b>1.89E-01</b>	<b>7.61E-01</b>	<b>1.53E-01</b>
42	<b>1.80E-01</b>	<b>6.19E-01</b>	<b>1.18E-01</b>
63	<b>1.75E-01</b>	<b>2.08E-01</b>	<b>3.71E-02</b>
66	<b>1.73E-01</b>	<b>-1.85E-01</b>	<b>-4.08E-02</b>
69	<b>1.72E-01</b>	<b>-5.91E-01</b>	<b>-1.21E-01</b>
40	<b>1.72E-01</b>	<b>-7.34E-01</b>	<b>-1.50E-01</b>

**BEAM4 MODEL**

<u>NODE</u>	<u>DX</u>	<u>DY</u>	<u>DZ</u>
28	<b>1.86E-01</b>	<b>7.15E-01</b>	<b>1.63E-01</b>
30	<b>1.85E-01</b>	<b>5.80E-01</b>	<b>1.31E-01</b>
33	<b>1.83E-01</b>	<b>2.04E-01</b>	<b>4.16E-02</b>
37	<b>1.82E-01</b>	<b>-1.78E-01</b>	<b>-4.92E-02</b>
40	<b>1.81E-01</b>	<b>-5.44E-01</b>	<b>-1.43E-01</b>
42	<b>1.81E-01</b>	<b>-6.78E-01</b>	<b>-1.77E-01</b>

As a final test, the natural frequencies and mode shapes of the SOLID95 and BEAM4 models are compared in Table 10. The BEAM4 model did not perform particularly well in this test, producing frequencies that are significantly lower than the corresponding SOLID95 modes. However, the two models do produce the same ordering of the three modes.

**Table 10. Pier Modal Analysis Comparison**

<b>Mode Shape</b>	<b>SOLID95 Model</b>	<b>BEAM4 Model</b>
Transverse bending in plane of pier	7.876 Hz	5.058 Hz
Bending out of plane of pier	8.503 Hz	5.720 Hz
Pier cap Twist with Column Torsion	13.445 Hz	8.557 Hz

## Wolf Creek Bridge Models

The vibration mode shapes of multi-girder bridges may be considered to consist of several ideal types, as shown in Figure 21, with reference to a non-curved bridge. Vertical bending modes, shown in Figure 21(a) represent simple “beam-like” bending of the entire bridge in the vertical plane. Lateral bending, which is a much less commonly observed mode, is the horizontal bending mode of the entire bridge, again acting as a beam. Lateral bending modes are not particularly important for straight bridges, except possibly under wind load. However, lateral bending will be potentially important for curved bridges, since not only can bending be accompanied by lateral motion, but vehicular traffic generates lateral forces as they traverse the curved surface. The torsional mode shown in Figure 21(c) represents somewhat similar motion of individual girders to those observed in the vertical bending modes, except bending is accompanied by twisting, and one side of the bridge translates downward, while the other translates upward. Typically, the vertical bending modes and torsional modes in straight bridges are located relatively close to each other, with the torsional modes having slightly higher frequencies. Finally the transverse bending mode shown in Figure 21(d) represents a mode similar to what might be found in an orthotropic plate, and combines slab and diaphragm bending with girder bending *across* the bridge.

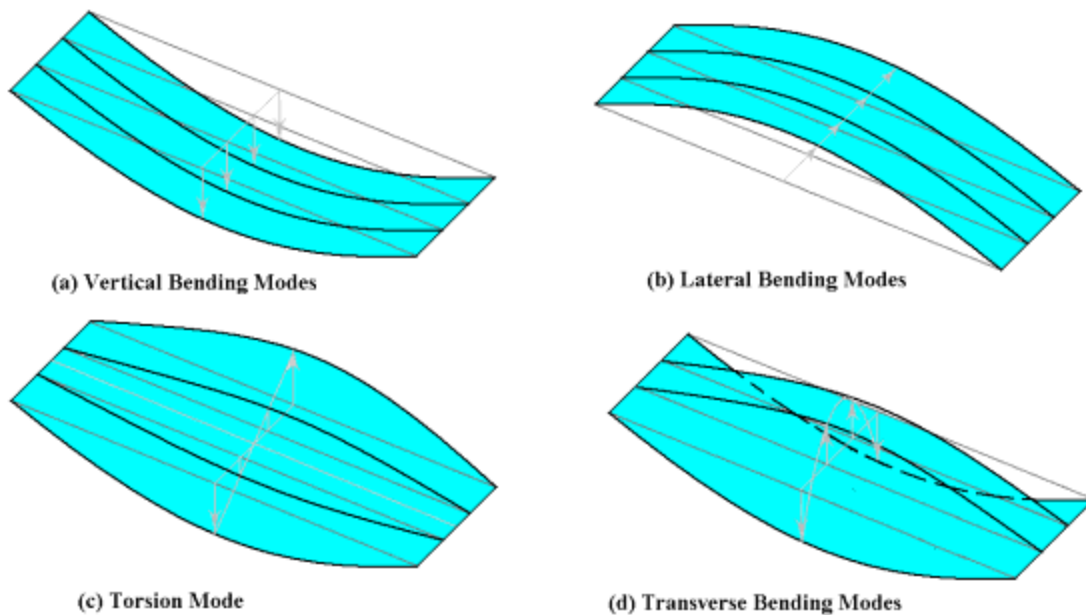


Figure 21. Idealized Vibration Mode Types

Multi-girder curved bridges, such as the Wolf Creek Bridge, behave in a somewhat more complicated manner. Vertical bending and torsion do not decouple, so most modes that show predominant vertical bending also show a certain amount of torsion, which is reflected in the fact that either the outer edge of the bridge undergoes larger displacements than the inner edge of the bridge, or the reverse occurs. In addition, several modes may be expected to show dominant torsion. In the following discussion, modes that do not show significant reversal of curvature across the bridge will be denoted as vertical bending modes, while modes that do reverse curvature across the bridge will be denoted as torsional modes. Finally, some modes in a

multispan bridge may show combinations of one mode type in one or more spans with another mode type in adjacent spans.

Using the block Lanczos method included in ANSYS, twenty modes were extracted for both the rigid pier and the flexible pier models. The natural frequencies obtained for the rigid pier model are given in Table 11 and are discussed in further detail shortly. The corresponding natural frequencies obtained for the flexible pier model are shown in Table 12.

**Table 11. Rigid Pier Model Natural Frequencies**

Mode	Frequency(Hz)	Mode Shape Summary
1	5.8715	First vertical bending, outside edge, span B dominant
2	7.407	First torsion, span B dominant
3	7.787	Vertical bending, outside edge, spans A and C antisymmetrical
4	8.9055	Vertical bending, outside edge, spans A and C symmetrical
5	10.359	First torsion, spans A and C dominant, Antisymmetrical
6	10.603	First torsion, spans A and C dominant, Symmetrical
7	14.221	Transverse bending, span B dominant
8	14.45	Lateral bending of deck, severe girder distortion over piers
9	15.295	Second Vertical bending, span B, outer edge dominant
10	16.294	Transverse bending, span A dominant
11	16.32	Transverse bending, span C dominant
12	17.111	Second lateral bending of deck; rotation about vertical axis through center span, significant girder distortion
13	18.965	Second torsion; Span B, some rotation about vertical axis, distortion
14	21.192	Third lateral bending of deck, severe girder distortion
15	22.893	Second transverse bending, Span B, reversal of curvature in longitudinal direction
16	24.057	Second vertical bending, outside edges spans A and C; antisymmetrical
17	24.351	Second vertical bending, outside edges spans A and C; symmetrical
18	27.051	Second torsion, spans A and C, antisymmetrical
19	27.259	Second Bending and Torsion, Spans A,B,C, outside edge dominant, sym.
20	28.246	Second Transverse bending, Span B, reversal of curvature in transverse direction

Upon comparing the two tables, it is immediately obvious that the natural frequencies computed using the flexible pier model are somewhat lower than those predicted by the rigid pier model. This result was expected because any softening of the boundary conditions of an otherwise identical FE model would be expected to lead to lower natural frequencies. A number of the mode shapes reveal interesting changes in shapes as well, reflecting the ways in which the flexible piers participate with the superstructure in the vibration. In order to investigate the systematic way in which modeling the piers has modified the response, it is useful to compare the mode shapes obtained from the two models on a mode by mode basis.

### **First Tangential (Longitudinal) Translation Mode**

The lowest natural frequency computed by the flexible pier model does not have a counterpart in the rigid pier model. The presence of fixed bearings at the piers, together with expansion bearings at the two abutments permits a motion of the entire superstructure as almost a rigid body rotation about the center of curvature. This mode shape is illustrated in Figures 22 and

**Table 12. Flexible Pier Model Natural Frequencies**

Mode	Frequency (Hz)	Mode Shape Summary
1	2.2815	Longitudinal translation (rotation about center of curvature)
2	3.6193	First Lateral bending of deck, with bending and pier motion
3	4.654	First vertical bending outer edge, span B dominant (A,C)
4	6.2713	First vertical bending inner edge, span B dominant
5	7.3379	First vertical bending, outer edge, spans A,C anti-symmetrical
6	8.23	First vertical bending, outer edge, spans A,C, symmetrical
7	8.8165	First anti-symmetrical torsion, spans A,C
8	9.6415	First symmetrical torsion, spans A,C
9	10.797	Second lateral bending plus anti-symmetrical torsion
10	13.478	Second vertical bending, outer edge, span B dominant
11	13.64	First transverse bending, span B
12	15.251	Second vertical bending inner edge, span B, transverse bending, spans A and C
13	15.79	First transverse bending, spans A and C, symmetrical
14	16.033	First transverse bending spans A and C, anti-symmetrical
15	17.979	General torsion of bridge, A,B,C, symmetrical
16	19.665	Third lateral bending, symmetrical Girder distortion at abutments
17	20.312	Second vertical bending outer edges, A,B,C, some torsion, anti-symmetrical
18	21.251	Second transverse bending, span B, longitudinal reversal of curvature, Antisym
19	22.83	Second vertical bending, spans A, C, significant pier participation, symm.
20	23.756	Fourth lateral bending, Antisymmetrical, Girder distortion at piers and abutment

23. Referring to Figure 22, it appears that a small amount of vertical bending occurs in the three spans of the bridge, but the oblique view indicates that this motion is not large. By comparison, the oblique view of the first mode indicates significant deformation of the pier columns. This is more easily seen from Figure 23(a) which indicates a significant rigid body rotation of the entire deck about the center of curvature, accompanied by pier motion. The participation of this mode of vibration could be significant for bridges subjected to vehicles undergoing braking, and the behavior can only be predicted by the flexible pier model, since the fixed bearings in the rigid pier model effectively preclude this motion.

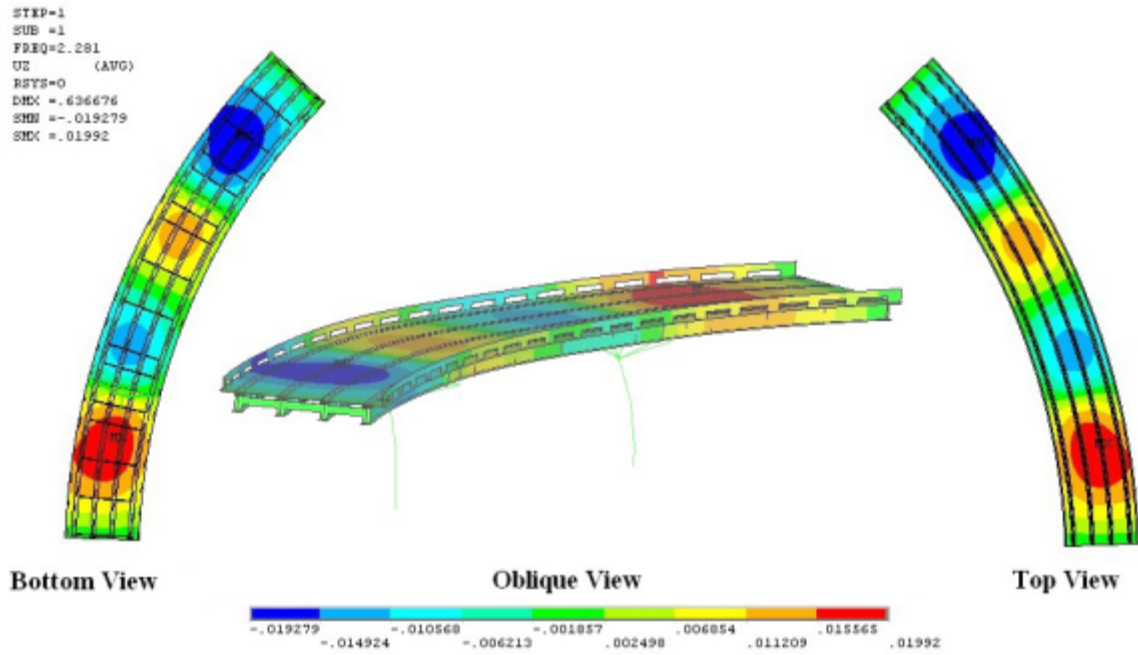


Figure 22. Flexible Pier Model – Longitudinal first mode with z displacement contours

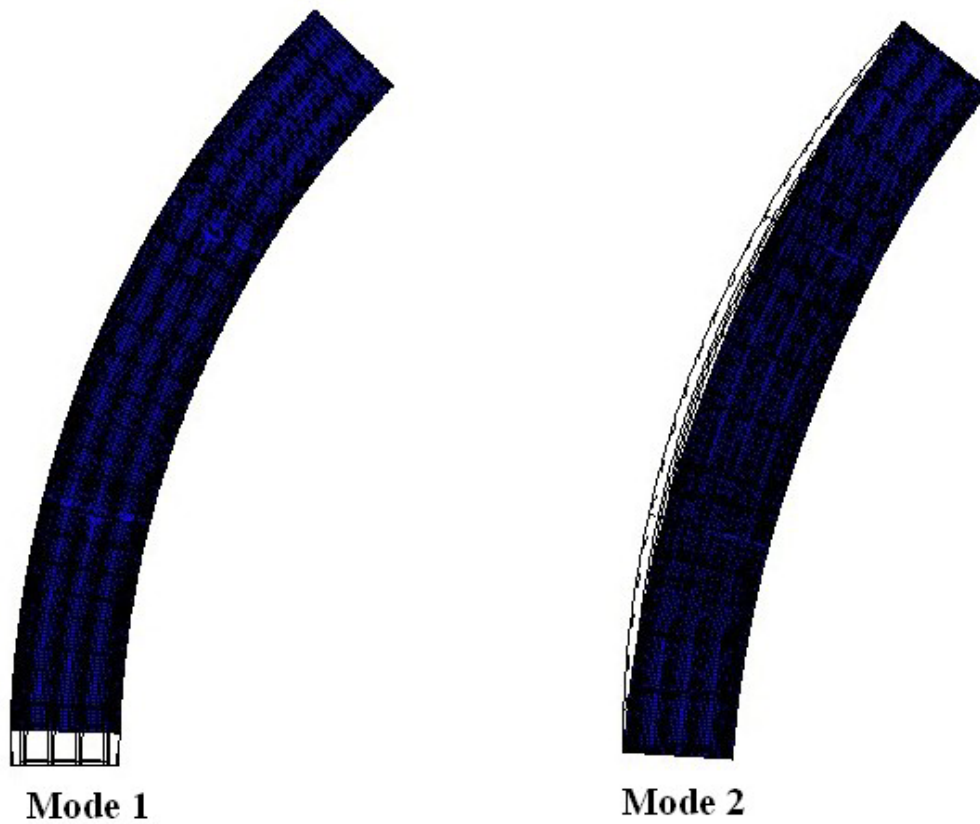


Figure 23. First Two modes of the flexible pier bridge - deformed shapes

## First Lateral Deck Bending Mode

Both the flexible pier model and the rigid pier model predict the existence of several lateral deck bending modes, but the frequencies and detailed deformation of these modes differ significantly. Figure 24 shows the first lateral deck bending mode for the flexible pier model, which is mode 2 in Table 12 with a frequency of 3.619 Hz while Figure 25 shows the first lateral deck bending mode for the rigid pier model, which is mode 8 in Table 11 with a frequency of 14.45 Hz.

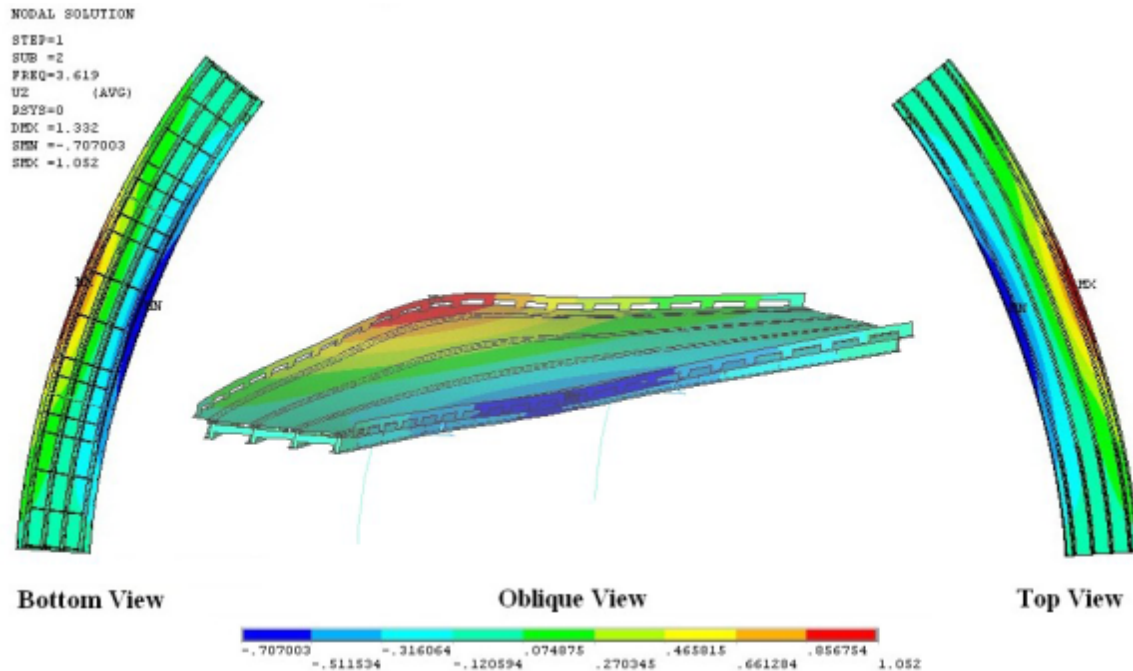


Figure 24. Flexible Pier Model - First Lateral Bending Mode (3.619 Hz)

In Figure 24, it is seen that some Span B torsion occurs along with the lateral bending. This is not surprising, since the driving mass is located at the deck level, which would not be the shear center of this non-symmetric section. Moreover, lateral pier motion is accompanied by rotation of the pier cap, which further exacerbates this motion. By comparison, Figure 25 shows insignificant torsion of any span accompanying lateral displacement, but the bottom view does reveal significant distortion of the girder webs at the pier locations, a phenomenon that would probably not be predicted had a beam element been used to model the girders. The presence of the partial depth diaphragms does not eliminate this mode of vibration, but does mean that, in the absence of pier bending, significant girder distortion is necessary in order for the predicted lateral bending of the deck to occur.

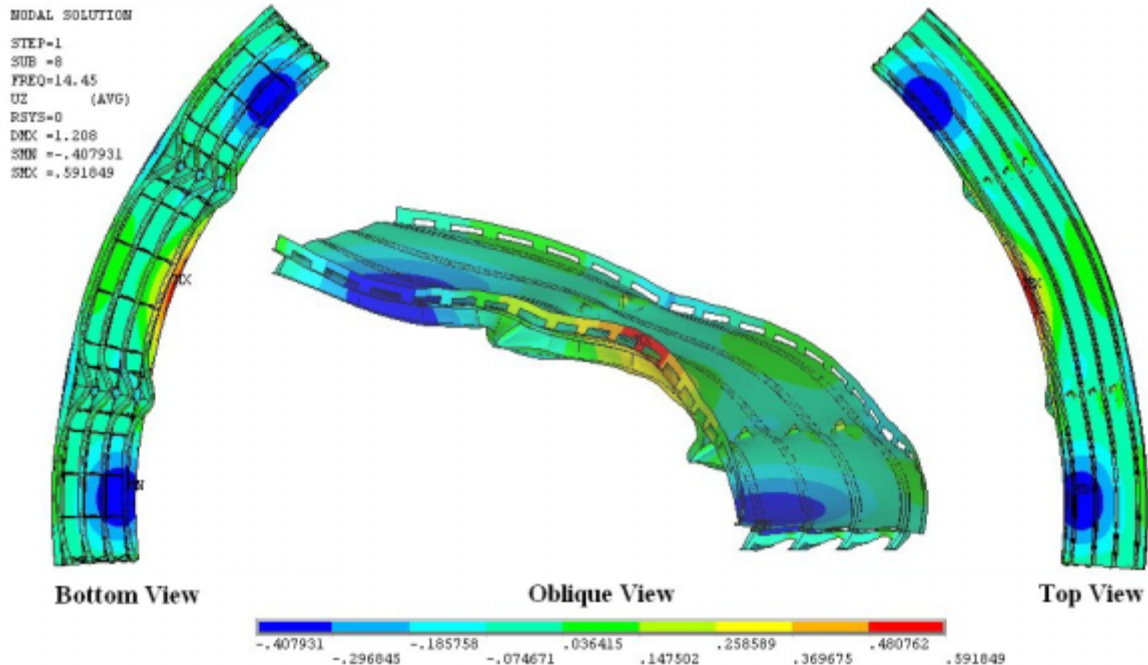


Figure 25. Rigid Pier Model - First Lateral Bending Mode

### First Vertical Bending Mode – Span B, Outer Edge Dominant

An interesting feature of both the rigid pier and flexible pier models is a tendency for the inner edge and outer edge motion to be dominant in different modes, and for span B to show significant motion when spans A and C are relatively inactive, or vice versa. The first mode of the rigid pier model (5.872 Hz) and the third mode of the flexible pier model (4.654 Hz) shown in Figures 26 and 27 respectively, reflect dominant bending motion of the outer edge of span B, with relatively small motion of the side spans, or the inner edge. These modes appear relatively similar to each other, except that some vertical translation of the deck occurs at the pier location in the flexible pier model, and the flexible pier model predicts somewhat larger side span displacements. Obviously, the rigid pier model overestimates the natural frequency by about 26%, relative to the flexible pier model. Both models predict that very little motion occurs on the inner edge of the bridge, a strong indicator that twisting is accompanying bending.

### First Torsion Mode – Span B, Inner Edge Dominant

The fourth mode of the flexible pier model (6.271 Hz) can be interpreted as the first torsion mode of the center span. In this case the inner edge, not the outer edge undergoes the dominant motion, but because the outer edge undergoes significant motion out of phase with the inner edge, this mode is interpreted as torsion and not inner edge bending. The rigid pier model predicts this mode as mode 2 (7.407 Hz) which is about 18% higher. These predicted modes are shown in Figure 28 and 29. It is seen from this figure that the rigid pier model predicts larger relative motion on the outer edge of the bridge than the flexible pier model.

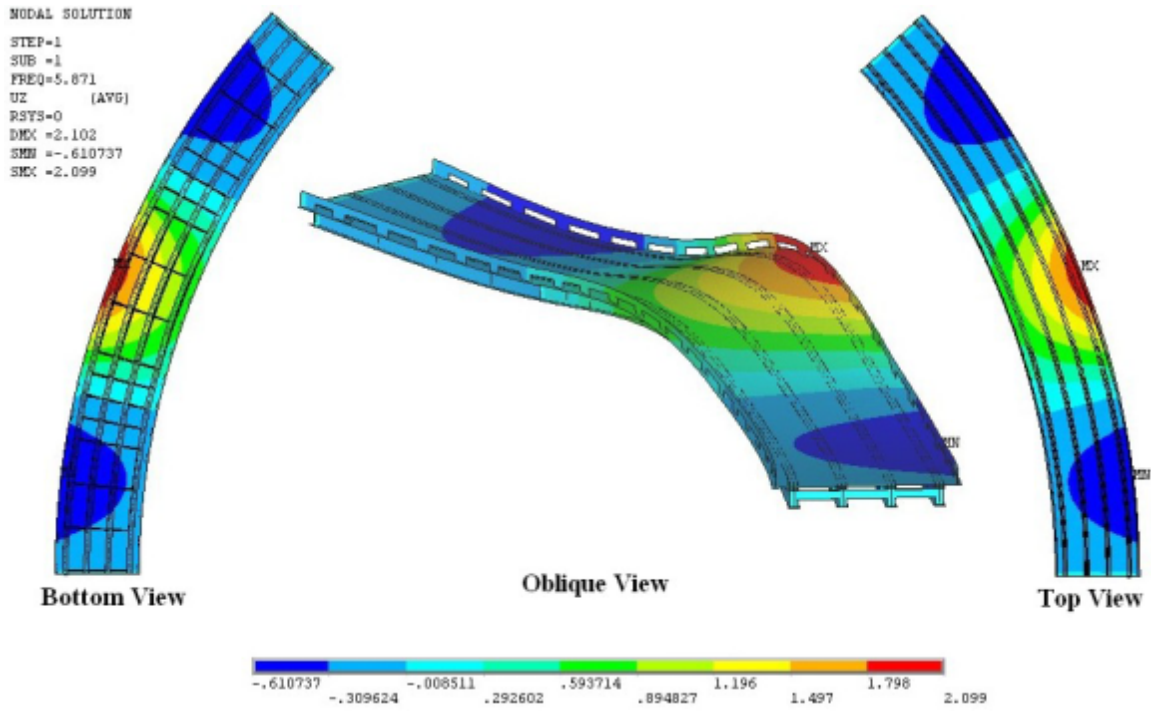


Figure 26. Rigid Pier Model - First Vertical Bending Mode, Outer Edge Dominant

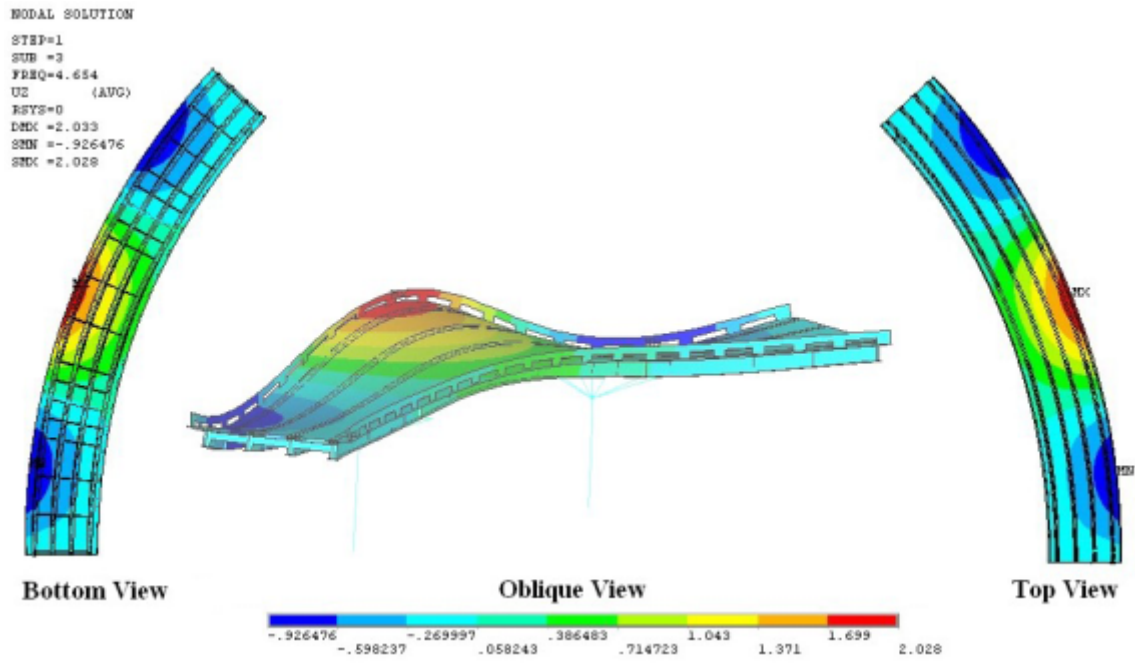


Figure 27. Flexible Pier Model - First Vertical Bending Mode, Outer Edge Dominant

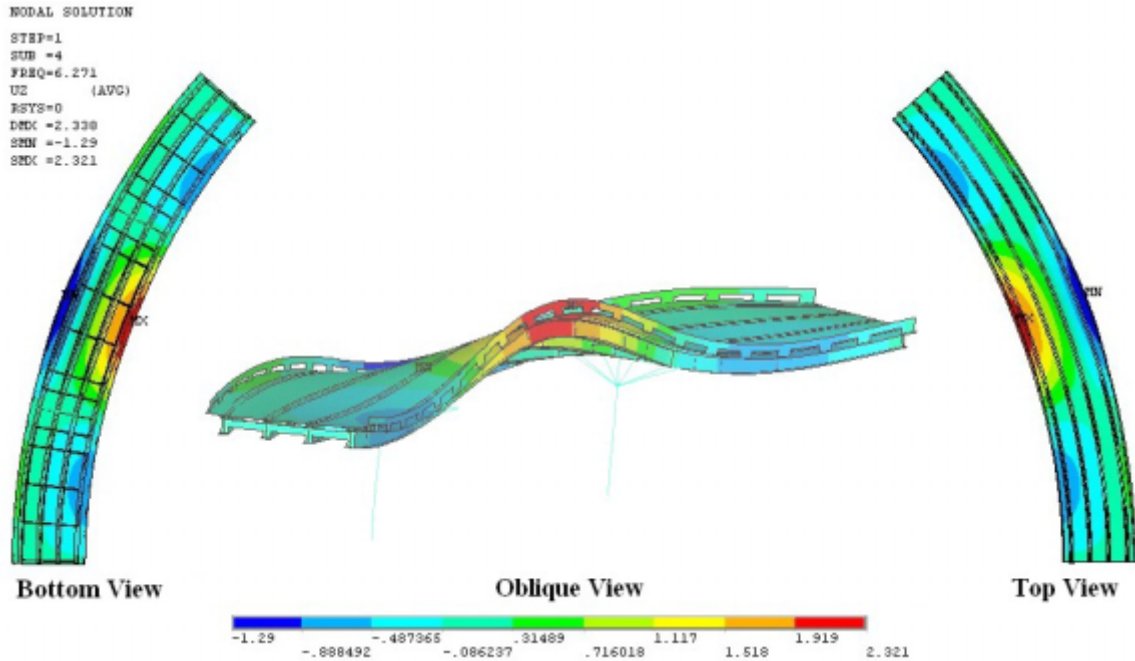


Figure 28. Flexible Pier Model -First Torsion Mode, Span B Dominant

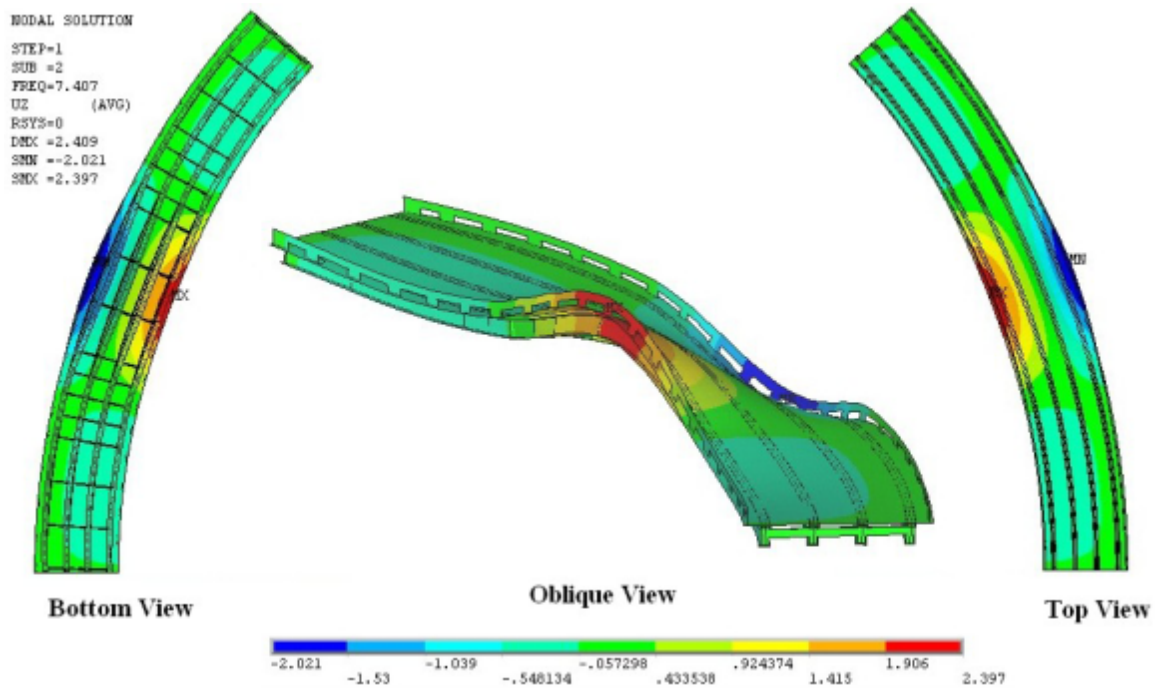


Figure 29. Rigid Pier Model - First Torsion Mode, Span B Dominant

### First Bending Mode – Outer Edges of End Spans (Antisymmetrical)

Mode 3 of the rigid pier model (7.787 Hz) and mode 5 of the flexible pier model (7.338 Hz) reflect bending of the end spans with outer edge motion dominant, and the two end spans moving out of phase. These modes are shown in Figures 30 and 31, respectively. The agreement between these natural frequencies is relatively good, with the rigid pier model prediction being

only about 6% higher than the flexible pier model. This suggests that pier participation is not very important in this mode. The rigid pier model does show somewhat larger bending motion on the inner edge than is seen in the flexible pier model, suggesting that a little pier rotation may be occurring in this mode as well.

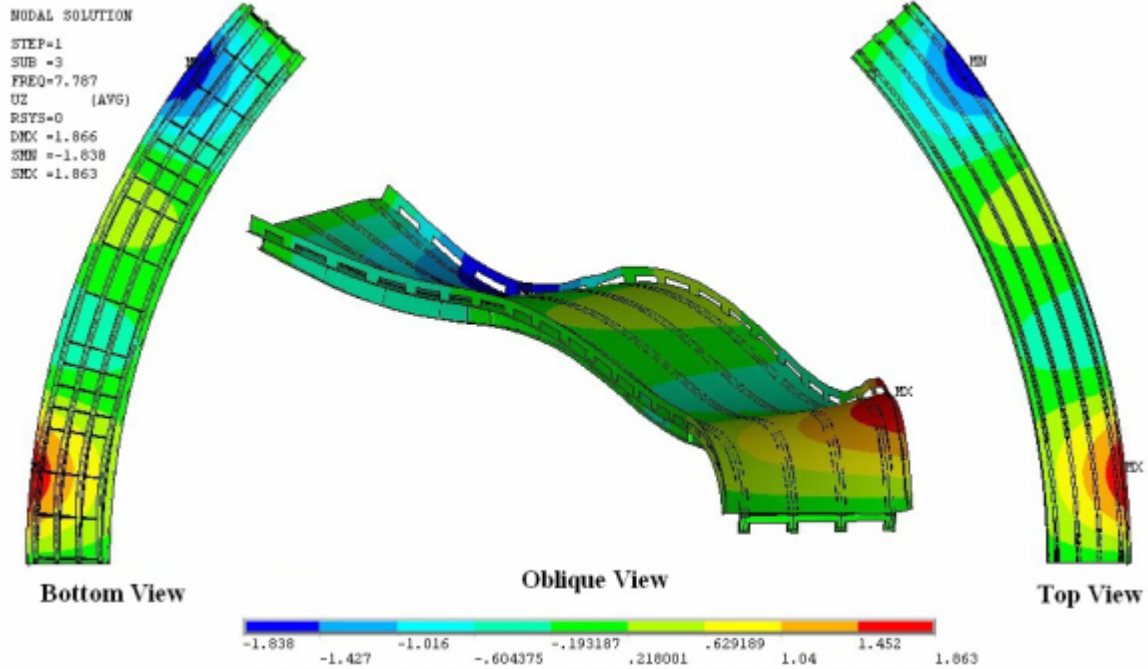


Figure 30. Rigid Pier model – End Spans Outer Edge Bending Mode One, Antisymmetrical

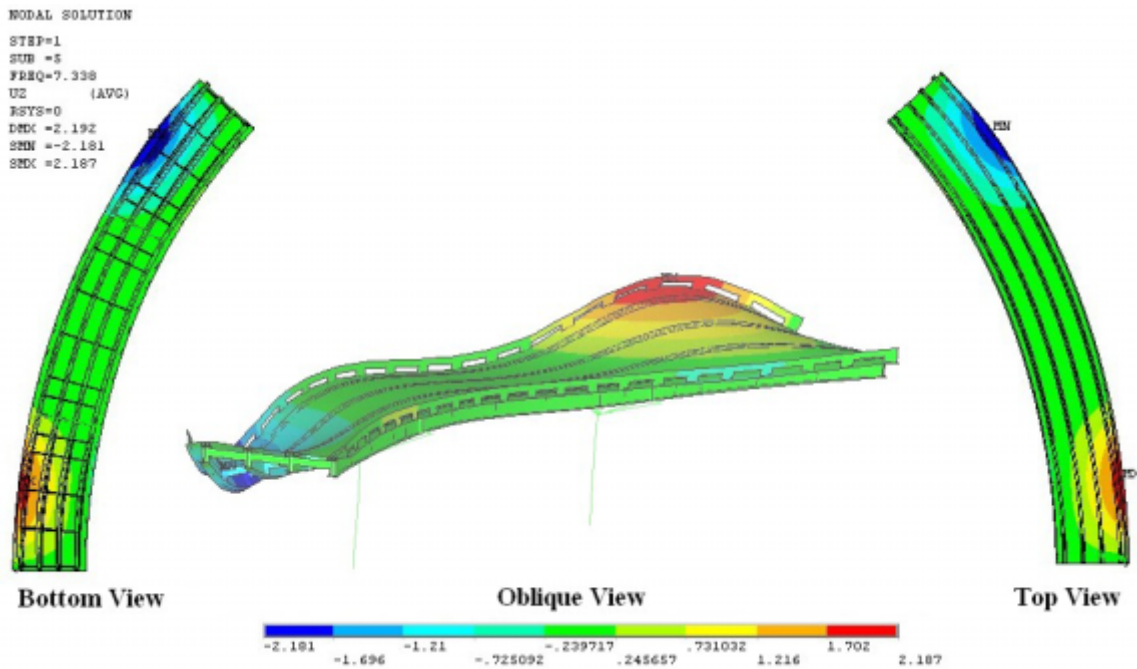


Figure 31. Flexible Pier Model – End Spans Outer Edge Bending Mode One, Antisymmetrical

### First Bending Mode – Outer Edges of End Spans (Symmetrical)

Mode 4 of the rigid pier model (8.906 Hz) and mode 6 of the flexible pier model (8.23 Hz) are also dominated by vertical bending of the outer edges of the end spans. In this case, however, the two end spans are in phase with each other. The fact that the in phase frequencies are higher than the out of phase frequencies indicates that the center span provides more stiffness for the symmetrical than for the antisymmetrical mode. These modes are also in relatively reasonable agreement with each other, with the rigid pier model being about 8% high. The mode shapes predicted for these two modes are shown in Figures 32 and 33 respectively. The similarity of these mode shapes indicates that the pier flexibility is not of great importance. Examining these figures, it is seen that the center span tends to participate more in this mode than in the anti-symmetric mode discussed above and is in phase with the motion of the end spans. This contributes a boundary condition that is nearly fixed for the end spans, and provides some indication as to why the frequencies of the predicted symmetrical modes are higher.

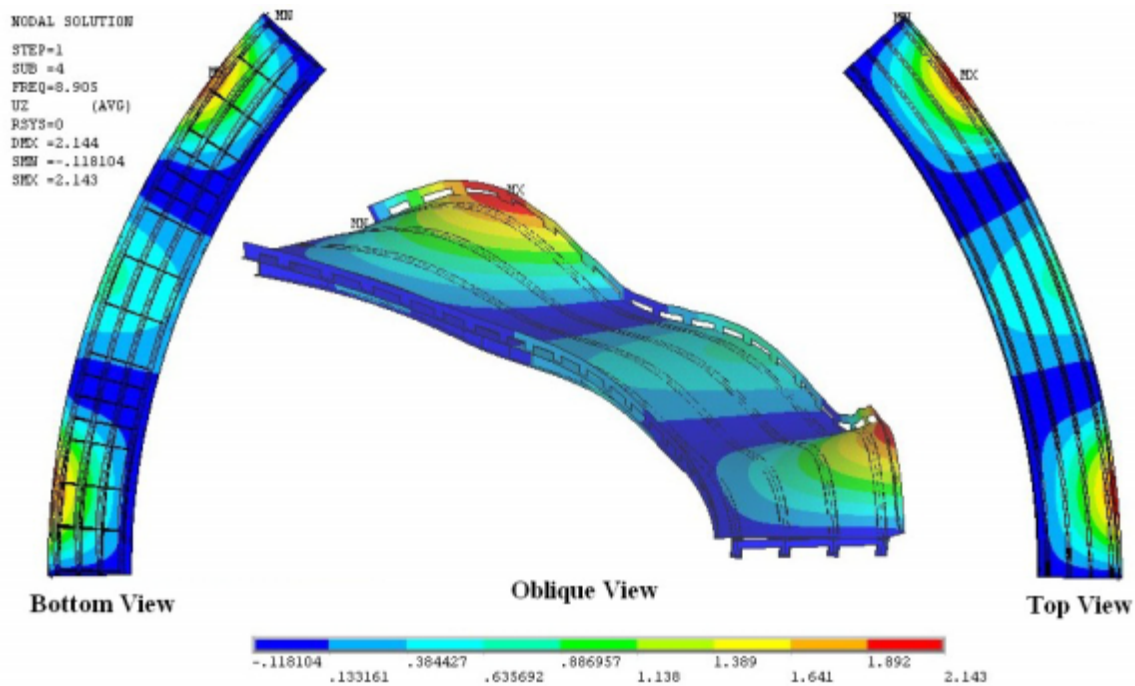


Figure 32. Rigid Pier Model – First End Span Symmetrical Bending Mode

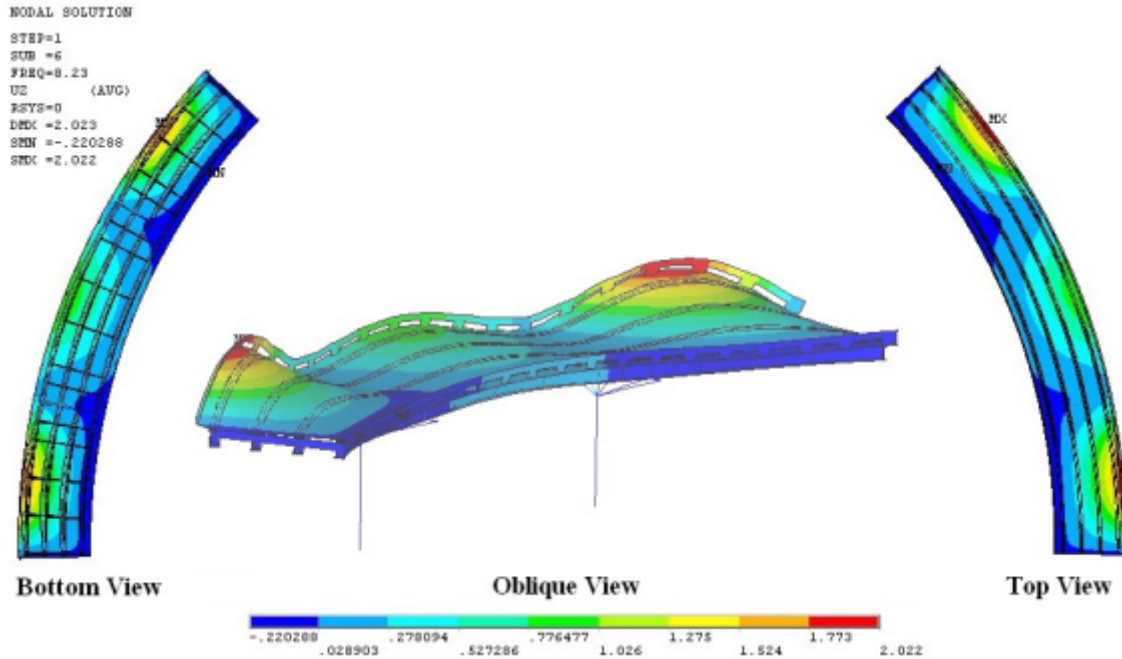


Figure 33. Flexible Pier Model – First End Span Symmetrical Bending Mode

### First End Span Antisymmetrical Torsion

As indicated in the earlier discussion, torsional modes typically occur in relatively close proximity to bending modes, but with slightly higher frequencies. The first end span torsional mode of the rigid pier model is mode 5, at 10.359 Hz, and the corresponding mode of the flexible pier model is mode 7 at 8.817 Hz.

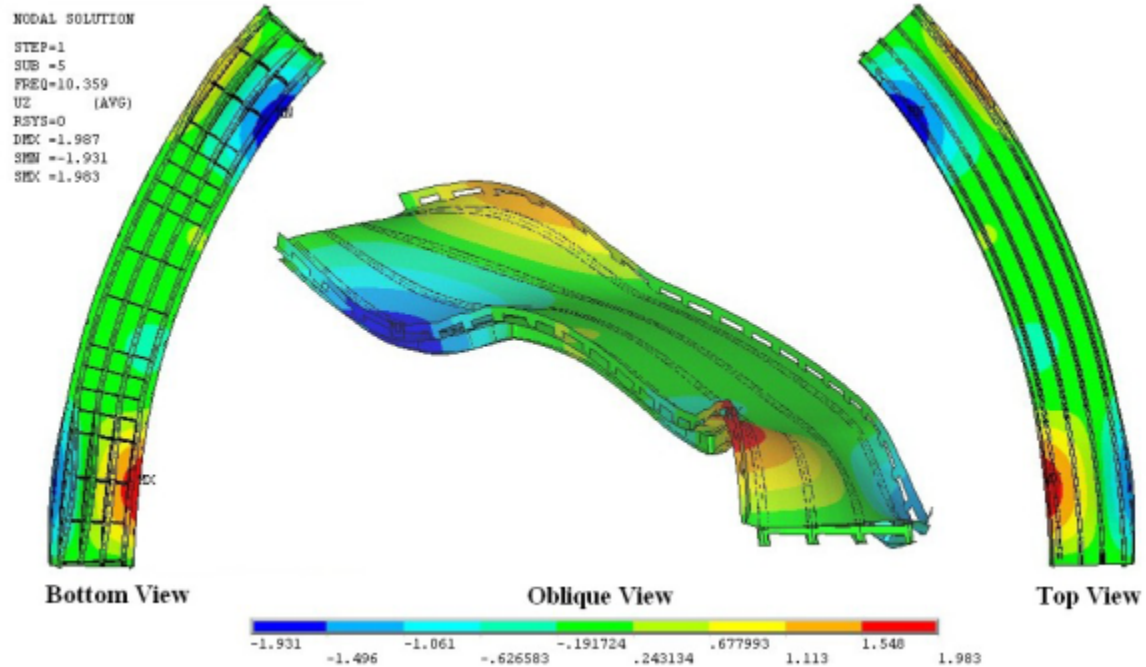


Figure 34. Rigid Pier Model, First End Span Antisymmetrical Torsion Mode

Pier participation is more important in this mode, as indicated by the 17% higher frequency predicted by the rigid pier model. These mode shapes are shown in Figures 34 and 35, respectively. The influence of the pier flexibility is seen by the smaller relative magnitudes of the outside edge displacements in the flexible pier model than in the rigid pier model. In fact, the flexible pier model could just as easily be described as an inner edge bending mode.

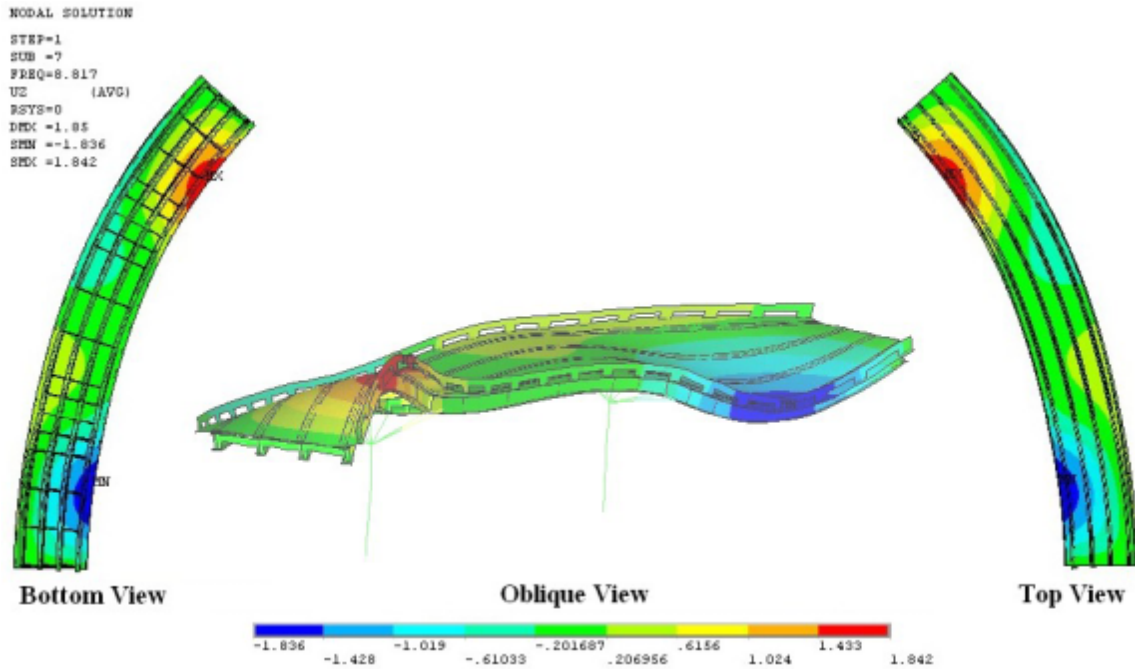
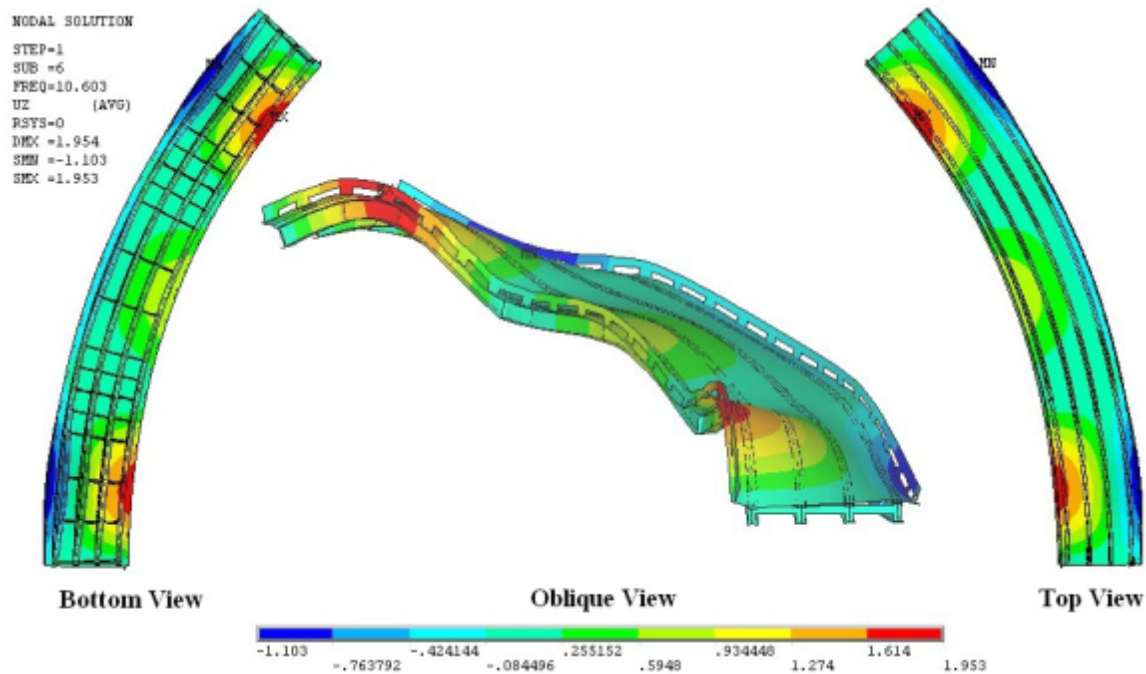


Figure 35. Flexible Pier Model - First End Span Antisymmetrical Torsion Mode

### First End Span Symmetrical Torsion Mode

The symmetrical torsion modes are slightly higher than the anti-symmetrical torsion modes, a situation similar to that observed with the exterior bending modes. The rigid pier mode 6 (10.603 Hz) (Figure 36) and the flexible pier mode 8 (9.642 Hz) (Figure 37) describe these modes. The rigid pier frequency of this mode is about 10% higher than that predicted by the flexible pier model. In the symmetrical torsion mode as well, the rigid pier model predicts larger outside edge displacements than does the flexible pier model. In this case, however, both the rigid pier and flexible pier models predict a clear reversal of signs from the inner to outer edges of the bridge.



**Figure 36. Rigid Pier Model – Symmetrical End Span Torsion Mode**

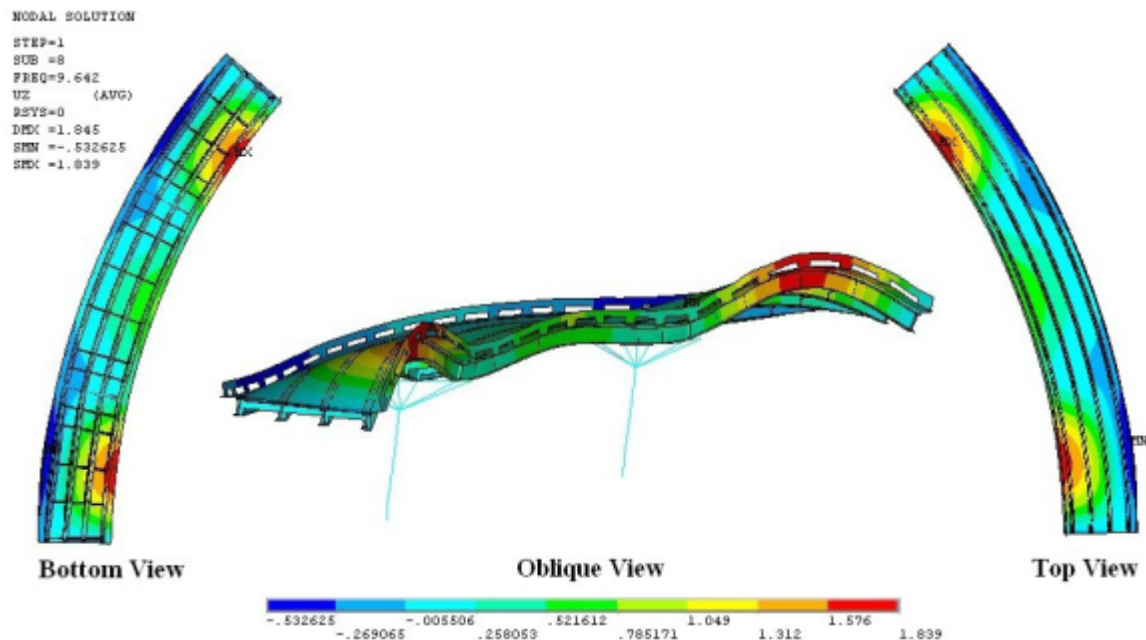


**Figure 37. Flexible Pier Model – Symmetrical End Span Torsion Mode**

### First Transverse Bending Mode – Span B

Mode 7 of the rigid pier model (14.221 Hz) and mode 11 of the flexible pier model (13.64 Hz) correspond to transverse deck bending of span B. There is only about 4% difference between these frequencies, so pier flexibility is not of great importance for this mode. The predicted mode shapes are shown in Figures 38 and 39. The mode shapes are quite similar. A small amount of pier bending probably accounts for the difference in predicted frequencies.

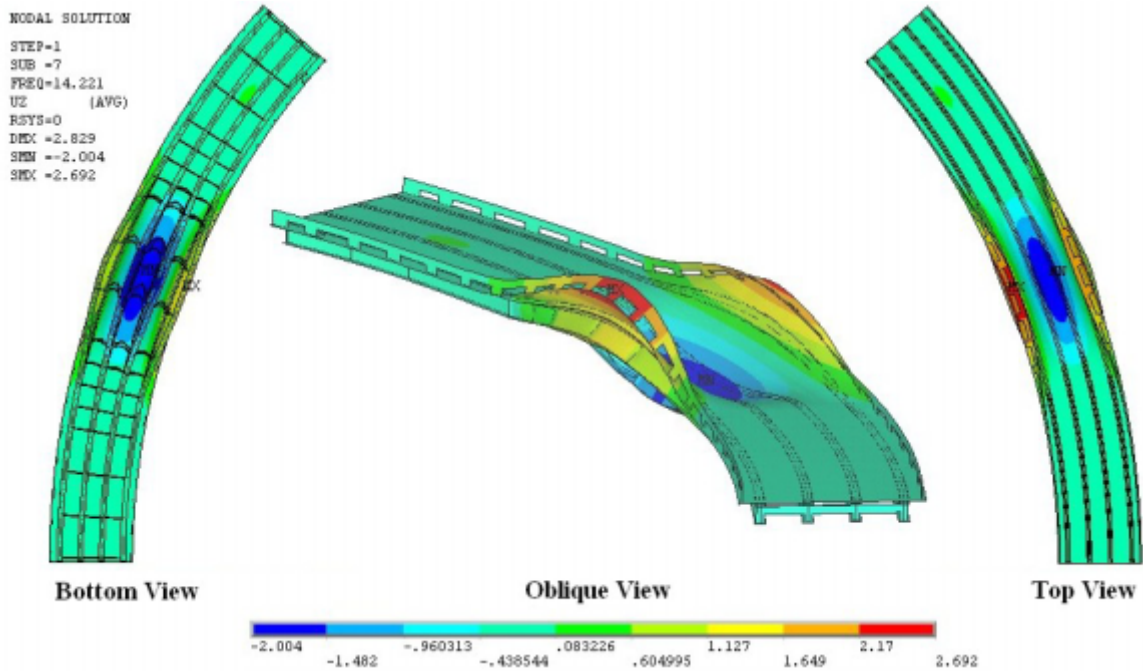


Figure 38. Rigid Pier Model – Span B First Transverse Bending Mode

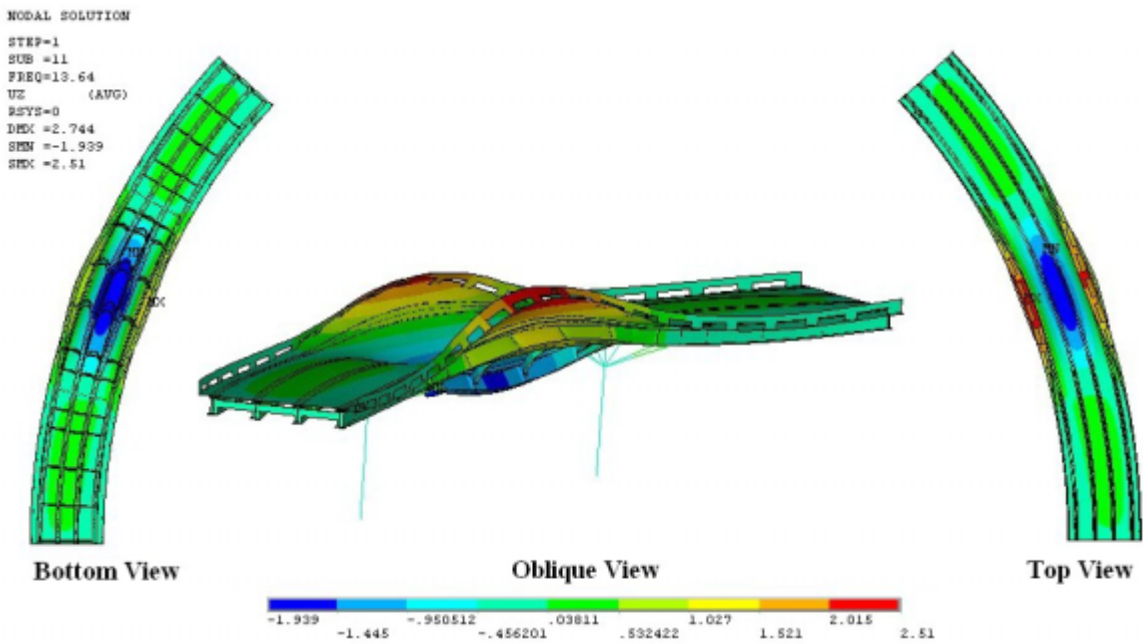


Figure 39. Flexible Pier Model - Span B First Transverse Bending Mode

### Second Vertical Bending Mode of Span B

Mode 9 of the rigid pier model(15.295 Hz) and Mode 10 of the flexible pier model (13.478 Hz) correspond to the second vertical bending mode of span B, with a single reversal of bending at midspan. There is about a 13% discrepancy between the predicted frequencies,

indicating that pier action is at least somewhat significant. The mode shapes are shown in Figures 40 and 41, respectively.

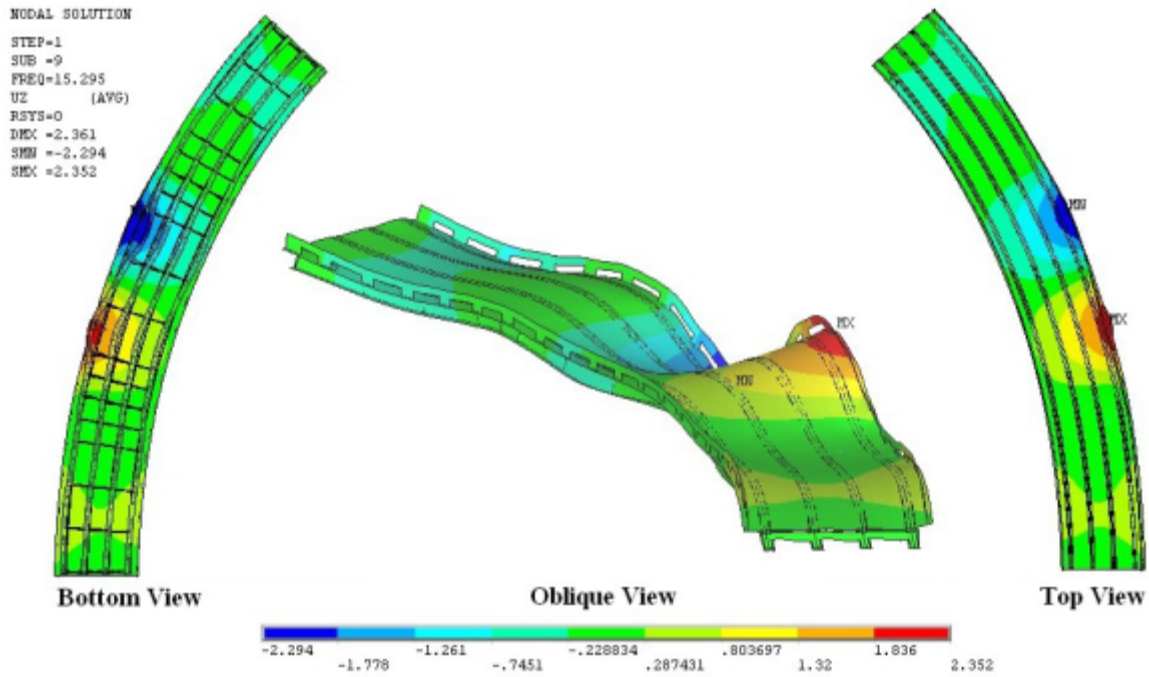


Figure 40. Rigid Pier Model – Second Longitudinal Bending Mode of Span B

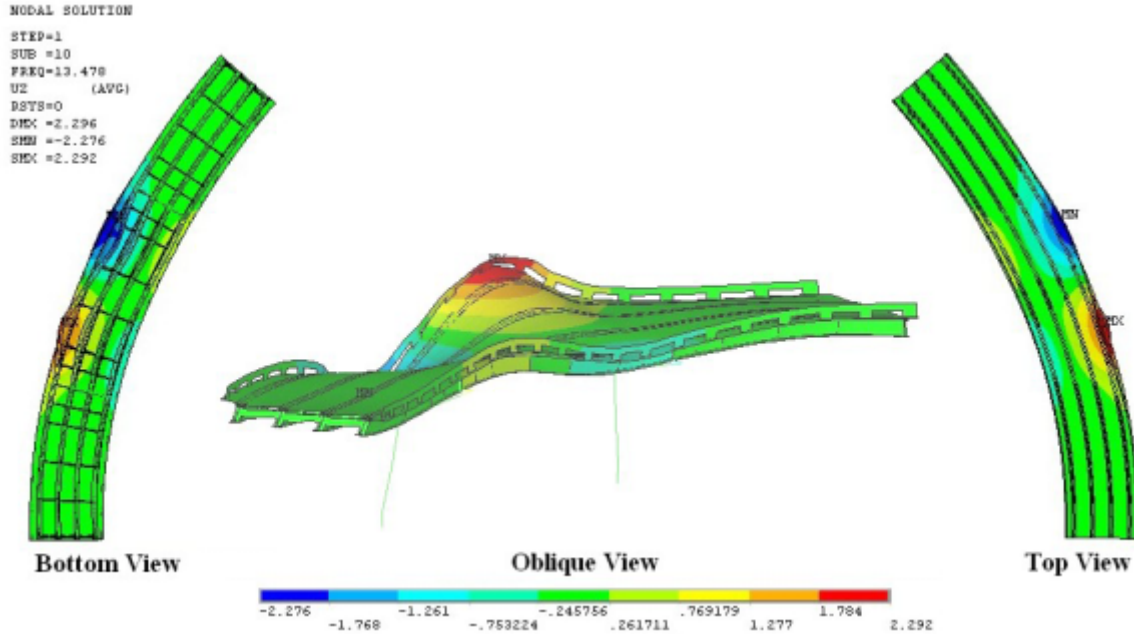


Figure 41. Flexible Pier Model – Second Longitudinal Bending Mode of Span B

Examining Figure 41, it is seen that at least some bending of the pier columns is occurring, indicating that some lateral displacement may be associated with this mode in the presence of flexible piers. The rigid pier model obviously cannot predict this behavior.

## Transverse Bending of End Spans

Several modes display transverse bending of the end spans. These are discussed together, since they represent quite similar phenomena. Mode 10 of the rigid pier model is predominantly transverse bending of span A at 16.294 Hz. Mode 11 of the rigid pier model at 16.32 Hz is quite similar, except that the transverse bending is primarily limited to span C. These two modes are shown in Figure 42.

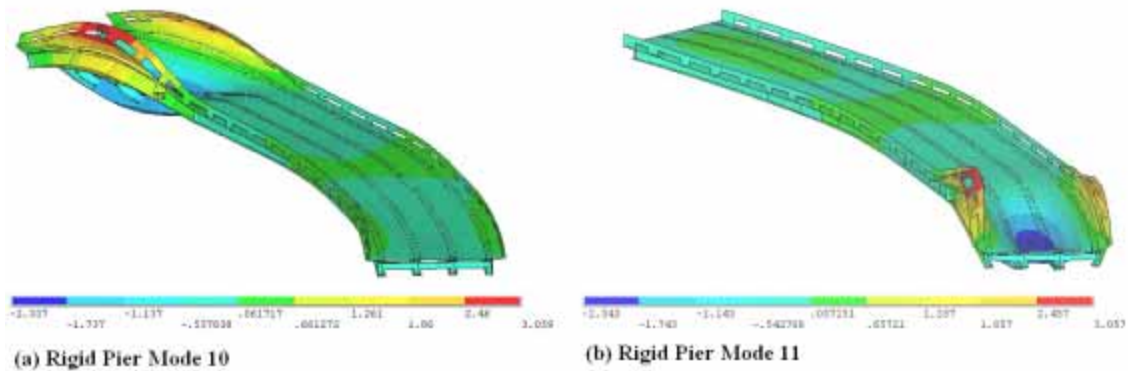


Figure 42. Rigid Pier Model – End Span Transverse Bending Modes

By comparison, the two flexible pier modes for end span transverse bending both combine bending of both end spans, but Mode 13 (15.79 Hz) is symmetric, with spans A and C in phase, and mode 14 (16.033 Hz) is anti-symmetric, with spans A and C out of phase. These modes are shown in Figure 43.

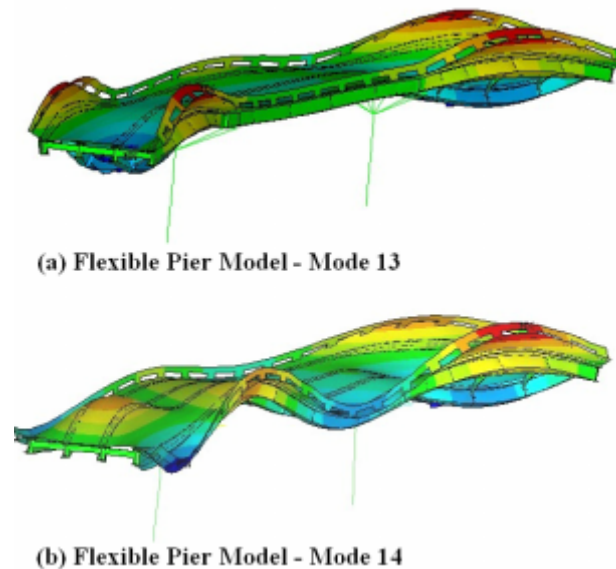


Figure 43. Flexible Pier Model – End Span Transverse Bending Modes

Thus, in this case, the rigid pier model effectively isolates the two end spans from each other, leading to two decoupled (but nearly identical) modes. The fact that the rigid pier

frequencies are not identical should be ascribed to small numerical asymmetries in the model. Interestingly, in the flexible pier model, the pattern we have seen before has reversed itself, with the symmetrical mode having a slightly lower frequency than the anti-symmetrical mode.

### Second Torsion Mode – Span B

Mode 13 of the rigid pier model (18.965 Hz), and mode 12 of the flexible pier (15.251 Hz) can be interpreted as the second torsion mode on span B. These modes are shown in Figures 44 and 45, respectively. The flexible pier model can also be interpreted as interior edge bending, since the outer edge of the deck undergoes only relatively small translation. These modes are beginning to show some of the complexity associated with modeling the girders as plates, since visible girder distortion is present along the overall superstructure bending. This is particularly evident in the bottom view of the rigid pier model shown in Figure 44. By comparison, the flexible pier model shows less girder distortion in span B, but does show some girder distortion and some transverse bending in spans A and C, as is evident from Figure 45.

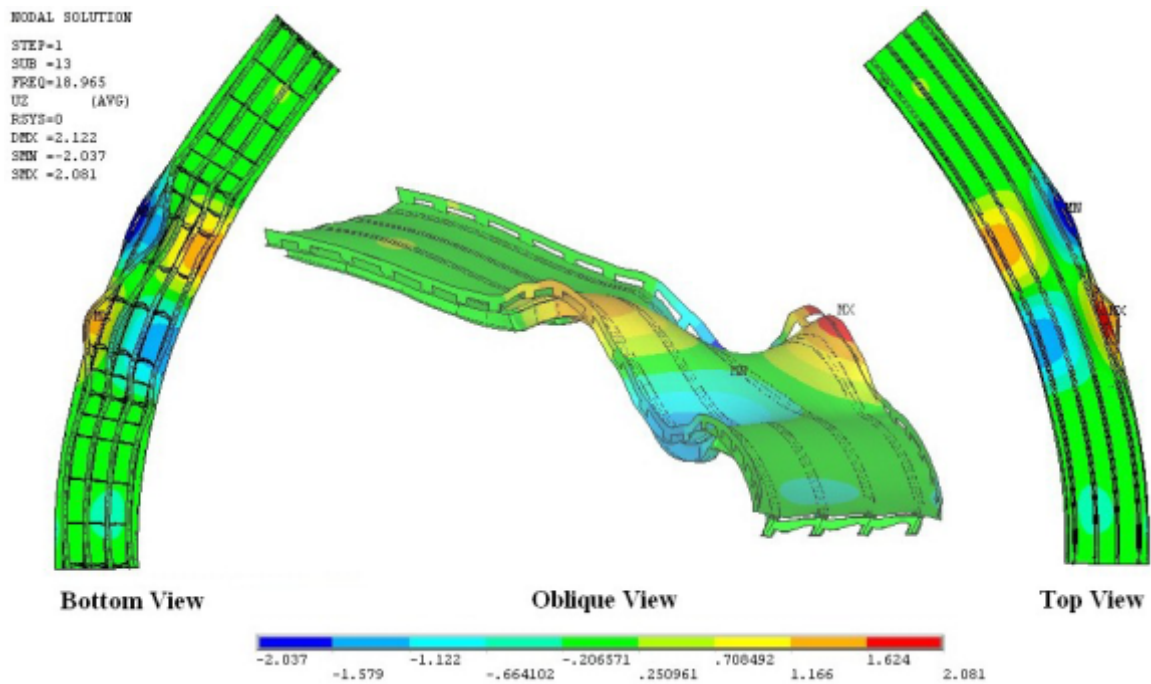


Figure 44. Rigid Pier Model – Second Torsional mode of Span B

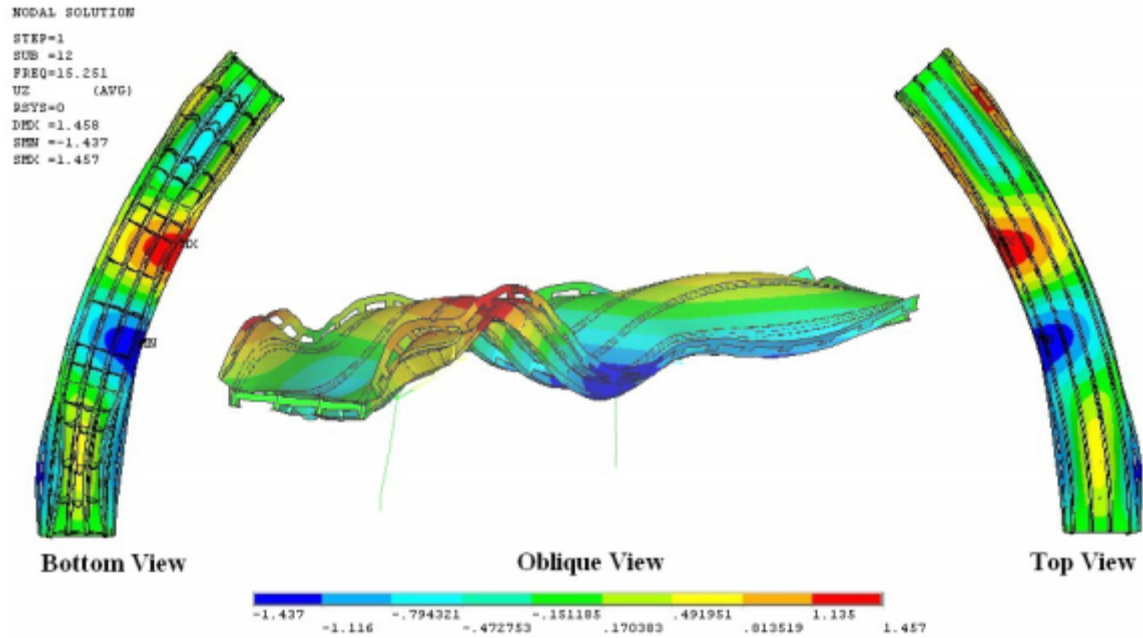


Figure 45. Flexible Pier Model –Second Torsional Mode of Span B

## Second and Third Lateral Bending Modes

Both the rigid pier model and the flexible pier model indicate the presence of second and third lateral bending modes. The predicted frequencies and local behavior of the two models differ significantly, however.

The rigid pier model's mode 12 (17.111 Hz), shown in Figure 46, appears to have a strong lateral displacement behavior, together with some tendency to distort into something of an "S" shape relative to the original line of curvature. This is consistent with the second lateral bending mode. In order for the deck to undergo significant lateral displacements, it is necessary for significant local girder distortion to take place at all four support points. This is evident from Figure 46, along with some inside edge bending (or torsion) on span B.

The flexible pier model's mode 9 (10.797), shown in Figure 47, reveals similar lateral bending, as shown in Figure 49, but with a more cleanly defined "S" shape distortion. The flexible pier model also shows significant girder distortion at the abutments, but has almost no girder distortion at the intermediate piers, which translate with the deck. However, the translation of the pier caps with the deck is accompanied by significant rotation, leading to much more pronounced torsion of the deck in the flexible pier model than was observed in the rigid pier model. As expected, the rigid pier model's natural frequency is nearly 70% higher than that predicted by the flexible pier model for this mode.

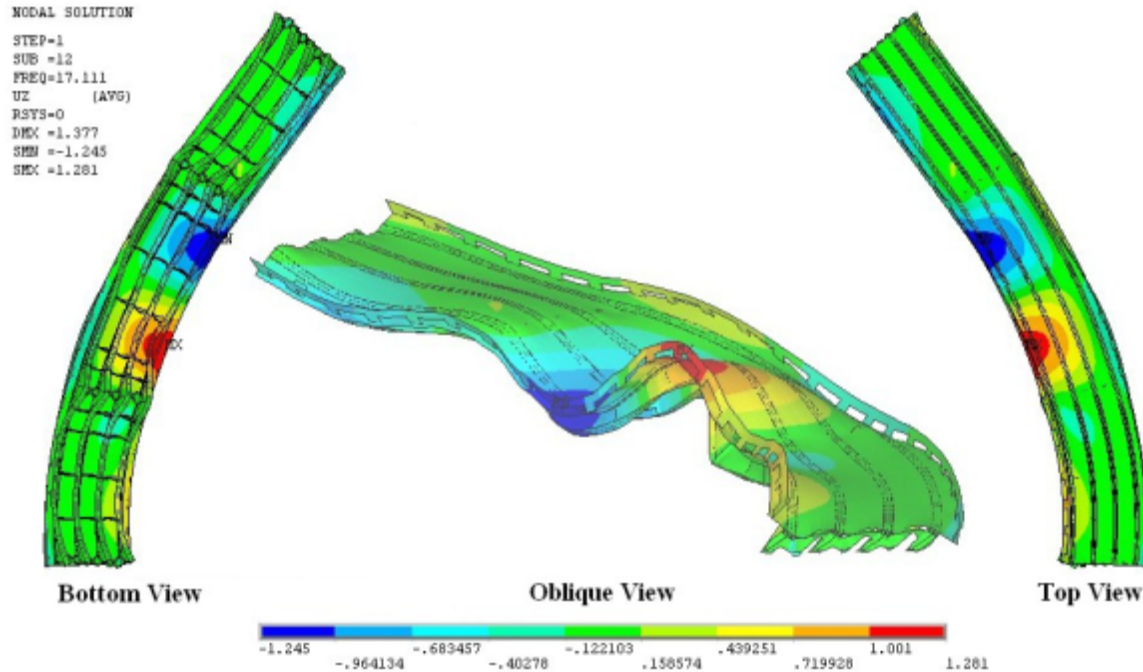


Figure 46. Rigid Pier Model – Second Lateral Bending Mode

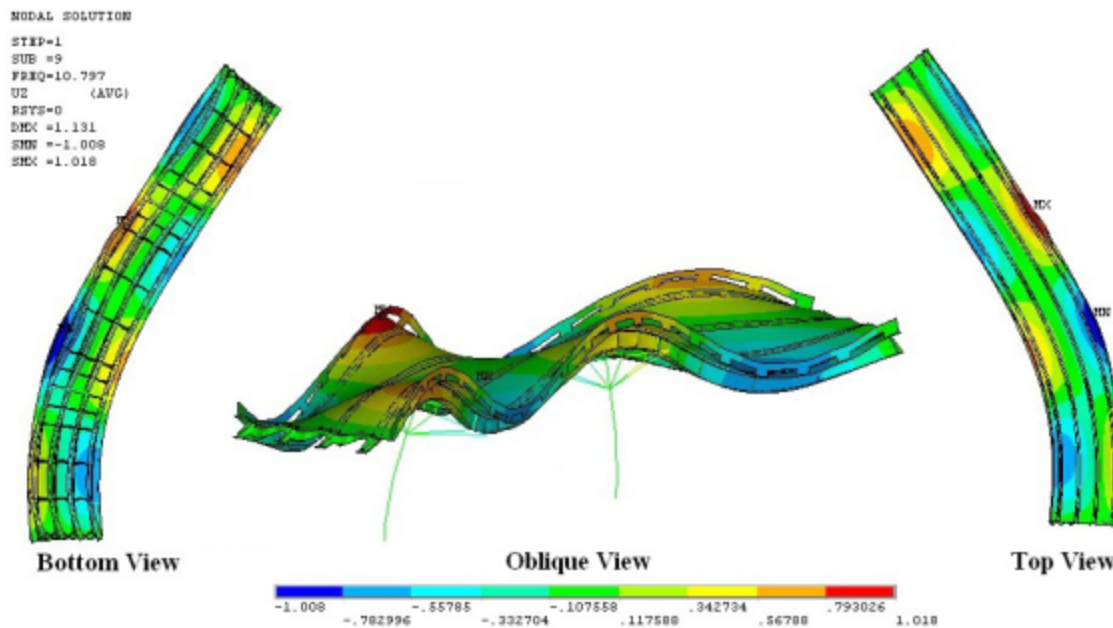


Figure 47. Flexible Pier Model – Second Lateral Bending Mode

The third lateral bending mode of the rigid pier model is mode 14 (21.192 Hz) and that of the flexible pier model is mode 16 (19.665 Hz). Apparently the third lateral bending mode does not involve as much pier motion as the second lateral bending mode, since the difference between the two predicted frequencies is much less than for the second lateral bending mode. This is easily seen from Figures 48 and 49. The mode shapes are relatively similar between the two models. The bottom views are particularly revealing, since they indicate significant local girder distortion at the abutments, but almost no girder distortion at the intermediate piers. The

difference between the frequencies is probably caused by the total restraint against vertical rotation of the deck that occurs at the pier locations in the rigid pier model. By contrast, the flexible pier model permits rotation about the vertical axis, accompanied by pier rotation about the same axis.

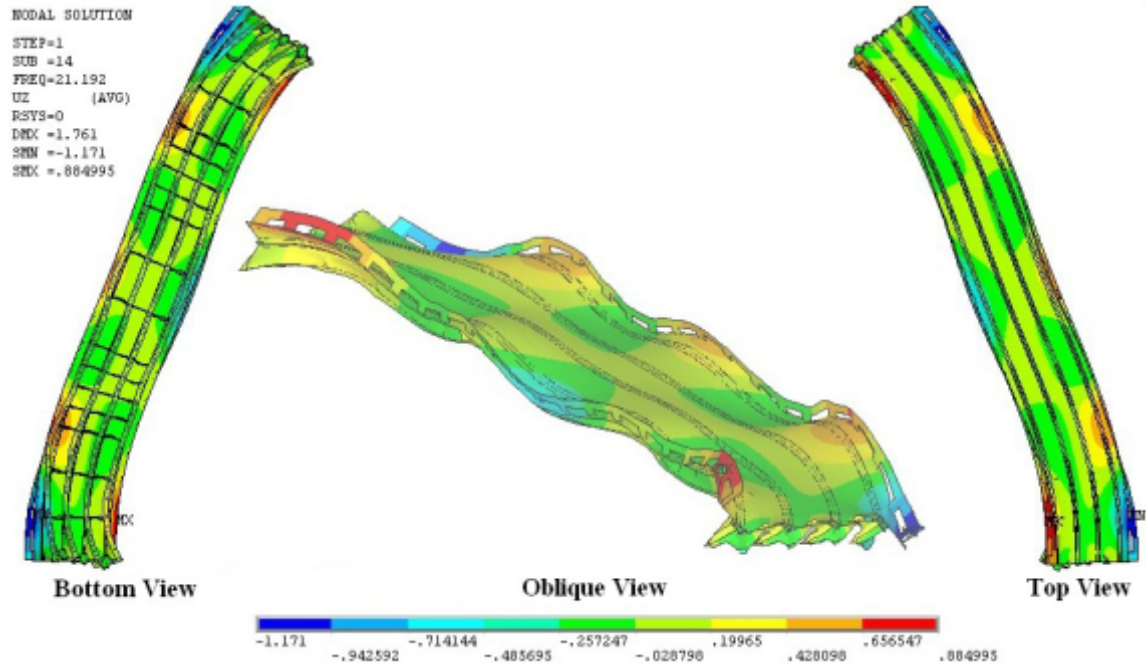


Figure 48. Rigid Pier Model – Third Lateral Bending Mode

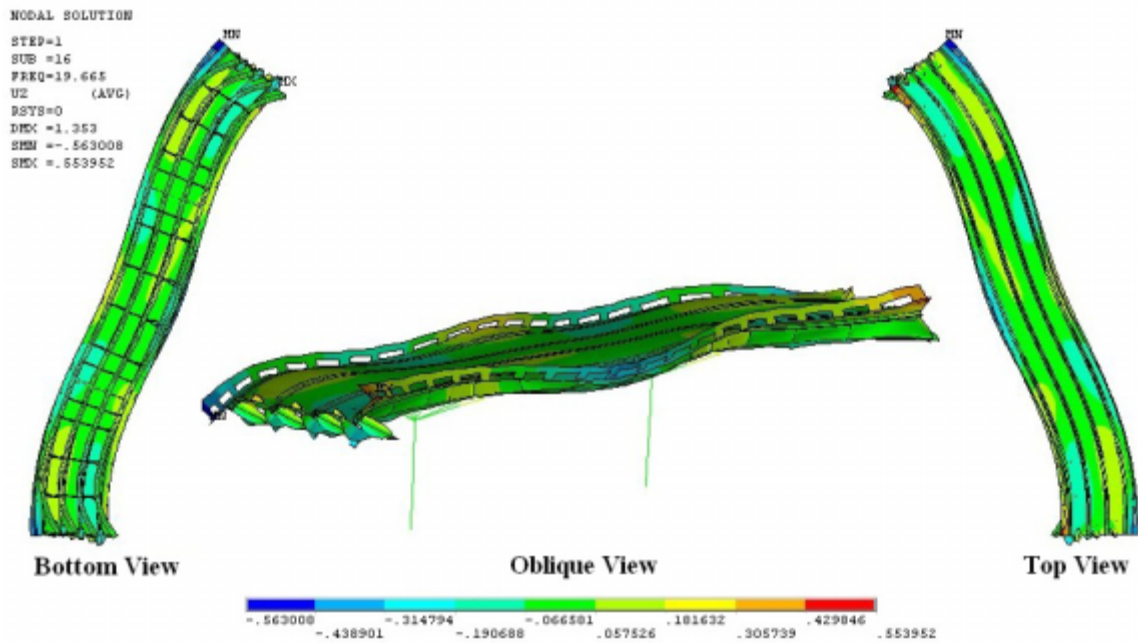


Figure 49. Flexible Pier Model – Third Lateral Bending Mode

## Second Transverse Bending – Span B

The fifteenth mode of the rigid pier model (22.893 Hz) and the eighteenth mode of the flexible pier model (21.251 Hz) indicate transverse bending of the deck on Span B, with a reversal of directions at midspan. These modes are shown in Figures 50 and 51, respectively.

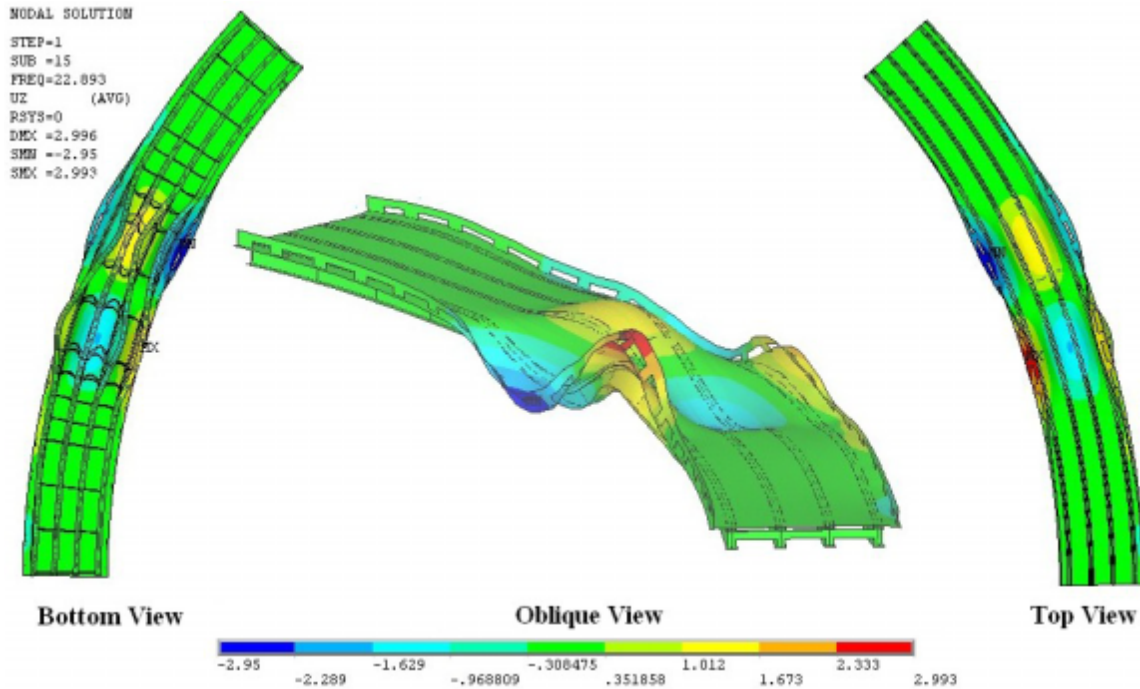


Figure 50. Rigid Pier Model – Second Transverse Bending Mode, Span B

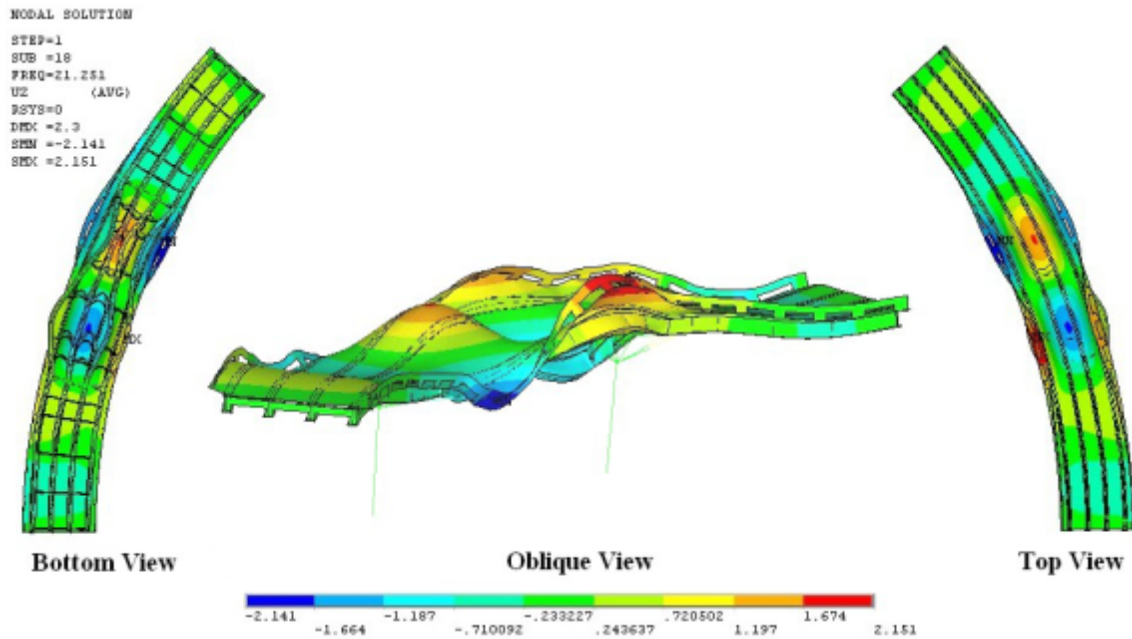


Figure 51. Flexible Pier Model - Second Transverse Bending Mode, Span B

The relatively close agreement between these frequencies and mode shapes indicate relatively insignificant participation of the piers in these modes. The bottom views of both figures suggest significant torsion of the girders accompanying this mode, and the top views indicate that significant torsion of the railing also occurs.

### **Additional Mode Shapes**

As the behavior of the modes becomes more complex, it becomes increasingly difficult to obtain detailed comparisons, between the rigid and flexible pier models. Even so, it does appear that mode 16 of the rigid pier model (24.057 Hz) and mode 17 of the flexible pier model (20.312 Hz) may correspond. Likewise mode 17 of the rigid pier model (24.351 Hz) bears strong similarities to mode 19 of the flexible pier model (22.83 Hz). In the case of many of the higher modes, pier action is not as important, so the agreement of the computed frequencies is fairly good.

## **DISCUSSION**

### **Convergence Studies**

The girder and girder/slab convergence studies suggest that the plate girders are relatively insensitive to the number of elements used to model the girder cross-section. The girder study indicates that negligible changes occur if the number of elements on the flange is increased from four to six, and if the number of web elements is increased from two to six. However, the number of elements used along the girder does have a significant influence, and it appears that elements should probably not be more than about 2% of the span length. These results are not surprising upon reflection. The girder behaves very much like a Bernoulli-Euler beam, for which the Navier assumption that plane sections remain plane is an excellent approximation. The plate elements used are capable of producing this effect, and in fact can reproduce cubic displacement variations over the height, because of the drilling degrees of freedom that are included in the SHELL63 element. Thus, as long as beam behavior is being considered, a relatively coarse discretization of the cross-section is possible. The displacement field does not vary linearly along the length of the girder, however. Thus more mesh refinement is needed along the length.

The girder/slab convergence study results show slightly greater sensitivity to the number of web elements, but was surprisingly insensitive to the number of slab elements, providing at least 8 elements was used to model the slab. This suggests that shear lag in the deck, although almost certainly present, does not have a pronounced influence on convergence of girder displacements. The slab/girder study also suggests that a reasonable model of stiffness requires elements to be on the order of 2% of the span, for the same reason as cited previously.

The diaphragm convergence study reveals somewhat more complex behavior. The midspan displacements are somewhat more sensitive to the cross-section discretization, showing approximately 2.5% change in displacements when the number of web elements is increased from two to nine. The sensitivity to mesh density along the length appears similar to that observed in the girders. The meshes used in the diaphragm convergence study were somewhat

coarser lengthwise than those used in the girder studies, so a more pronounced influence of mesh refinement is evident. It does appear that a fully converged mesh may require elements to be no longer than 2% of the diaphragm length, but that reasonable behavior may be obtained with somewhat coarser meshes, since the diaphragm are secondary members. The increased sensitivity to cross-section mesh density suggests that the diaphragm member does not behave as simply as the girder and the girder slab combination. The most likely reason is that the loading in the plane of the web does not pass through the shear center of the non-symmetrical channel section, so the Navier assumption is not fully accurate. The actual behavior of the channel is a combination of bending, for which the Navier assumption is largely valid, and restrained warping torsion, for which plane cross-sections do not remain plane. The presence of this latter effect, plus the accompanying St Venant torsion both indicate a more complex cross-section deformation pattern that will require a finer mesh within the cross-section for adequate representation. In this regard, the convergence study probably provides an overly severe test. Because the diaphragm member is loaded at mid-span, it has a shear span, and a corresponding span over which full reversal of warping constraint is achieved of only four feet, as compared with seven feet in the actual diaphragm. Moreover, the ends of the diaphragm convergence model flanges are fixed, which will increase the warping restraint over that expected in the actual diaphragm members, which are only restrained in the web.

### **Pier Models**

The pier studies were directed at producing an efficient, yet reasonably accurate model of the piers. Tests one through four indicate that the BEAM4 pier model reproduce the stiffness of the SOLID95 model reasonably well. By comparison, the natural frequencies of the BEAM4 pier model are considerably lower than those predicted by the SOLID95 model, indicating that the use of multiple beam elements to reproduce the pier cap tends to overestimate the effective mass of the pier cap. This result could be improved somewhat by introducing a reduced mass density in the pier cap elements of the frame model. However, the superstructure's effective mass considerably exceeds the effective mass of the pier cap, so it was decided not to modify the model in this way.

Perhaps the most significant result of this study is that the process of approximating a solid element model using frame elements is not altogether trivial, and such models should not be applied to the construction of a bridge model without being tested for their accuracy as stand-alone structures. Several trial models were constructed during this process, and the final model, while acceptable, cannot be considered to be an exact representation of the solid model.

A more fundamental question may concern the approximations inherent in the SOLID95 model, which greatly simplify the behavior of the reinforced concrete structure. Ideally, field tests of pier structures should be used to verify or refute the approximations. However, the difficulty in any such field tests is that significant cracking of the pier cap is unlikely to become evident until the superstructure is in place and live loads have been applied. In this state, a number of additional approximations in the bridge model will make it difficult to isolate any modeling errors in the piers.

## **The Wolf Creek Bridge Models**

The rigid pier and flexible pier models of the Wolf Creek Bridge predict natural frequencies and mode shapes that can, in general, be compared with each other. Although the mode shapes of a curved girder bridge are significantly more complicated than those of a comparable span straight bridge, the idealized mode shape types: vertical bending vibration, lateral bending vibration, torsional vibration, and transverse vibration can still be recognized in the curved girder bridge, with proper interpretation. Using the similarities in mode shape types between the two models permits the stiffening influence of the rigid pier approximation to be evaluated.

The flexible frequency model consistently predicted lower frequencies than those of the rigid pier model, an expected result. The magnitude of the difference between the frequencies predicted by the rigid pier and flexible pier models depends largely upon the amount of pier translation or rotation of the individual modes. Modes for which the piers displace or rotate significantly in the flexible pier model tend to have significantly lower frequencies, and significantly different mode shapes than those predicted by the rigid pier models, with the rigid pier model over-estimating the natural frequency by as much as 70% for certain modes. By contrast, modes that have little pier participation tend to have frequencies that agree within 10%. In particular, with reference to the pier analyses, the lowest pier mode is a combination of lateral translation and rotation of the pier cap in the plane of the pier, accompanied by column bending. Given the fact that the curved superstructure also tends to rotate during vertical loading, as a result of the transfer of load toward the outer edge, the influence of pier flexibility is significant.

Although it is beyond the scope of the present study to conduct vehicular loading studies, one potential drawback of the finite element method as implemented here is apparent. Structural engineers typically base their designs upon composite and non-composite girder moments, in order to conduct a limit state based design of the girder/slab combination. The direct output of the plate based finite element model consists of element stresses, not member moments, so a substantial amount of post-processing would be required to convert the results of a plate based FE analysis to a form that is suitable for girder design.

## **SUMMARY**

This research study has developed and analyzed a finite element based, horizontally curved bridge model for the purpose of comparing the dynamic and static model response with future field test data of the Wolf Creek Bridge in Bland County, Virginia. The bridge model was generated using the finite element program ANSYS. The curved bridge model was developed through a series of studies by first running convergence tests on straight plate girders and girder/deck composite assemblages of comparative length. This was done in order to determine the necessary plate discretization for the bridge in order to generate a satisfactory model, while keeping the model size within the software limitations. A nearly 30,000-element model of the bridge superstructure, comprised of SHELL63 plate elements, was subsequently developed based on the convergence study results.

The substructure, or central piers, was modeled by first generating a large three-dimensional replica of one of the two identical central piers, using solid elements. Because of the large size of the superstructure model, a much smaller version of the two central piers' models was needed for implementation into the bridge model. Using beam elements, various combinations of element dimensions and material properties were attempted until a beam element pier was generated that displayed similar frequency response and displacement characteristics, under various loadings, to the significantly larger three-dimensional brick element pier. The curved bridge model was completed by connecting the piers to the bridge superstructure, using contact nodes, and the results of this model were compared with those obtained using a typical rigid support approximation.

The focus of the current report is a comparison of the free vibration characteristics of the rigid pier and flexible pier models of the bridge. Additional studies, not reported here include responses to forced excitations, which were conducted as a feasibility study for upcoming bridge tests, and construction period studies to investigate the rotational tendencies of the non-composite girders (Lydzinski; 2006).

Because of license restrictions imposed on this research project, several key components of the Wolf Creek bridge had to be modeled in a simplified fashion. These features of the bridge can be developed in future studies to create improved approximations.

Of particular interest is the modeling of the bearing components between the girders and the piers. In this project the piers were joined directly to the superstructure using contact nodes, therefore the true bearing properties are completely neglected. There is a strong possibility that the bearings could somewhat significantly impact the dynamic results in this research.

The other primary approximation of the developed model is the method used to represent the connections between the girder and diaphragm members. The bridge construction drawings specify that these connections be completed through a series of bolts that would join the diaphragm members to the connection plates, which are welded directly to the girders. Due to the complexities involved, this project modeled the diaphragms and connection plates as a single joined entity, thus neglecting any flexibility enabled by the bolted connections.

## CONCLUSIONS

- Curved multi-girder composite bridges can be comprehensively modeled using a combination of plate elements. Advantages of this approach include the ability to model local plate bending behavior of girder elements and girder-diaphragm interaction that cannot be captured using beam elements.
- Relatively coarse meshes can be used to define the cross-section of girders with reasonable accuracy, since the cross-section displacement pattern is relatively simple, but considerably more refinement is needed along the girder length. The amount of cross-section refinement of

the web is controlled by the need to model lateral plate bending of the web, and by the need to accommodate the connection plate-diaphragm details.

- Haunches modeled using plate elements do not appear to cause some of the local girder flange distortion that has sometimes been observed using rigid link models. The plate element model is known to underestimate the lateral shear stiffness of the haunch, but no extraneous displacements caused by this approximation were observed in the current studies, because the haunch lateral stiffness is much larger than that of the elements to which it is connected.
- Small pier models using beam elements can be developed that display similar stiffness properties to significantly larger three-dimensional pier replicas. Simultaneously replicating both stiffness and mass properties accurately is more difficult.
- Direct comparison of mode shapes between rigid and flexible pier models indicate the importance of including pier models in order to accurately determine the response of a curved girder bridge. Although comparison studies were not conducted using other types of piers, it is thought that the hammerhead type piers used on the Wolf Creek Bridge may display a particularly strong rotational coupling with the tendency of the curved bridge cross-section to rotate under load that would probably not be present with multi-column piers.
- Simply supported boundary condition models on rigid piers result in different mode shapes and natural frequencies from those values with the added central piers. Most importantly, the rigid pier approximation changes the dynamic bridge response model, not only in the immediate region of the piers, but throughout the entire structure. The importance of these changes is particularly noticeable in modes that have significant lateral displacements or rotations at the piers.
- It may be necessary to introduce numerous approximations in order to develop a curved bridge model, even using finite elements. Thus, exactly replicating the actual bridge response in detail may be difficult. Specific problems encountered in this project include parapet modeling, concrete deck and pier modeling in negative moment regions, and adequate specification of boundary conditions.

## RECOMMENDATIONS

1. *VDOT's Structure & Bridge Division should consider the use of the finite element method as an analysis tool in the design of curved girder bridge structures.*
2. *VDOT's Structure & Bridge Division should consider incorporating pier flexibility in the analysis of curved girder bridge structures.*

## CONSIDERATIONS FOR FURTHER RESEARCH

The next logical step in furthering the development of finite element modeling capability for curved girder bridges is to conduct field tests on the Wolf Creek Bridge. This study is currently underway as a joint test venture between the University of Virginia and the Virginia Transportation Research Council to conduct field studies on the bridge following its completion in 2006. Goals for this field study are centered on the dynamic testing and subsequent strain instrumentation of the bridge. Results from such a field study will be extremely useful in determining the accuracy of the generated computer models, and in evaluating the quality of several of the approximations introduced during the modeling process. Subsequent modifications of the model can then be done in an attempt to better match the model with the actual bridge response. Improvements to the model accuracy can be made in several areas. One way is in the creation of more accurate parapet, or railings models, using the as-built parapet characteristics.

One significant conclusion of this study is that incorporating pier flexibility is particularly important in the analysis of curved girder bridges. This study introduced a simple approximate beam model for the piers in an attempt to maintain a manageable model size, while retaining the essential anticipated behavior. As noted, simultaneously matching stiffness and mass on this model proved to be somewhat difficult. Further studies of alternative simplified pier models that will be suitable for finite element modeling are needed, possibly using plate elements to replicate the behavior of the pier cap. Since superstructure and substructure design often proceed concurrently, studies are also needed to provide guidelines for modeling pier influence during the design period.

At several points during the modeling process, it was necessary to introduce the approximation that concrete cracking is relatively unimportant. The validity of this approximation needs to be evaluated using field data, and determine the conditions under which alternative modeling approaches are needed.

Following model modification to better match the experimental results, future studies will help further the understanding of horizontally curved bridges' behavior. Some suggested studies might include static load analysis on the bridge to examine resulting stresses and strains in the girders and diaphragms, as well as a study of transient or moving loads to examine the effects of passing vehicles.

The design process for curved girder bridges is often based upon the approximation of rigid substructures. While some design software permits foundation flexibility, most either does not, or provides a very simplified substructure model that does not capture the nature of flexible piers, such as T-piers. The current studies strongly suggest that such approximations may be inadequate. A critical analysis of the distribution of moments along the span, and the distribution of moments between girders at a location in the presence of flexible piers should be undertaken.

In addition, it may be beneficial to look at how other types of piers, especially those with greater rotational stiffness than the hammerhead pier on the Wolf Creek Bridge, affect the

dynamic disparity between the rigid support model and the flexible pier model. The single column of a hammerhead pier provides relatively low stiffness against pier cap rotation, which can lead to significant rotation and translation of the pier cap, coupled with the bridge deck. It would be a valuable study to examine how the dynamic response of piers, with multiple columns, or wider column bases, differs from the results obtained with the single column piers used in this analysis.

The model developed in this study, along with proper correlation to the Wolf Creek field studies and the steps involved in its creation, may be very beneficial not only to the understanding of the Wolf Creek Bridge itself, but to other researchers who are seeking to enhance multispan horizontally curved bridge design through modeling analyses.

### **COSTS AND BENEFIT ASSESSMENT**

The finite element method provides a very useful tool for modeling multispan curved girder bridges, being able to model details of structural behavior that cannot be modeled any other way. In the current project, a combination of plate elements and beam elements were used to gain considerable insight into several important aspects of the Wolf Creek Bridge that would have been difficult to obtain with any other modeling tool. Specific positive benefits include:

- the ability to model plate behavior of plate girders within the overall structure
- the ability to model the complete structure behavior, including substructure contributions
- the ability to model the diaphragm/girder interaction in detail
- numerous options for modeling the girder/slab interaction
- complete modeling of the girder warping torsion/bending interaction through the use of shell elements
- the potential for design modifications that could lead to more economical superstructures of curved girder bridges.

These benefits are particularly useful during the research process, but as this study has shown also have the potential to provide insight into structural behavior that would be difficult to obtain in other ways.

There are, however, significant costs associated with this modeling process, not all of which were encountered in the current project, but which would be encountered in the use of finite element analysis in a design setting. Several of these costs have been mentioned before, but a brief list includes:

- a time-consuming model construction process, in particular if convergence for a particular purpose is to be assured
- lengthy program execution times, not always convenient in a design procedure
- an additional lengthy process (not considered here) of load modeling

- a lengthy post-processing analysis to extract girder moments for design purposes that was not undertaken during this study
- the use of a numerical approximation procedure (finite elements) that is not guaranteed to provide good quantitative results when used by inexperienced analysts.

It is difficult to place a specific monetary value on the costs of finite element analysis when used in a design setting, since the added benefit to be gained by the more detailed structural analysis is likely to counteract many of these costs.

## ACKNOWLEDGMENTS

The authors thank the Virginia Transportation Research Council for the financial support provided to this project. Dr. Jose Gomez of VTRC is also acknowledged for his comments and critiques throughout the project.

## REFERENCES

- Brennan, P.J., and Mandel, J.A. (1973). Users Manual- Program for Three Dimensional Analysis of Horizontally Curved Bridges, *Rep., Res. Project HPR-2(111)*, Syracuse University, Syracuse, N.Y.
- Chang, T.C., and Volterra, E. (1969). Upper and Lower Bounds for Frequencies of Elastic Arcs, *The Journal of the Acoustical Society of America* 46, 1165-1174.
- Culver, C. G. (1967). Natural frequencies of horizontally curved beams, *Journal of the Structural Division*, ASCE, 93, 2, 189-203.
- Culver, C. G., Dym, C. L., and Brogan, D. K. (1972a) Bending behavior of cylindrical web panels, *Journal of the Structural Division*, ASCE, 98, 10, 2291-2308.
- Culver, C. G., Dym, C. L., and Uddin, T. (1973) Web slenderness requirements for curved girders, *Journal of the Structural Division*, ASCE, 99, 3, 417-430.
- Culver, C. G. and Frampton, R. E. (1970) Local instability of horizontally curved beams, *Journal of the Structural Division*, ASCE, 96, 2, 245-265.
- Culver, C. G., and Nasir, G. (1971) Inelastic flange buckling of curved plate girders, *Journal of the Structural Division*, ASCE, 97, 4, 1239-1256.
- Dabrowski, R. (1968). *Curved Thin-Walled Girders*, translated from the German by C. V. Amerongen, Cement and Concrete Association, London. (Original German version by Springer Verlag, Berlin.)

- Davidson, J. S., Ballance, S. R., Yoo, C. H. (1999a), Analytical Model of Curved I-Girder Web Panels Subject to Bending, *Journal of Bridge Engineering*, ASCE, 4(3), 204-212.
- Davidson, J. S., Ballance, S. R., Yoo, C. H. (1999b). "Finite displacement behavior of curved I-girder webs subjected to bending." *Journal of Bridge Engineering*, ASCE, 4(3), 213–220.
- Davidson, J. S., Ballance, S. R., and Yoo, C. H. (2000a). Behavior of Curved I-girder Webs Subjected to Combined Bending and Shear, *Journal of Bridge Engineering*, ASCE, Vol. 5, No. 2.
- Davidson, J. S., Ballance, S. R., and Yoo, C. H., (2000b), Effects of Longitudinal Stiffeners on Curved I-Girder Webs, *Journal of Bridge Engineering*, ASCE, 5, 2, 171-178.
- Davidson, J.S., Abdalla, R.S., Madhavan, M. (2004). Stability of Curved Bridges During Construction, University Transportation Center of Alabama, Report Number 03228.
- Fukumoto, Y., and Nishida, S., (1981). Ultimate load behavior of curved I-beams, *Journal of Engineering Mechanics*, ASCE, 107, 2, 367-385.
- Galambos, T. V., Hajjar, J. F., Huang, W. H., Pulver, B. E., Leon, R. T., and Rudie, B. J., (2000). Comparison of measured and computed stresses in a steel curved girder bridge. *Journal of Bridge Engineering*, ASCE, 5(3), pp. 191-199.
- Gendy, A.S., and Saleeb, A.F. (1992). On the Finite Element Analysis of the Spatial Response of Curved Beams with Arbitrary Thin-Walled Sections, *Computers and Structures*, 44, 639-652.
- Gottfeld, H. (1932). *The Analysis of Spatially Curved Steel Bridges*, (In German) Die Bautechnik, p. 715.
- Hall, Dann H. (1996). Curved Girders are Special, *Engineering Structures*, 18, 769-777.
- Huang, C.S., Chang, S.H., and Tseng, S.H. (1998). Out-of-Plane Dynamic Responses of Non-Circular Dynamic Curved Beams by Numerical Laplace Transform, *Journal of Sound and Vibration*, 407-424.
- Lavelle, F.H., and Boick, J.S. (1965). A Program to Analyze Curved Girder Bridges, *Engineering Bulletin-8*, University of Rhode Island, Kingston.
- Lee, S. C., Davidson, J. S., and Yoo, C. H. (1994). Shear buckling coefficients of plate girder web panels. *Computers & Structures*, Vol. 59, No. 5, pp. 789-795.
- Lee, S. C. and Yoo, C.H. (1996). Ultimate Strength of Plate Girder Web under Pure Shear. *Journal of Structural Engineering*, ASCE, 125(8), August, pp. 847 - 853.

- Liew, J.Y., Shanmugam, N.E., Tan, L.O., and Thevendran, V. (1995). Behavior and Design of Horizontally Curved Steel Beams, *Journal of Construction and Steel Research*, 32, 37-67.
- Linzell, D., Hall, D., and White, D., (2004). Historical Perspective on Horizontally Curved I Girder Bridge Design in the United States, *Journal of Bridge Engineering*, ASCE, 9, 3, 218-229.
- Lyzdzinski, J. (2006) *Finite Element Analysis of the Wolf Creek Multi-span Curved Girder Bridge*, M. S. Thesis, Department of Civil Engineering, University of Virginia.
- Nakai, H., and Yoo, C. H. (1988). *Analysis and Design of Curved Steel Bridges*, McGraw-Hill.
- NCHRP. (1999) *Improved Design Specifications for Horizontally Curved Steel Girder Highway Bridges*, Report 24, NCHRP. Washington D.C.: National Academy Press.
- Oden, J.T. (1967). *Mechanics of Elastic Structures*, McGraw-Hill.
- Piovan, M. T., Cortinez, V. H. and Rossi, R. E. (2000). Out-of-Plane Vibrations of Shear Deformable Continuous Horizontally Curved Thin-Walled Beams, *Journal of Sound and Vibrations*, 237, 101-118.
- Rajasekaran, S. and Padmanabhan, S., (1989). Equations of Curved Beams, *Journal of Engineering Mechanics*, 115, 5, 1094-1111.
- Rajasekaran, S. and Ramm, E. (1985) Local and member stability of thin-walled straight and curved beams of open section, *Proceedings, 2d International Conf. Computer Aided Analysis and Design in Civil Engineering*, Roorkee India.
- Saje, M. and Zupan, D. (2003). The Three-Dimensional Based Theory: Finite Element Formulation Based on Curvature, *Computers and Structures*, 81, 1875-1888.
- Shore, Sidney. (1975). *Horizontally Curved Highway Bridges*, Interim report for the U.S. Department of Transportation as part of the CURT project, University of Pennsylvania.
- Shore, S. and Landsberry, C. (1975). *A Fully Compatible Annular Segment Finite Element*, Interim report for the U.S. Department of Transportation as part of the CURT project, University of Pennsylvania.
- Simons, D.C., (2005), *AASHTO LRFD Impact upon Bridge Stiffness and Strength*, M.S. Thesis, University of Virginia, Charlottesville.
- Snyder, J.M., and Wilson, J.F. (1992). Free Vibrations of Continuous Horizontally Curved Beams, *Journal of Sound and Vibration*, 157, 345-355.

- Tan, C. P. and Shore, S. (1968). Response of a horizontally curved bridge to moving load, *Journal of the Structural Division*, ASCE, 94, 761-781.
- Tilley, Matthew R. (2004). Analysis of a Curved Girder Bridge, Thesis University of Virginia.
- Topkaya, Cem, and Williamson, Eric. (2003). Development of Computational Software for Analysis of Curved Girders Under Construction Loads, *Computers and Structures*, 81, 2087-2098.
- Umanskii, A.A. (1948). *Spatial Structures*, (in Russian) Moscow.
- Vlasov, V. Z. (1961). *Thin-walled Elastic Beams*, 2d Edition, National Science Foundation, Washington, D. C.
- Yang, Y.B., Wu, C.M. and Yau, J. D. (2001). Dynamic Response of a Horizontally Curved Beam Subjected to Vertical and Horizontal Moving Loads, *Journal of Sound and Vibration*, 242, 519-537.
- Yoo, C. H. (1979). Matrix Formulation of Curved Girders, *Journal of the Engineering Mechanics Division*, ASCE, 105, 6, 971-988.
- Zureick, A. and Naqib, R., (1999). Horizontally Curved Steel I-Girders State of the Art Analysis Methods, *Journal of Bridge Engineering*, ASCE, 4, 1, 38-47.